LUND UNIVERSITY

Synthetic studies on naphthoxylosides - labeled compounds and mechanistic studies on acetals

Johnsson, Richard

2008

SYNTHETIC STUDIES ON NAPHTHOXYLOSIDES

LABELED COMPOUNDS AND MECHANISTIC STUDIES ON ACETALS

LUND
UNIVERSITY

RICHARD JOHNSSON ORGANIC CHEMISTRY LUND UNIVERSITY

Akademisk avhandling som för avläggande av teknologie doktorsexamen vid tekniska fakulteten vid Lunds Universitet kommer att offentligen försvaras fredagen den 25 april 2008, kl. 9.30 i sal B, på Kemicentrum, Getingevägen 60, Lund.

A doctoral dissertation at a university in Sweden is produced as a monograph or as a collection of papers. In the latter case, the introductory part constitutes the formal dissertation, which summarizes the accompanying papers. These have already been published or are manuscripts at various stages.

SYNTHETIC STUDIES ON NAPHTHOXYLOSIDES
Labeled compounds and mechanistic studies on acetals

Organic Chemistry
Department of Chemistry
Lund University
P.O. Box 124
SE-221 00 Lund
Sweden

ISBN 978-91-628-7473-5

Printed in Sweden by Media-Tryck, Lund 2008

"If I had to go back and do it all again, I wouldn't change a thing."

Joe Strummer (1952-2002)

ABSTRACT

Labeled analogs to an antiproliferative naphthoxyloside have been synthesized and evaluated. Our investigations have shown that the fluorescently labeled analogs are poor structural analogs, and the physical and biological properties are altered to a large extent. Instead, a radioactively labeled compound was synthesized, which made it possible to follow the pathway in the cell. The results showed a difference between a normal and a transformed cell line based on accumulation of the naphthoxyloside and it appears that the transformed cells process the naphthoxylosides faster than the normal cells do.

This work also involved mechanistic studies for regioselective openings of benzylidene acetals with boranes and a new mechanism has been proposed. As it turns out, the regioselectivity can be controlled by the choice of borane, Lewis acid and solvent. When the borane is activated by a Lewis acid, the reaction rate is increased and the borane is the most electrophilic species, thus directing the regioselectivity. In contrary, when the borane is not activated, the Lewis acid is the most electrophilic species that directs the regioselectivity.

LIST OF PAPERS

This dissertation summarizes the following papers. Papers I-V and VIII are reprinted with kind permission from the publishers (Paper I Georg Thieme Verlag; II, IV, V, VIII Elsevier; III American Chemical Society).

I. Richard Johnsson, Ulf Ellervik
"Selective 1-O-deacetylation of carbohydrates using polymer-bound benzylamine"
Synlett **2005**, 2939-2940.

II. Richard Johnsson, Katrin Mani, Ulf Ellervik
"Synthesis and biology of bis-xylosylated dihydroxynaphthalenes"
Bioorganic & Medicinal Chemistry **2007**, *15*, 2868-2877.

III. Richard Johnsson, Katrin Mani, Fang Cheng, Ulf Ellervik
"Regioselective reductive openings of acetals; mechanistic details and synthesis of fluorescently labeled compounds"
Journal of Organic Chemistry **2006**, *71*, 3444-3451.

IV. Richard Johnsson, Katrin Mani, Ulf Ellervik
"Evaluation of fluorescently labeled xylopyranosides as probes for proteoglycan biosynthesis"
Bioorganic & Medicinal Chemistry Letters **2007**, *17*, 2338-2341.

V. Richard Johnsson, Andréas Meijer, Ulf Ellervik
"Mild and efficient direct aromatic iodination"
Tetrahedron **2005**, *61*, 11657-11663.

VI. Richard Johnsson, Ulrika Nilsson, Lars-Åke Fransson, Ulf Ellervik, Katrin Mani
"Expression of glycosaminoglycans by tritiated 2-(6-hydroxynaphthyl-β-D-xylopyranoside"
Preliminary manuscript

VII. Richard Johnsson, Dan Olsson, Ulf Ellervik
"Reductive openings of acetals; explanation of regioselectivity in borane reductions by mechanistic studies"
Journal of Organic Chemistry, Accepted for publication

VIII. Richard Johnsson, Gustav Träff, Martin Sundén, Ulf Ellervik
"Evaluation of quantitative thin layer chromatography using staining reagents"
Journal of Chromatography A **2007**, *1164*, 298-305.

ABBREVIATIONS

3T3 A31	Mouse 3T3 fibroblast
3T3 SV40	Virus transformed mouse 3T3 fibroblast
CS	Chondroitin sulfate
DS	Dermatan sulfate
GAG	Glycosaminoglycan
HA	Hyaluronic acid
HFL-1	Human fetal lung fibroblast
HS	Heparan sulfate
KS	Keratan sulfate
PAPS	3'-phosphoadenosine 5'-phosphosulfate
PG	Proteoglycan
SCID	Severe combined immunodeficiency
T24 cells	Human bladder carcinoma cells

CONTENTS

1 INTRODUCTION

1.1 Carbohydrates

The word carbohydrates origins from *hydrate of carbon*, and was originally a description for monosaccharides, where the general structural formula is $C_n(H_2O)_n$. Carbohydrates can exist in a variety of different forms and sizes, from monosaccharides up to complex polysaccharides of more then 10,000 monosaccharide units, such as in cellulose. Since monosaccharides have several hydroxyl groups, oligo- and polysaccharides can be built up in many ways; thus giving considerable diversity.

The grandfather of carbohydrate chemistry, Emil Fischer, elucidated the structure of (+)-glucose already in 1891 and introduced carbohydrates in synthetic organic chemistry.[1,2] Despite this early start, carbohydrate chemistry did not develop as a thriving research area until the 1960's. The slow progress was most certainly the unawareness of the biological importance of carbohydrates (except as energy source or cellular building material) in biological systems. The biological importance of carbohydrates is today well accepted,[3-5] and synthetic carbohydrate chemistry is extensively reviewed in books and the primary literature.[6-9]

When a carbohydrate is attached to different chemical species (i.e. not a carbohydrate) it is named a glycoconjugate, with examples such as glycoproteins, glycolipids and also the naphthoxylosides, discussed in this dissertation.

1.1.1 Nomenclature

The full nomenclature of carbohydrates is too complex to be discussed in detail but some concepts, essential for this dissertation are discussed below. Four common monosaccharides are shown in Figure 1.1.

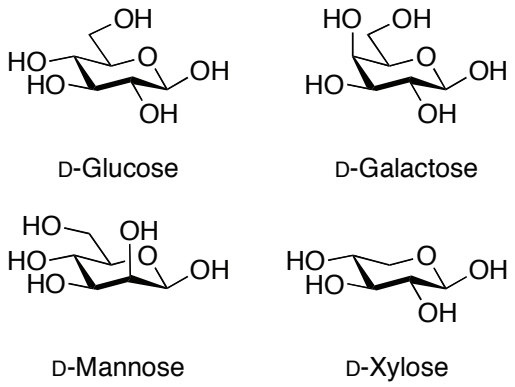

Figure 1.1 Common monosaccharides.

Carbohydrates can be seen as polyhydroxylated ketones (ketoses) or aldehydes (aldoses) with the possibility of ring closing to get hemiacetals (Figure 1.2). The monosaccharides are numbered along the carbon chain, in their open form, and the numbering extends to the oxygens.

When the carbohydrate forms the hemiacetal, it can become a six-membered (pyranose) or five-membered (furanose) ring. The pyranoses dominate, for most sugars, in aqueous solution, but the furanose form is quite common in biomolecules (Figure 1.3).

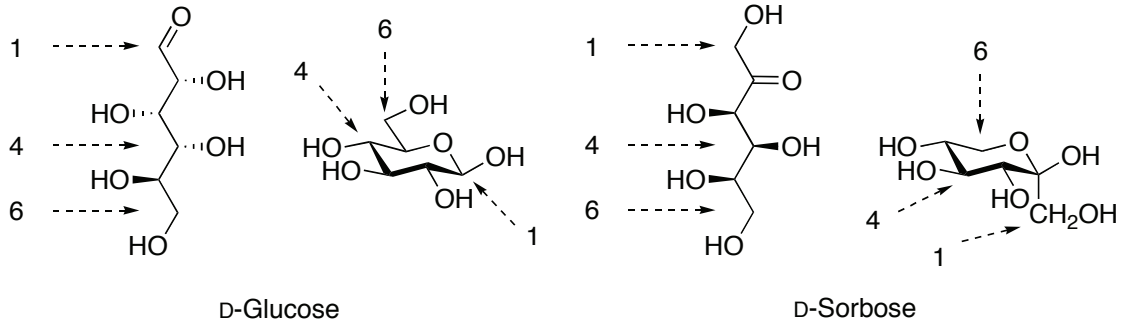

Figure 1.2 Open and closed pyranosidic forms of glucose and sorbose.

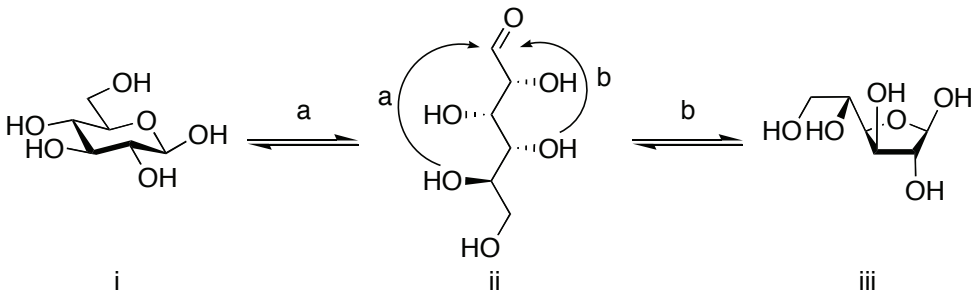

Figure 1.3 Pyranose (i), open chain (ii) and furanose (iii) form of D-glucose.

The carbohydrate nomenclature is based on the stereogenic centers as can be seen in Figure 1.1. If we change one of these stereocenters, a new carbohydrate will be formed. For example, if we invert position 2 in glucose we will get mannose. If we invert all the stereogenic centers in a monosaccharide, we will get its enantiomer and the saccharide prefix will change from D to L (Figure 1.4).

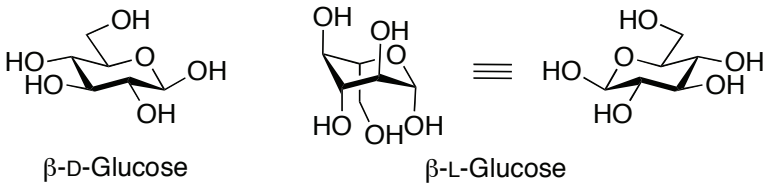

Figure 1.4 D- and L-glucose.

This nomenclature is derived from glyceraldehyde and is most easily explained using a Fischer projection.[1,2,10] In the Fischer projection, all vertical bonds are below the plane and the horizontal bonds above. Fisher decided that D-(+)-glucose should have the same configuration of the highest numbered stereogenic center as D-(+)-glyceraldehyde,[i] that is if the highest numbered stereogenic center has the hydroxyl group to the right in the Fischer projection, the carbohydrate belongs to the D-series.

The stereogenic center formed upon ring closure to the hemiacetal is called the anomeric center and the two different stereoisomers are called anomers. The anomers are referred to as α or β according to their configurational relationship to the anomeric reference atom, i.e. the highest numbered stereogenic center. In the α-anomer, the relationship between the atoms is formally cis (easiest to see in Fischer and Haworth projections) and in the β-anomer the relationship is formally trans. In Figure 1.5 the Fischer projection of the open

[i] Fisher decided that the highest numbered stereogenic center in (+)-glucose should have the same configuration as (+)-glyceraldehyde, as it turns out he was proven to be right 75 years later.

form of D-glucose (highest numbered stereogenic center has the hydroxyl to the right), followed by the closed form Fischer projection. In the closed Fischer projection the trans-relationship can be seen, representing a β-glucose. The Haworth projection, another way to represent cyclic carbohydrates, in this projection groups to the left in the Fischer projection are above the plane.

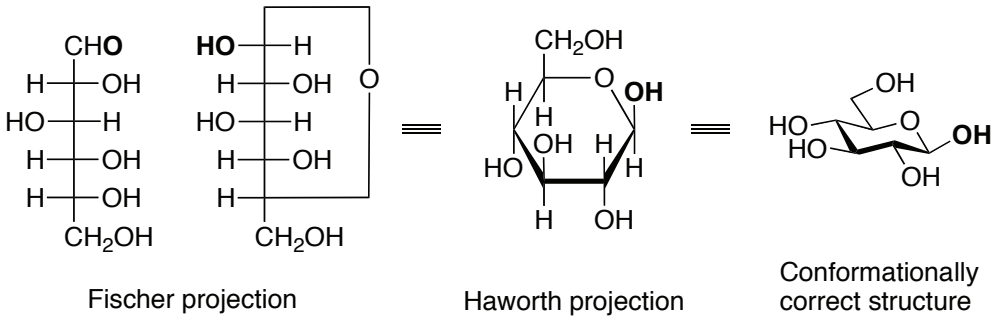

Figure 1.5 Anomeric configuration of glucose and the relationship between different projections.

1.1.2 Protecting group chemistry

Since a monosaccharide has several hydroxyl groups of similar reactivity, it is important to couple the different hydroxyl groups independently. The use of protecting groups are thus of great importance. By introducing orthogonally protecting groups, it is possible to derivatize specific hydroxyl groups. The anomeric hydroxyl group is of different reactivity compared to the other hydroxyl groups and can be selectively modified, as exemplified in section 2.1.2 of this dissertation. The most common protective groups in carbohydrate chemistry are ethers, esters and acetals, illustrated by benzyl ethers, acetate esters and benzylidene acetals (Figure 1.6).

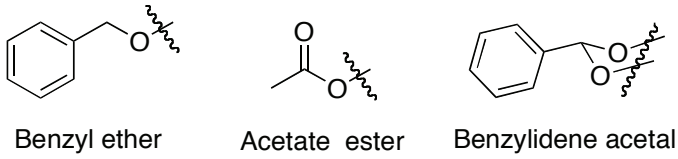

Figure 1.6 Common protective groups.

1.2 Aromatic glycosylation

In a glycosylation, the hemiacetal of a carbohydrate is coupled to another fragment, forming an acetal. The fragment can be a carbohydrate, forming a disaccharide, or a non-carbohydrate, termed an aglycon. Generally the carbohydrate, the donor, has a leaving

group (LG) in the anomeric position that is activated by a promoter (P), forming an oxocarbenium ion that subsequently reacts with the free hydroxyl group of the acceptor (Scheme 1.1).

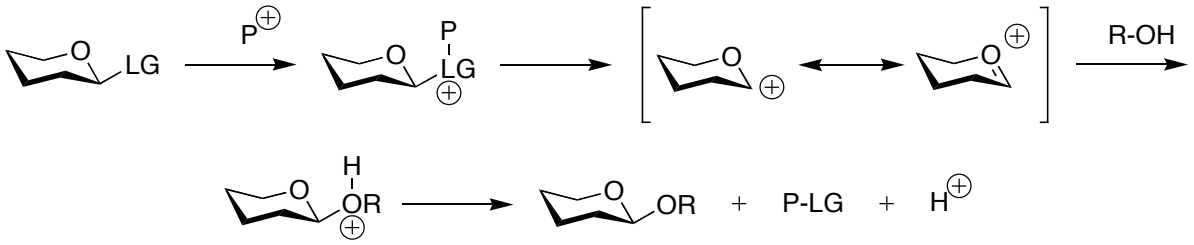

Scheme 1.1 The general mechanism for acid promoted glycosylation.

If the reaction follows an S_N1 mechanism, the oxocarbenium ion can be attacked from both sides. The anomeric effect promotes the formation of the α-anomer, but participating groups can direct the attack to the 1,2-*trans* product. Examples of participating groups are C2-esters that can stabilize the oxocarbenium ion by forming an acyloxonium ion, and the reaction proceeds in an S_N2 manner (Figure 1.7). It the acceptor instead attacks the acyloxonium instead, an orthoester, a common byproduct, is formed.

The mechanism for aromatic glycosylation do not differ from other glycosylations, but there are some differences in the procedures.[11] A glycosylation can proceed by three different reaction pathways; acid promoted reactions (S_N1 type), base promoted reactions (S_N2 type), and nucleophilic reactions were the anomeric hydroxyl group is the nucleophile. Nucleophilic glycosylation does not work on aromatic systems, and is thus not discussed in this dissertation.

Three methods for aromatic glycosylation has been used in this work, i.e. peracetylated carbohydrates and trichloroacetimidate donor, both promoted by acid, and halide sugars promoted by base.

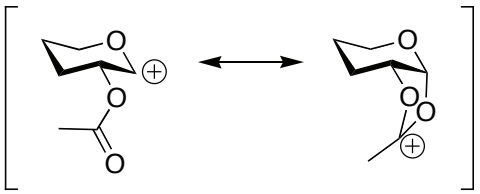

Figure 1.7 Illustration of the participating group.

1.2.1 Glycosyl acetates

Since peracetylated carbohydrates are easily prepared, and in many cases commercially available, the use of glycosyl acetates as donors is often the first method to investigate. A standard procedure is activation with BF_3•OEt_2 in dichloromethane or acetonitrile. There are some drawbacks, such as somewhat lower yields and anomerization to the thermodynamically more stable α-anomer.[12] The yield is also dependent on the nucleophilicity of the phenol, and electron-donating groups on the aromatic ring usually give better yields. Lee et al. demonstrated that sub-equimolar amounts of triethylamine prevented anomerization of the formed product.[13] They showed that the use of 2.5 equivalents of BF_3•OEt_2 with 0.5 equivalents of triethylamine gave high β-selectivity in excellent yields using different phenols. If the amount of base is higher than the amount of acid, the reaction do not proceed.[14]

1.2.2 Glycosyl trichloroacetimidates

Trichloroacetimidate donors usually give better yields compared to reactions using anomeric acetates.[15,16] Normally the reaction is run in dichloromethane and the promoter, usually BF_3•OEt_2 or TMSOTf, is used in sub-stoichiometric amounts. Anomerization is not a problem in this reaction, probably due to the low amount of acid used.

1.2.3 Glycosyl halides

The third method of aromatic glycsosylation is the use of a glycosyl halide, most commonly the bromide, which is more reactive than the chloride and more stable than the iodide. There are different reaction conditions for the aromatic halide, e.g. the use of phase transfer conditions[17] or Koenigs-Knorr conditions with silver salts (e.g. Ag_2O,[18] Ag_2CO_3[19]). The base promoted reaction proceeds via an S_N2 like mechanism, and the stereochemistry is directed by the starting material.

Dihydroxynaphthalenes are highly activated due to the electron donating effect from the hydroxyl groups. This renders the glycosylation intricate and we have thus developed a standard procedure for aromatic glycosylation. The first method to be used is peracetylated glycosyl donor, promoted with BF_3•OEt_2, in dichloromethane with addition of triethylamine, a mild activation method that minimize anomerization. The second choice is

to use the same conditions without triethylamine, a somewhat stronger activation and hence a higher risk for anomerization. The third method is the glycosyl trichloroacetimidate activated by TMSOTf with molecular sieves present. This method gives a strong activation of the donor, but the glycosyl trichloroacetimidates are more complicated to synthesize. As a last resort we turn to halide sugars, that usually give low yields, but the mechanism is completely different and thus, making it a versatile method.

1.3 Proteoglycans and glycosaminoglycans

Xylose, or wood sugar, is widely expressed in plant cells but is unusual in mammalian cells, and has, so far, only been found in the unique position as the linker between protein and glycosaminoglycan (GAG) chains in proteoglycans (PG).

Müller described the first GAG in 1836, when he isolated "chondrin" from cartilage. The first report on the possible existence of chondroitin sulfate (CS) proteoglycan complex came 1889 by Mörner and the name chondroitsäure was introduced. Following the discovery of hyaluronic acid (HA) in 1934, the GAGs were studied in detail and in the past half century a lot of studies of GAG structure, biochemistry and biological functions have been performed.[20,21] GAGs are polydisperse acidic polysaccharides that often are covalently linked to a protein, forming a proteoglycan. The synthesis of GAG starts with formation of a linker tetrasaccharide, β-D-GlcA-(1-3)-β-D-Gal-(1-3)-β-D-Gal-(1-4)-β-D-Xyl, that is the same in all PGs except for keratan sulfate (KS),[22] followed by polymerization and addition of repeating disaccharides. During the polymerization the GAG chains undergo serial modifications including N-deacetylations/N-sulfations, epimerizations, and O-sulfations.

PG core proteins range from 10 kDa to more then 500 kDa and may contain one or more GAG chains covalently linked to the core protein.[23] Practically all mammalian cells produce proteoglycans, that can be secreted to the extracellular matrix, inserted into the plasma membrane or stored in secretory granules.

The four most common GAG chains are; hyaluronic acid (HA), keratan sulfate (KS), chondroitin sulfate (CS)/dermatan sulfate (DS), and heparan sulfate (HS)/heparin. With exception of HA that is not attached to a core protein, the GAGs may be O-linked, (CS/DS and HS/heparin), or N-linked, (KS), to the core protein.

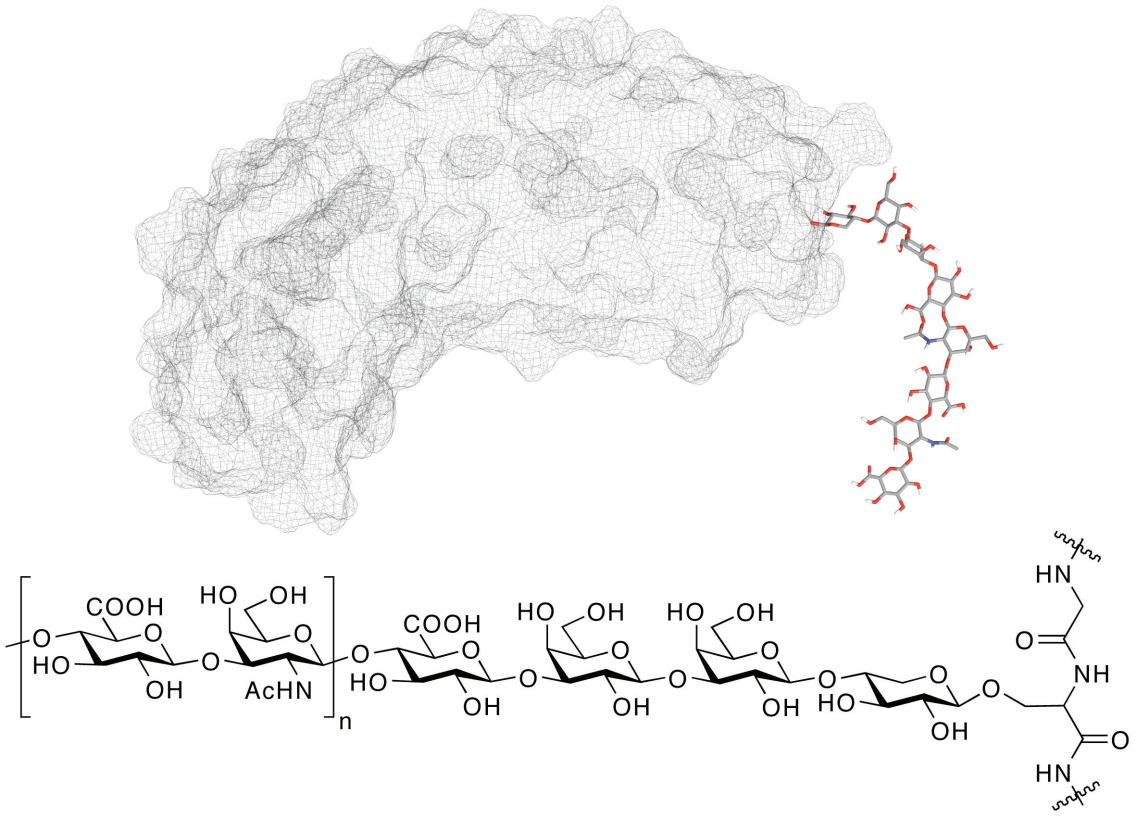

Figure 1.8 The PG decorin[i] with an assembling CS chain. The protein couples the GAG chain on serine-4 and starts with the linker tetrasaccharide (-4)-β-D-GlcA-(1-3)-β-D-Gal-(1-3)-β-D-Gal-(1-4)-β-D-Xyl-(1-).

HA was first isolated in 1934 by Meyer and co-workers from the vitreous of the eye.[27] The repeating disaccharide unit is (-4)β-D-GlcA(1-3)-β-D-GlcNAc-(1-) (Figure 1.9). HA is the only GAG that is not attached to a core protein and has a typical polymer structure containing around 25,000 disaccharide units.[28] The HA is present in virtually all vertebrate tissues and fluids but is most abundant in the skin, which holds 50% of the HA in the body, the vitreous of the eye, skeletal tissue and umbilical cord.[29] HA is highly viscous (about 5000 times that of water) and gives rise to the rigidity of the organ when present in high concentrations, e.g. in rooster combs.

KS is either N-linked or O-linked to the core proteins, where the N-link is to asparagine residues and the O-link is to serine or threonine residues.[30,31] KS is a polylactosamine with the repeating disaccharide unit of (-4)-β-D-Gal-(1-3)-β-D-GlcNAc-(1-) (Figure 1.9), which

[i] The secondary structure of the protein was elucidated in a rough homology model in Prime[24], based on the X-ray structure of decorin's amino acids 22-326.[25,26]

is partially sulfated at position 6.[32,33] KS is found in cornea (hence the name keratin from Greek *keratos*), cartilage, brain and in bone.

The galactosaminoglycans CS/DS are the most abundant GAGs in the body and exist in both skeletal and soft tissue. CS/DS are synthesized by alternating addition of GalNAc and GlcA. GlcA can then be epimerized into IdoA. Thus disaccharide unit for CS consist of (-4)-β-D-GlcA-(1-3)-β-D-GalNAc-(1-) (Figure 1.9) with sulfate on GalNAc position 4 or in position 6. The number of sulfate groups varies from zero to three in the GalNAc unit, and the average size is around 40 disaccharides.[34] DS is built up of the repeating disaccharide unit (-4)-α-L-IdoA-(1-3)-β-D-GalNAc-(1-) (Figure 1.9), with various amounts of sulfates on both monosaccharide units.[35]

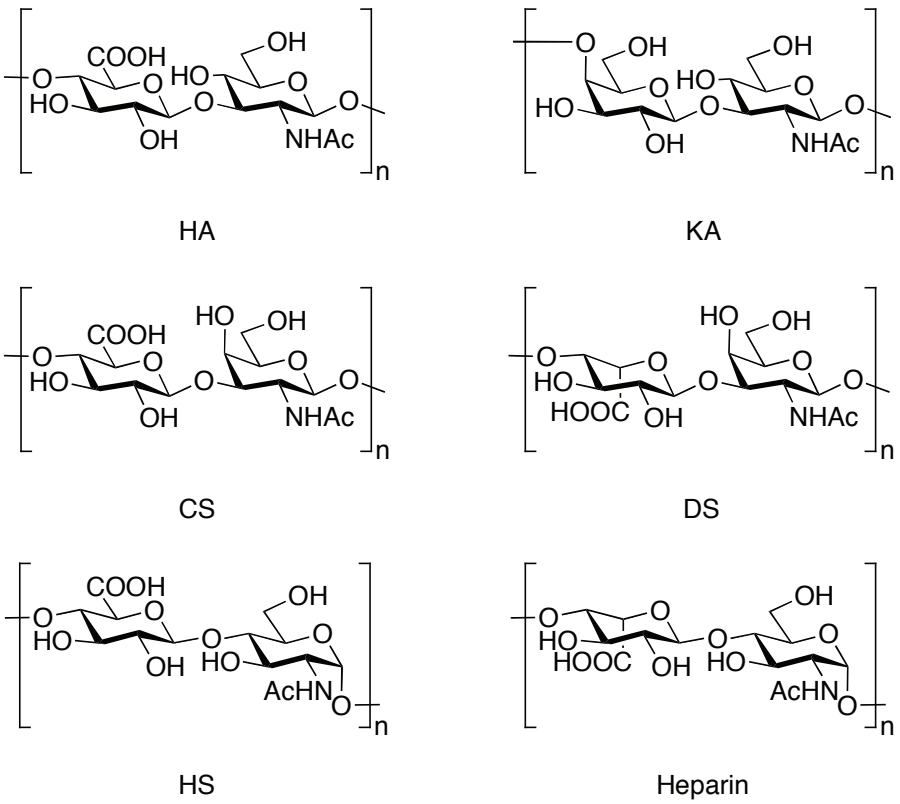

Figure 1.9 The major disaccharide units of the different GAG chains. These are subjected to various degrees of modifications including N-deacetylation/N-sulfation, epimerization, and O-sulfation.

The glucosaminoglycans HS and heparin are linked to the protein by the same linker tetrasaccharide as CS and DS. The common backbone in HS/heparin is build up of the repeating disaccharide (-4)-β-D-GlcA-(1-4)-α-D-GlcNAc-(1-) (Figure 1.9). The amount of modifications of the saccharides, e.g. sulfation and epimerization varies.[36] Heparin is a highly modified and highly sulfated HS. HS is produced in almost all cells whereas heparin is only produced in mast cells.[23] HS is primarily found in the extracellular matrix and in cell membrane whilst heparin is only intracellular.[37] Heparin usually consist of 100-200 disaccharide units.[38]

1.3.1 Applications of proteoglycans and glycosaminoglycans

PG have complex biological functions, mainly due to the presence of GAG chains.[39] PGs are bulk material in cartilage, but they are also involved in numerous cellular processes such as cell growth, adhesion, and migration.[40] Many biological functions arise from the interaction of GAG chains with a variety of molecules and pathogens, such as coagulation factors and other proteases, enzymes and enzyme inhibitors, growth factors, cytokines, polyamines, viruses and prion protein.[41-44]

Heparin has an anticoagulant activity and low molecular heparin has been administered as an anticoagulant for the last 70 years.[45] DS does also have anticoagulant properties, but is not as efficient as heparin.[46] DS binds to collagen thereby influencing the elasticity of the tissue.[47] HA is used as biomaterial and also as supportive material in eye and ear surgeries.

1.3.2 Biosynthesis of proteoglycans

The biosynthesis of the core protein of proteoglycans starts in the rough endoplasmic reticulum, followed by transport via smooth vesicles to the Golgi complex where the glycosylation takes place. After the formation and modification of the GAG chain in the Golgi they are transported by secretory vesicles to the cell surface, where the cell-associated PGs usually reside.[39]

The cell takes up the building blocks in form of monosaccharides and sulfates, that are activated in the cytosol to form UDP-sugars and 3'-phosphoadenosine 5'-phosphosulfate (PAPS)[i]. The UDP-sugars and PAPS are then transported into the endoplasmic reticulum

[i] PAPS is the universal donor of sulfate to all sulfotransferases.

and Golgi lumens. The biosynthesis of the linker tetrasaccharide starts with xylosylation of a serine residue of the PG, followed by two galactose units and then a glucuronic acid. The lumen of the Golgi apparatus is the main site for the GAG synthesis, but the synthesis of the linker tetrasaccharide is probably started earlier in the secretory pathway.[22] The fifth saccharide determines the formation of CS/DS (GalNAc) or HS/heparin (GlcNAc).

It is still unclear what determines the formation of CS/DS or HS/heparin, but a variety of factors affect the distribution. For example a repetitive serine-glycine sequence flanked by a cluster of acidic amino acid residues promote HS formation.[48] Lander and co-workers have also shown that sequences in the protein outside the immediate GAG attachment site (more then 70 amino acids) regulate the formation of CS or HS.[49]

1.4 Exogenous xylosides for biosynthesis

The priming ability, i.e. the ability to start GAG synthesis of different, exogenous xylosides was observed in 1968 by Helting and Rodén. They studied the enzymes involved in the addition of galactose and glucuronic acid to serine-linked xylose (**1**).[50-52] In 1973 Okayama and co-workers made a similar study, but with xylose linked to *p*-nitrophenol.[53] The Okayama group continued their study and tested different aglycon structures, and they also made the first systematic study with alkyl ethers of different length (**2**) and compared thiophenol with phenol.[54] Later reports showed that several aromatic structures, including 4-methyl-umbelliferyl β-D-xylopyranoside, can initiate priming of HS, and also that the α-anomers of phenyl and methyl xyloside were inert.[55] In 1991 Esko and co-workers xylosylated a range of aglycons and showed that xylosylated estradiol (**3**), and some other xylosides carrying an aromatic ring was the only ones that primed HS efficiently.[56] This was further developed into naphthol based xylosides, and it was shown that the fused aromatic system primed HS efficiently (**4**).[57] The Esko group also showed that naphthogalactosides, were poor GAG-primers.[58,59]

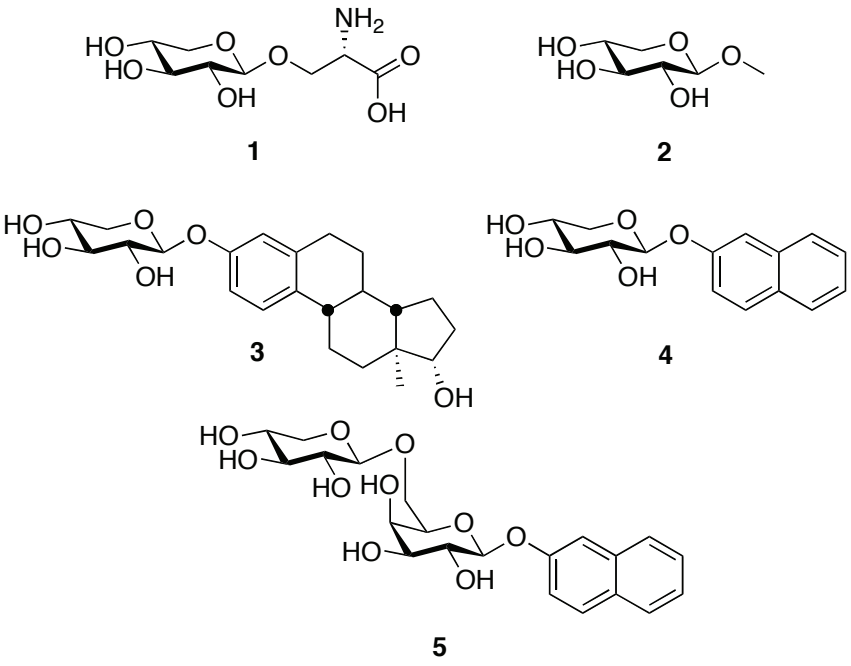

Figure 1.10 Previously studied GAG primers.

In 1998 Mani observed that **6**, the first hydroxynaphthyl xyloside, primed HS and inhibited cell growth in several cell types.[60] It was later shown by the group that this xyloside was active in vivo and reduced tumor load in a SCID mouse model by 70-97%.[61] **6** is considered as a reference compound in the group and new compounds are compared to this molecule.

Ellervik and co-workers then studied the fourteen mono-xylosylated dihydroxynaphthalenes and it was shown that the antiproliferative activity varied depending on the aglycon structure.[62,63] The response to the xylosides was relative slow indicating that it could be a biotransformation of the xyloside to get the bioactivity. It was also shown that **6** induce apoptotic cell death in human bladder carcinoma (T24) cells.

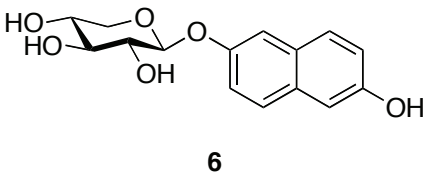

Figure 1.11 Compound **6**, our reference compound.

Ellervik and co-workers have also evaluated a carbon-analog to **4**, that did not initiate GAG synthesis to a large extent (**7**).[64] Later studies in the group involved thio-analogs, which gave no selective antiproliferative effect, but primed GAG chains efficiently (**8**).[65] Another recent study involves synergistic effects of an acetylated disaccharide (**9**) and acetylated **6**. Together with α-difluoromethylornithine and spermine NONOate, a lower dose of the xyloside still gives an antiproliferative activity.[66]

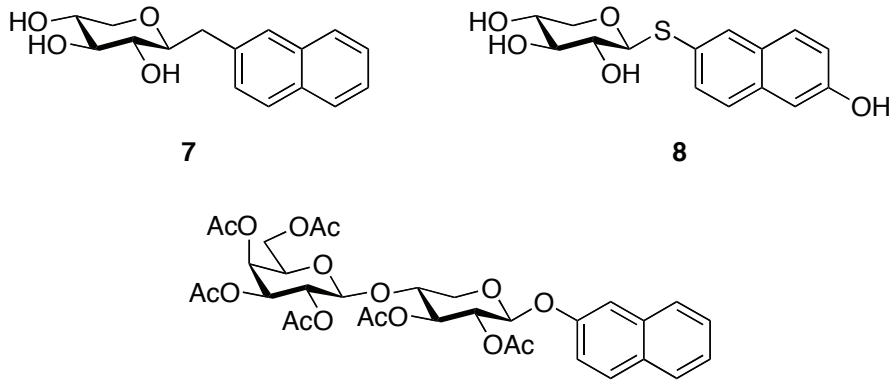

Figure 1.12 Some of the GAG primers synthesized by the Ellervik group.

2 BIS-XYLOSIDES

2.1 Synthesis of bis-xylosides

As previously reported by our group, 14 mono-xylosylated dihydroxynaphthalenes have been synthesized and evaluated for their biological action.[62,63] As it turned out 1-(4-hydroxy)-β-D-xylopyranoside and 2-(1-hydroxy)-β-D-xylopyranoside in particular, but also 1-(3-hydroxy)-β-D-xylopyranoside and 7-(1-hydroxy)-β-D-xylopyranoside were degraded in the medium used for the cell experiments. This is probably due to activation of the free hydroxyl group, since a poly-hydroxylated compound was isolated from the stability study. To minimize degradation, and to investigate if it is possible to induce bidirectional priming, we initiated a study of bis-xylosides.

2.1.1 Bis-xyloside synthesis with glycosyl acetate

As described previously the glycosylation of dihydroxynaphthalenes can be difficult due to the highly activated aromatic system. Other circumstances that can render problems are steric hindrance as well as internal hydrogen bonding. At first we attempted to perform xylosylations using peracetylated xylose in dichloromethane activated by $BF_3 \bullet OEt_2$ and with NEt_3 added to suppress anomerization.[13] This gave bis-xylosylated 2,6-dihydroxynaphthalene (**24**), 2,7-dihydroxynaphthalene (**25**), 1,6-dihydroxynaphthalene (**28**) and 1,7-dihydroxynaphthalene (**29**) in excellent yields of 81-96%. However, bis-xylosylated 1,4-dihydroxynaphthalene (**20**), 1,5-dihydroxynaphthalene (**21**) and 1,3-dihydroxynaphthalene (**27**) gave only 22-64% yield, with some mono-xylosylated product as well. More interestingly, bis-xylosylated 1,8-dihydroxynaphthalene (**22**), 2,3-dihydroxynaphthalene (**23**) and 1,2-dihydroxynaphthalene (**26**) could not be

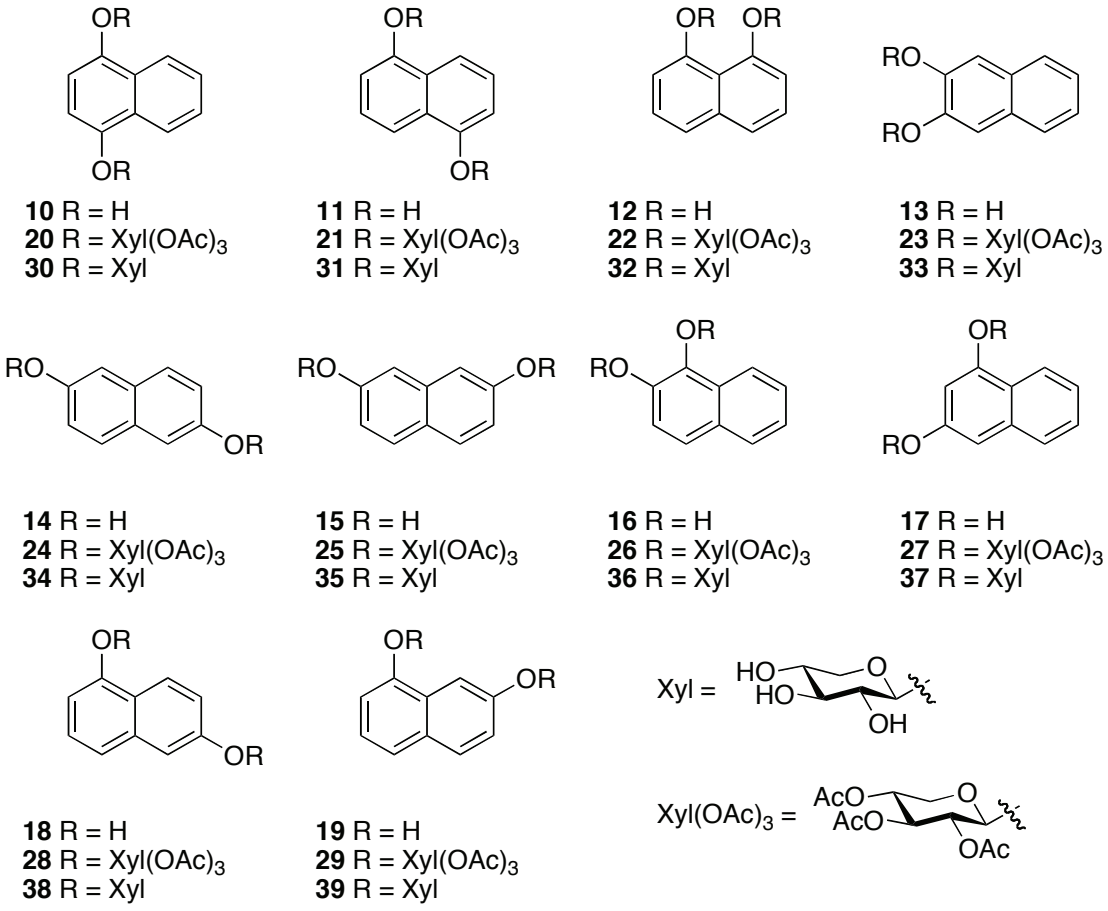

Chart 2.1 Dihydroxynaphthalenes (**10**-**19**), and the bis-xylosylated analogous (**20**-**39**).

synthesized at all under these conditions. In the synthesis of **26** small amounts of mono-xylosylated product was isolated, but in the synthesis of **22** and **23** only degradation of starting material was observed.

To glycosylate the three unreactive dihydroxynaphthalenes, we turned to the trichloroacetimidate donor in dichloromethane with TMSOTf as promoter and molecular sieves present.[67-69] The trichloroacetimidate donor is known to be a more activated donor compared to the corresponding acetate and hence more suitable for the less reactive phenols.

2.1.2 Selective deacetylation

The synthesis of trichloroacetimidate donors are frequently performed using the corresponding anomerically deprotected carbohydrate. This hemiacetal can be synthesized from, for example, the corresponding thioglycoside or an anomeric acetate. Since peracetylated xylose was available, anomeric deacetylation was of interest. The most

common reagent is hydrazine acetate, which unfortunally is severely toxic.[70] Other methods involve heavy metal salts, such as bis(tribulyltin) oxide,[71] tributyltin methoxide[72,73] or mercury salts (mercuric chloride/mercuric oxide[74]). More environmentally friendly alternatives are also available, such as benzylamine[75] or sodium methoxide[76] as summarized in Table 2.1.

Table 2.1 Methods of anomeric deacetylation.

Entry	Reagent	Yield (β-glucose)	Best yield	Reference
1	NH_2NHAc	92%	96% (α-cellobiose)	70
2	$(Bu_3Sn)_2O$	93%	93% (β-glucose)	71
3	Bu_3SnOMe	70%	80% (β-galactose)	72,73
4	$HgCl_2/HgO$	70%	74% (β-ribose)	74
5	$BnNH_2$	91%	91% (β-glucose)	75
6	NaOMe	82%	90% (α-galactose)	76
7	KCN	97%	99% (β-mannose)	71
8	KOH	93%	99% (β-mannose)	71
9	NH_3	100%	100% (β-glucose)	77
10	NH_4CO_3	87%	95% (α-mannose)	78
11	Piperidine	-[a]	81% (β-cellobiose)	79
12	MgO	-[a]	89% (4,6-benzyliden-α,β-glucosamine)	80
13	$H_2N(CH_2)_2NH_2$	92%	>95% (β-galactose[b])	81

a) Not tested on β-glucose, b) Same result for β-xylose, α-mannose and α-cellobiose.

As can be seen from Table 2.1, most methods give reasonable to excellent yields but they involve drawbacks such as the use of hazardous substances, time-consuming purification steps and low selectivity due to very short reaction times. Since our group previously has been using the benzylamine method (entry 5, Table 2.1) with good results, we decided to investigate solid supported benzylamine. Benzylamine resin is inexpensive and can be filtered off the reaction without any additional purification steps. At first we tested a range

of solvents, using the conversion of peracetylated glucose (**40**) into 1-O-deacetylated glucose (**41**) (Scheme 2.1).

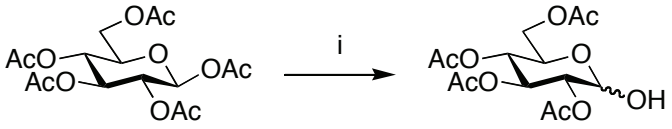

40 **41**

Scheme 2.1 Anomeric deacetylation of glucose. i) aminomethylated polystyrene, solvent (Table 2.2), 2 days.

The reactions were run at room temperature for two days, filtered and concentrated and the conversions were measured by NMR. The conversion was highest in DMF followed by THF. The conversions were good in ethanol and diethyl ether and acceptable in ethyl acetate, toluene and dioxane. The slowest conversions were found in dichloromethane and acetonitrile (Table 2.2). A polystyrene resin swell in some solvents that makes the functional group more available. However, no correlation between the solvents ability to swell the resin and the conversion in the reaction could be observed, e.g. DMF and dichloromethane swell the resin but ethanol and acetonitrile do not.

Table 2.2 Conversion of **40** to **41**.

Solvent	**Conversion (%)**[a]
DMF	79
THF	76
EtOH	70
Et_2O	67
EtOAc	55
Toluene	51
Dioxane	47
CH_2Cl_2	22
MeCN	4

a) Estimated by NMR after 2 days at room temperature.

Since the method should be easy, the decision fell on THF, which can easily be removed (compared to DMF). However, the conversion was only 76% after two days reaction, which was less than perfect. The reaction was thus tested in a sealed tube and at 75 °C, the conversion was raised to 78%. We reasoned that the incomplete reaction might be a result of poor diffusion due to charge build-up on the resin. To overcome this problem, three equivalents of triethylamine were added, giving a conversion of 96% after 18 h. With a working protocol for the 1-O-deacetylation, a range of monosaccharides were subjected to these conditions, which gave the deprotected products in 90-96% yield (Table 2.3). The reaction conditions were also tested on β-lactose, which only gave 67% conversion, but by prolonging the reaction time to 44 hours, the conversion increased to 88% (Table 2.3).

Table 2.3 Anomeric deacetylation of peracetylated carbohydrates.

Entry	Starting material	Conversion (%)[a]	α/β
1	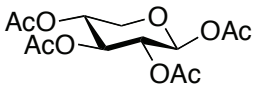	96	5:3
2	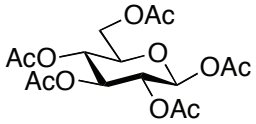	96	3:1
3	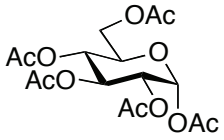	96	2:1
4	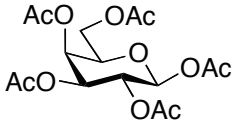	90	5:2
5	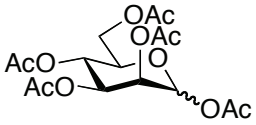	95	1:0
6	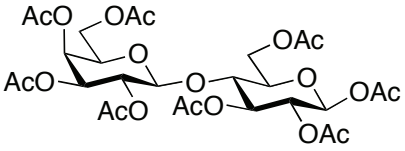	88	4:3

a) The reaction times were 18 h (entry 6: 44 h) and the conversions were estimated by NMR.

To verify the usefulness of the method, peracetylated glucose was deacetylated using polymer bound benzylamine and then converted to the corresponding trichloroacetimidate without any purification of the hemiacetal (Scheme 2.2). This reaction gave 2,3,4,6-tetra-*O*-acetyl-D-glucopyranosyl trichloroacetimidate (**42**) in 85% yield, a yield that is similar to other reported syntheses from the hemiacetal.[82,83]

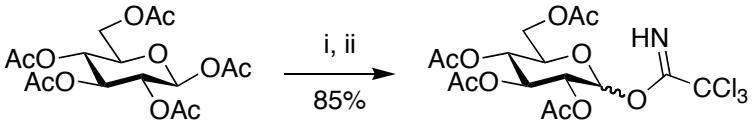

40 **42**

Scheme 2.2 Synthesis of **42** from **40**. i) aminomethylated polystyrene, NEt_3, THF; ii) Cl_3CCN, DBU, CH_2Cl_2.

2.1.3 Bis-xyloside synthesis with other donors

Using the trichloroacetimidate donor, **23** was synthesized in 58% and **26** in 33%. However, 1,8-dihydroxynaphthalene (**12**) was still inert. The reason that makes **12** so unreactive is probably the internal hydrogen bond between the hydroxyl groups. This makes the compound less nucleophilic and with a pK_a as low as 6.71, it is less prone to react in acid-mediated glycosylation.[84] Instead, a basic method was tested, starting with xylosyl bromide. At first the reaction was performed under Koenigs-Knorr conditions with Ag_2O, using quinoline as solvent. This was however not a good method and only degradation was observed. Some other solvents (acetonitrile, DMF, dichloromethane) were also tested but none of these gave any product. Instead, we turned to phase-transfer conditions with aqueous NaOH in dichloromethane and tetrabutylammonium bromide as phase-transfer catalyst.[15] These reaction conditions gave **22** in a low but, after all, acceptable 13% yield.

The acetylated bis-xylosides were then deacetylated in methanolic NaOMe. Problems emerged when the deprotected products should be chromatographed. The highly symmetric **30**, **31** and **34** were too crystalline to be chromatographed under normal phase conditions and they were virtually insoluble in anything, except DMSO. These compounds were instead purified using reverse phase HPLC.

2.2 Computational chemistry on dihydroxynaphthalenes

The electrostatic potentials of the ten dihydroxynaphthalenes (**10**-**19**) were calculated using density functional theory at the B3LYP/6-31G* level.[85] From the minimized structures, the distances between the two oxygen atoms were measured (Table 2.4).

The electrostatic potential can be seen as a way to measure the nucleophilicity of the compounds, i.e. a lower electrostatic potential means a higher nucleophilicity. In some cases, e.g. 1,8-dihydroxynaphthalene (**12**) the difference in potential of the two oxygen atoms are large (-152.7 and -44.8 kJ/mol) indicating an internal hydrogen bond. Since our attention was on the bis-xylosylation, the average electrostatic potentials were plotted versus the yields of bis-xylosylation with peracetylated xylose (Figure 2.1). As can be seen from Figure 2.1, the yields correlate well with the electrostatic potential.

Table 2.4 Average electrostatic potential of dihydroxynaphthalenes and the distances between the two oxygen atoms.

Compound	Average electrostatic potential (kJ/mol)	Distance between oxygen atoms (nm)
10	-126.9	0.56
11	-117.2	0.60
12	-98.7	0.26
13	-96.7	0.27
14	-133.9	0.78
15	-129.3	0.73
16	-99.2	0.27
17	-115.1	0.48
18	-125.1	0.63
19	-118.8	0.51

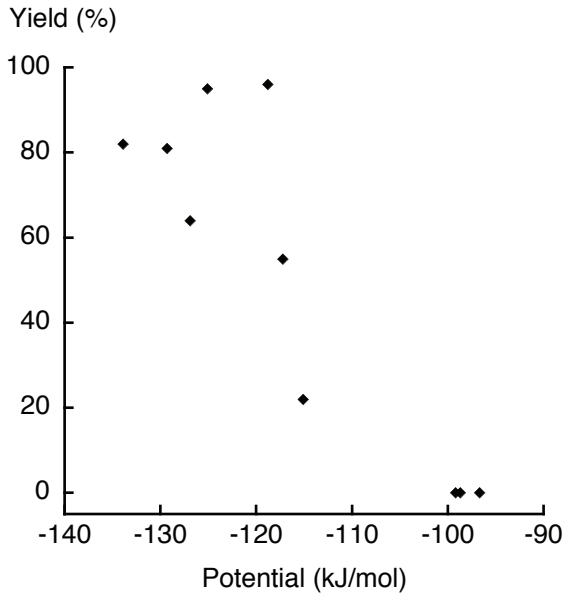

Figure 2.1 Yield of glycosylation versus electrostatic potential of dihydroxynaphthalenes.

However there are more factors affecting the yield of the bis-xylosylation that makes this correlation less accurate. For example some portions of mono-xylosylated product was isolated indicated that there are steric factors involved in the reaction. Interestingly, the distances between the two oxygen atoms was to some extent correlated to the polarity of the compounds, measured by HPLC retention time.

2.3 Biology of bis-xylosides

Initially, the stabilities of the bis-xylosylated dihydroxynaphthalenes were tested. The bis-xylosylated dihydroxynaphthalenes were thus subjected to the same conditions as for the growth assay, i.e. 0.2 mM in Ham's F-12 medium[i] incubated at 37 °C. Samples were analyzed with HPLC and no degradation of xyloside was observed within 96 hours, compared to the previous results with complete degradation of two of the fourteen mono-xylosylated dihydroxynaphthalenes in less than 70 hours.[63] The addition of the second xylose residue apparently gives a shielding effect that inhibits oxidation and degradation of the naphthoxyloside.

The priming of the bis-xylosylated compounds were tested on T24 cells. The cells were treated with the xylosides and [^{35}S]-sulfate, which makes it possible to detect the sulfated

[i] Ham F-12 medium contains a mixture of glucose with inorganic salts, amino acids, vitamins and some other additivs, i.e. a perfect medium for cell growth.

GAG chains.[86,87] All cells secreted proteoglycans, and some also initiated synthesis of free GAG chains. All of the bis-xylosylated compounds seemed to initiate priming to a lower extent than the mono-xylosylated compounds tested, except for **31** and **34**, which showed a slightly higher priming. After priming of GAG chains, size-exclusion chromatography was performed to separate proteoglycans from free GAG chains. In the separation of the GAG chains initiated by the bis-xylosylated naphthoxylosides, it was seen that the GAG chains were bigger compared to those isolated from the corresponding mono-xylosylated compounds. The size variation could depend either on the priming of longer chains or, bidirectional priming. To test this, three bis-xylosides (**31**, **34** and **38**) were, after GAG priming, subjected to oxidative reaction conditions that selectively cleave the xylose structure. The size exclusion chromatography was repeated, and shorter chains, similar to the ones isolated from mono-xylosylated compounds, were isolated. These results verify bidirectional priming (Figure 2.2).

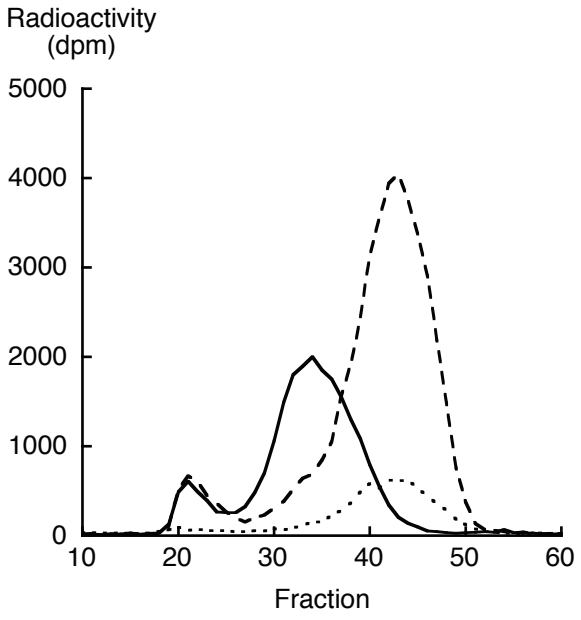

Figure 2.2 Priming of GAG chains in T24 cells incubated with **34** (solid line) compared to **6** (dashed line). The dotted line represents oxidatively cleaved GAG chains primed by **34**.

The antiproliferative properties of the bis-xylosylated dihydroxynaphthalenes were also investigated. Although several of the mono-xylosylated dihydroxynaphthalenes show antiproliferative properties, down to 25 μM, none of the tested bis-xylosylated compounds showed any strong growth inhibition. The reason for the lack of antiproliferative activity can be several-fold. For example it has been shown that priming of HS is required, but

insufficient for antiproliferative activity. The structure of the aglycon may give a different composition of the GAG chains and this may endow them with different possibilities to enter the cell nuclei and exert antiproliferative activity. The compounds could also be too big or too polar to be transported to the correct compartment of the cell for antiproliferative activity.[i] Another reason could be the stability of the bis-xylosides. It is well known that polyhydroxylated naphthalenes such as juglone, are toxic due to the redox cycling between semiquinone and quinone.[88-90] The reason for the lack of antiproliferative activity can thus be related to the lack of the free hydroxyl group, which inhibits oxidation and hence the antiproliferative effect.

[i] See section 4.4 for a discussion regarding the impact of molecular size and lipophilicity on GAG priming.

3 OBJECTIVES

The antiproliferative effect of **6** is known and studied by the group. However the underlying mechanisms for this antiproliferative effect is not known and the objectives for this dissertation is to gain more knowledge in order to design more selective and effective anti-cancer drugs. The tools for this is fluorescently and radioactively labeled analogs to **6** and this dissertation is focused on various aspects of these topics.

4 FLUORESCENT LABELING

4.1 Background

Fluorescent molecules are used as probes to investigate chemical and biological systems. Fluorescent probes can give important information, such as visualization of membranes and proteins in living cells or helix structures in nucleic acids.[91]

There are three different kinds of fluorescent probes, i) intrinsic, ii) extrinsic covalently bound and iii) extrinsic associated. Intrinsic probes, i.e. naturally occurring probes such as tryptophan, are preferable but rare. Extrinsic covalently bound probes are usually better than the associated ones, since the location of the probe is known.

The choice of fluorescent probe is based on a variety of requirements, e.g. emission wavelength, coupling method and polarity. There are fluorescent groups available with emission from UV to near IR. The emission wavelength, is dependant on several factors such as solvent, polarity and temperature.

Common organic fluorescent probes are anthracene (**43**) (blue emission, 401 nm), dansyl chloride (**44**) (blue emission, 492 nm) and fluorescein (**45**) (green emission, 514 nm). Example of other probes are; nile red (**46**) with a red emission spectra (635 nm) and NIR 4f (**47**)[i] that have an emission in the near IR region (822 nm).

[i] NIR 4f, 1,1'-Bis(3-isothiocyanatopropyl)-11-chloro-3,3,3',3'-tetramethyl-10,12-trimethylenindotricarbocyanine bromide

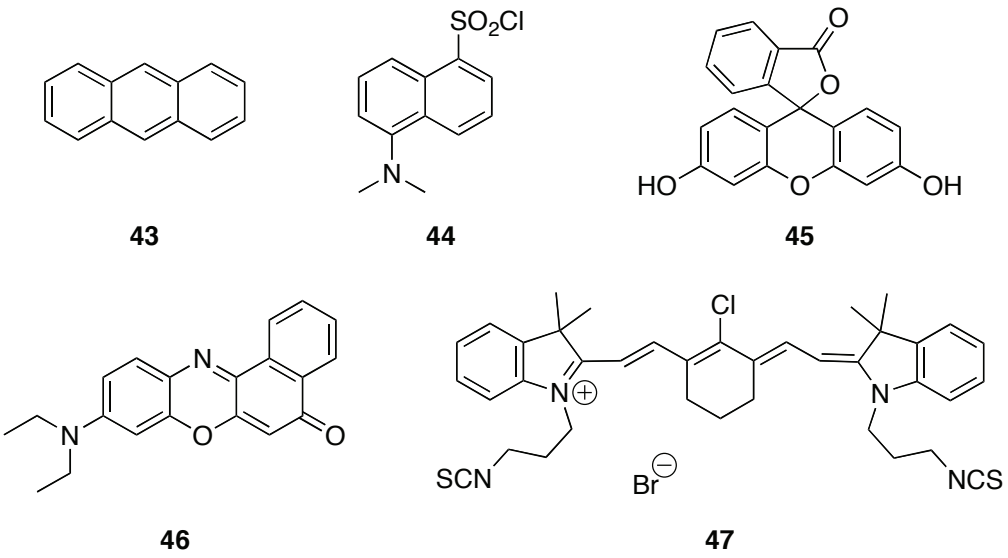

Figure 4.1 Different fluorescent probes.

The most apparent way to introduce a fluorescent probe in our active molecule, (**6**) is to substitute the naphthalene part for anthracene (Figure 4.2). This way, the fluorescently labeled compound would not differ much from the evaluated molecule. The synthesis of **48** has been performed by Ellervik et al. but absorbance/fluorescence analysis indicated that the compound was unstable and another way to introduce the fluorescent probe had to be designed.

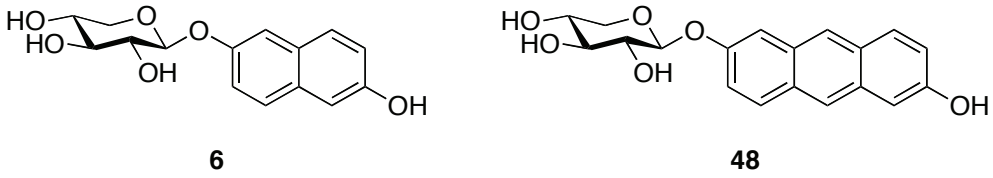

Figure 4.2 Fluorescent analog **48** to **6**.

4.2 First generation fluorescent xylosides

4.2.1 Synthesis of first generation

Ellervik et al. has previously introduced 9-anthraldehyde as a fluorescent protecting group for carbohydrates (Scheme 4.1).[92] The protecting group is an O-4/O-6 acetal that can be regioselectively opened using a range of reagents.[i] The anthracene moiety was thus decided

[i] A more detailed discussion regarding reductive opening of acetals is found in chapter 6.

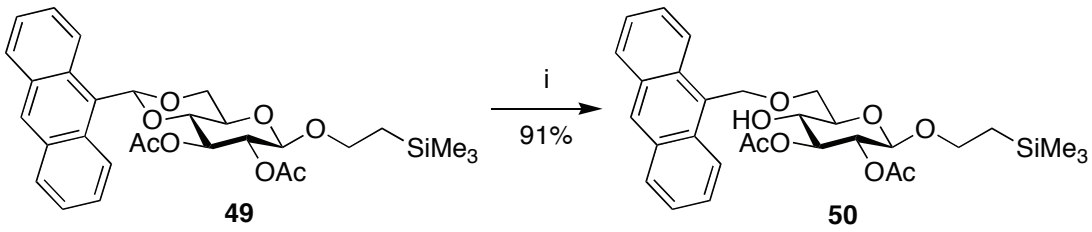

Scheme 4.1 Anthracenylidene acetal. i) $NaCNBH_3$, HCl/Et_2O, THF, 2 h.

to be used as fluorescent probe and the 9-antraldehyde dimethylacetal was selected to be a good way to introduce the fluorescent probe.

Since the knowledge of benzylic-phenolic acetals is scarce and the conditions for the regioselective opening were not known, a model system was synthesized (Scheme 4.2). Salicylic alcohol was thus coupled with the 9-anthraldehyde dimethylacetal under acid conditions to give **52** in 78% yield.[92]

Acetals can be opened with $NaCNBH_3$/HCl/THF, the reagent combination used for **49**, a method referred to as Garegg-opening.[93] This is one of the most common conditions for regioselective openings to give the 6-O protected carbohydrate. However, in our case this only gave degradation of **52** and no product could be isolated. Apparently these mixed benzylic-phenolic acetals are more sensitive to hydrolysis compared to the corresponding protected carbohydrates. Instead we used BH_3•$NMe_3/AlCl_3$, another well known reagent in carbohydrate chemistry for the regioselective opening of benzylidene acetals. With this reagent, the regioselectivity depends on the solvent; i.e. when it is used in combination with THF the product is the 6-O protected carbohydrate, while reaction in toluene, gives the 4-O protected carbohydrate (Scheme 4.3).[94]

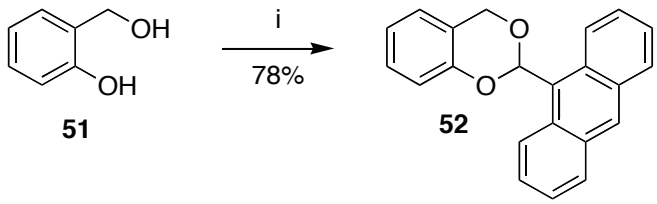

Scheme 4.2 Synthesis of model system. i) anthraldehyde dimethyl acetal, *p*TSA, MeCN, 2 h.

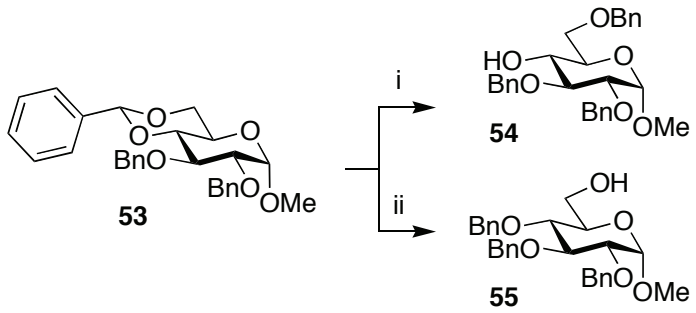

Scheme 4.3 Opening of benzylidene acetals with BH_3•NMe_3, $AlCl_3$ with i) THF or ii) toluene as solvent.

When the model compound **52** was subjected to the conditions in THF it opened to give the free phenol (**56**) in 83% yield. However, when **52** was subjected to the toluene conditions only degradation was observed.[i]

The first step in the synthesis was to make the 2,6-dihydroxy-3-(hydroxymethyl)-naphthalene (**58**) from commercially available 3,7-dihydroxy-2-naphthoic acid (**57**). At first the reduction was tested using $NaBH_4$ and I_2 in THF, a system previously used on the similar compound 3-hydroxy-2-naphthoic acid, which was reduced in 60% yield.[95] However, this method gave only small amounts of impure product in our system.

BH_3•THF was thus tested as reducing agent to give **58** in 58% yield.[96] The triol was then treated with 9-anthraldehyde dimethyl acetal, in acidic acetonitrile to give the acetal protected naphthol **59** in 76% yield. Since the acetal is acid labile, and prone to hydrolysis as observed above, the glycosylation was performed using the trichloroacetimidate donor.

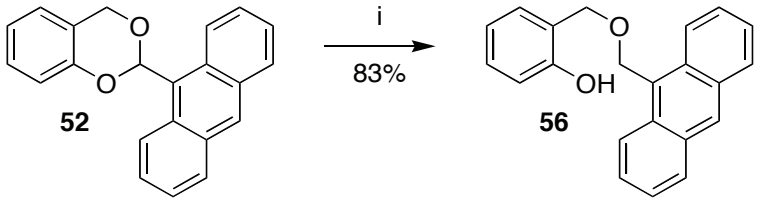

Scheme 4.4 The synthesis of **56**. i) BH_3•NMe_3, $AlCl_3$, THF, 0 °C, 3 h.

[i] This is an interesting observation and the regioselective opening of acetals are discussed in more detail in chapter 6.

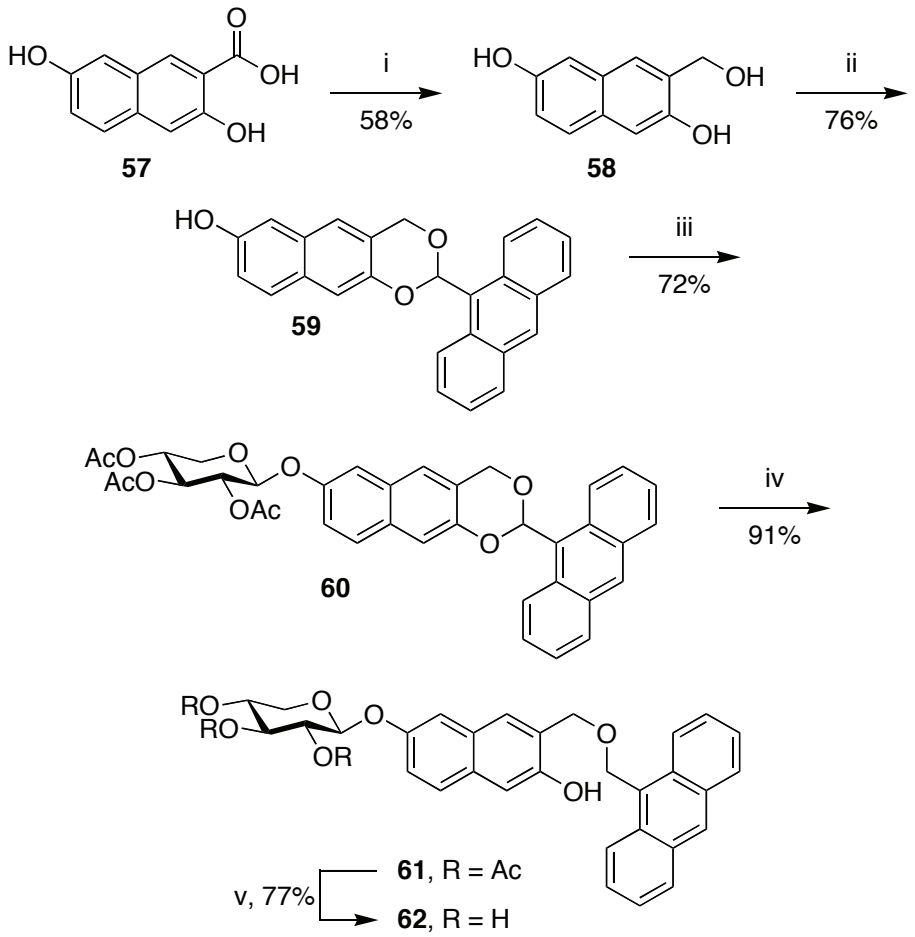

Scheme 4.5 The synthesis of fluorescent probe **62**. i) BH_3•THF, THF, 0-60 °C, 3.5 h; ii) anthraldehyde dimethyl acetal, *p*TSA, MeCN, 1 h; iii) 2,3,4-tri-*O*-acetyl-D-xylopyranosyl trichloroacetimidate, TMSOTf, MS 300AW, CH_2Cl_2, 3 h; iv) BH_3•NMe_3, $AlCl_3$, THF, 0 °C, 45 min; v) guanidine-guanidinium nitrate, 30 min.

The glycosylation was performed in dichloromethane with TMSOTf as promoter and molecular sieves present to give **60** in 72% yield.[67,69,97] The same reductive opening conditions as for **52**, were used on **60** to give **61** in 91% yield. The last step in the synthesis was deprotection of the three acetates. Deacetylation using standard Zemplén conditions (0.05 M NaOMe/MeOH), gave a low yield and instead guanidine/guanidinium nitrate, a less basic method, was used, which gave the final product **62** in 77% yield.[98]

4.2.2 Physical properties of first generation

Log *P*, is the measurement of the partitioning of a substance between two immiscible liquids, usually octanol and water, and is an expression of the lipophilicity. Log *P* measurements require substantial amounts of material and are time consuming to perform. Fortunately, it has been shown that both log *P* values and gradient HPLC retention times

can be treated as linear free-energy relationships.[99] Thus, the retention time can be calculated to a log *P* value, and for a series of similar compounds, the retention time itself can be used to estimate the lipophilicity.

The retention time for **62** was measured using a C-18 column and a mobile phase of water with a gradient of acetonitrile. The retention times were measured three times and the standard deviations were calculated.(Table 4.1).

Table 4.1 Gradient HPLC retention times and p*K*a for **6** and **62**.

Compound	Retention time	pK_a
6	17.73 ± 0.03	9.63 ± 0.02
62	43.40 ± 0.02	10.52 ± 0.09

The pKa of phenolic compounds are usually difficult to determine by computational methods, but they are easily measured using spectroscopic methods.[100] The *p*K$_a$ for **62** was thus measured using UV-spectroscopy at p*H* 9, 10 and 11 and the result can be seen in Table 4.1. The absorbance spectrum and fluorescent spectrum were also determined (Figure 4.3). Unfortunately, **62** was almost insoluble in water and instead the absorbance and fluorescent spectra were measured in acetonitrile.

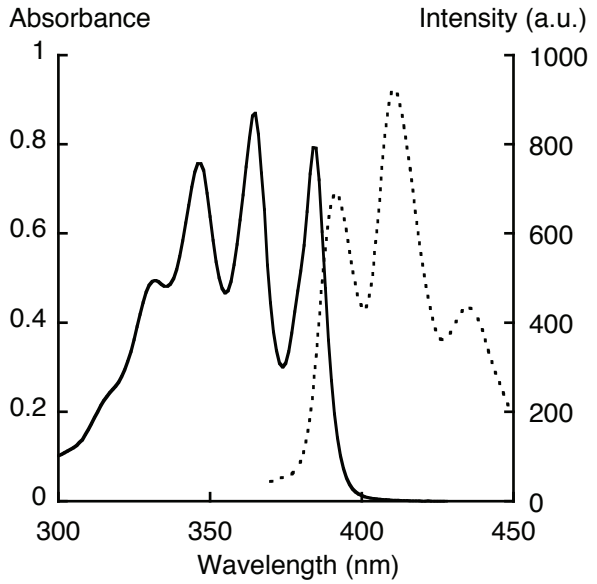

Figure 4.3 Absorbance spectrum of compound **62** (1.15 mM in MeCN, solid line) and fluorescence spectrum of compound **62** (1.15 mM in MeCN, λ_{EX} = 350 nm, dotted line).

4.2.3 Biology of first generation

Since compound **62** is highly lipophilic and uncharged it has the features to penetrate cell membranes and initiate GAG synthesis. By the initiation of GAG synthesis, various cellular processes can be affected. The fluorescent analog **62** was thus tested for uptake, antiproliferative activity and GAG priming in different cell lines.

The antiproliferative activity was tested on three cell lines; mouse 3T3 fibroblast (3T3 A31), virus transformed mouse 3T3 fibroblast (3T3 SV40) and T24. The cells were treated with **62** at different concentrations, 0.010, 0.025, 0.050, 0.100, 0.200 and 0.500 mM for 96 h. The proliferation was then compared to untreated cells using the crystal violet method.[101] All three cell lines were growth inhibited by **62** in a dose dependent manner. At the concentration 0.100 and 0.200 the transformed T24 and 3T3 SV40 cells were growth inhibited to a larger extent than in normal 3T3 A31 cells.

To evaluate if the growth inhibition was correlated to the uptake of **62**, the cells were treated with 0.100 mM **62** for 16 h, and then fixed and studied using fluorescence microscopy. All used cell lines took up the xyloside. In 3T3 A31 and 3T3 SV40 cells **62** was located largely inside the cytoplasm whereas in T24 cells it was accumulated in para- and peri-nuclear compartments.

The GAG priming ability of **62** was studied on 3T3 A31 cells. After priming, the GAG chains were separated from proteoglycans using size-exclusion chromatography. The 3T3 A31 cells secreted proteoglycans but also a very small amount of free xyloside primed GAG chains to the medium.[87,86] The HS proportion was determined to 4% by chemical depolymerisation of HS by nitrous acid.[102] In the cells, no xyloside primed GAG chains were isolated.

4.2.4 Summary of first generation

The fluorescent naphthoxyloside **62** was a poor structural analog to **6**, and no insight into the cellular mechanism could be deduced. The compound was too lipophilic as could be seen from the HPLC retention time, and it was probably also too big (75% higher molar mass).

4.3 Second generation fluorescent xylosides

4.3.1 Synthesis of second generation

Since **62** did not function as a good fluorescent analog, a new analog had to be designed. We therefore turned to the dansyl group, a probe with two aromatic rings, a sulfonyl group and a dimethyl amino group that will increase the hydrophilicity. The group is commercially available as the sulfonyl chloride, which easily can be coupled to a hydroxyl group, e.g. the phenolic oxygen of **6**. Another option was the possibility to couple to **58** but in that case there would be some time consuming protective group chemistry, since the aliphatic alcohol is not as reactive towards the sulfonyl chloride. It would also be possible to start with 2,3,6-trihydroxynaphthalene and couple position 3 to the dansyl group. In this case there will also be some time consuming and difficult protecting group chemistry. The most attractive option was therefore to couple the dansyl group directly to the 6-hydroxyl group of **6**. The phenolic group is necessary for the antiproliferative activity of the compound but not for the GAG priming ability.

The key intermediate in this synthesis is compound **63** with a free phenolic hydroxyl but a fully protected carbohydrate.

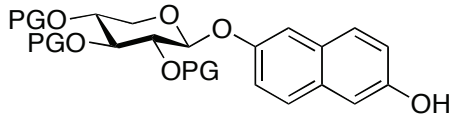

63

Figure 4.4 Key intermediate in the synthesis of second generation labeled xyloside.

If the use of protecting groups can be avoided, the synthetic route can often be shortened. At first 2,6-dihydroxynaphyhalene was xylosylated using BF_3•OEt_2 as acid. This gave a mixture of bis-xylosylated, mono-xylosylated and unreacted naphthol and this simple method was discarded. The next step was to use a mono-protected naphthol and 6-methoxy-2-naphthol was glycosylated to give **65** in 46% yield. However, deprotection using BBr_3 in dichloromethane gave impure **70** in a low yield. Since the deprotection did not work well, another mono-protected dihydroxynaphthalene was tested, 6-benzyloxy-2-naphthol (**66**). **66** was thus glycosylated to give **67** in 58% yield. The subsequent removal of the benzyl group by hydrogenolysis, using Pd/C in ethanol/ethyl acetate 1:1 at

atmospheric pressure failed. Increasing the hydrogen pressure to 500 psi quenched all chromophores, according to TLC analysis, and this synthetic route was abandoned. Instead of optimizing the deprotection of the methoxy ether and benzyl ether, we turned to selective removal of the aromatic acetate in the presence of aliphatic acetates.

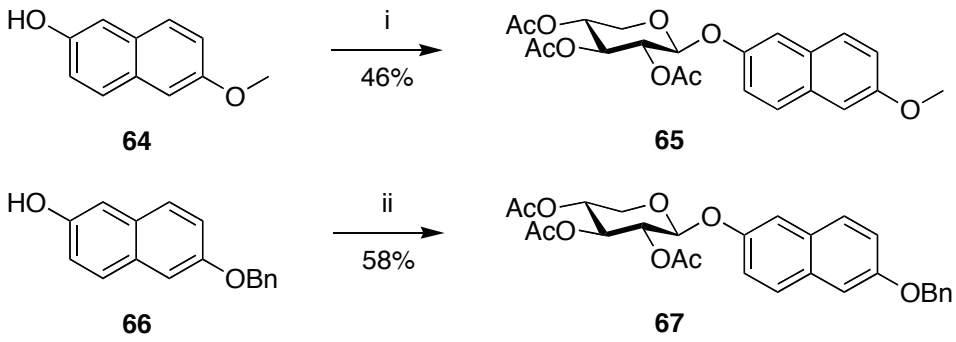

Scheme 4.6: Glycosylations. i) 1,2,3,4-tetra-*O*-acetyl-β-D-xylopyranose, BF_3•OEt_2, NEt_3, CH_2Cl_2, 3 h; ii) 1,2,3,4-tetra-*O*-acetyl-β-D-xylopyranose, BF_3•OEt_2, NEt_3, CH_2Cl_2, 1 h.

6-Acetoxy-2-naphtol (**68**) was glycosylated with peracetylated xylose in the presence of BF_3•OEt_2 and a catalytic amount of NEt_3 to suppress anomerization, which gave **69** in 81% yield.[13] Next, the aromatic acetate was selectively removed in the presence of aliphatic acetates. At first guanidine was tested, a method that is selective to aromatic acetates over primary and secondary aliphatic acetates.[103] The method can also be used for deacetylation of carbohydrates and the selectivity is deduced from the amount of guanidine used. When **69** was subjected to these conditions, only fully deacetylated product was isolated.

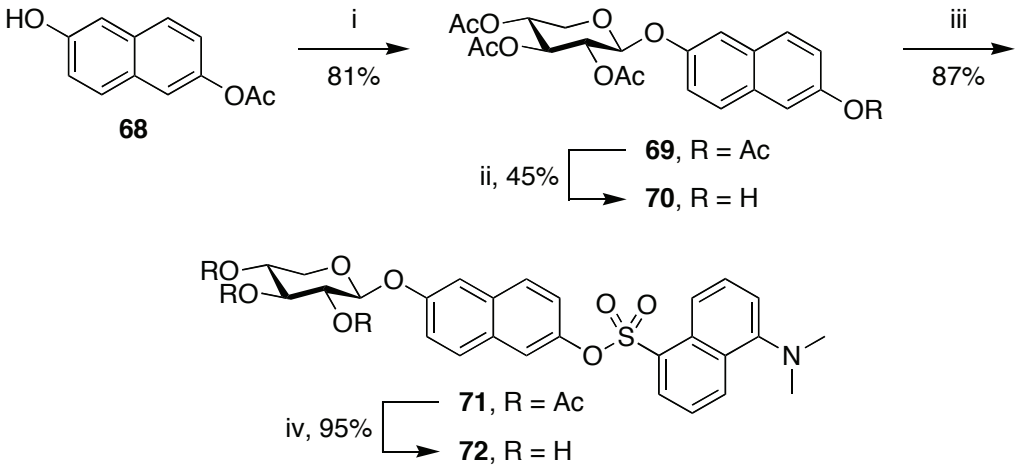

Scheme 4.7: Synthesis of fluorescent analog **72**. i) 1,2,3,4-tetra-*O*-acetyl-β-D-xylopyranose, BF_3•OEt_2, NEt_3, CH_2Cl_2, 2.25 h; ii) KCN, MeOH, 0 °C, r.t., 1.7 h; iii) dansyl chloride, NEt_3, CH_2Cl_2, 1.5 h; MeOH/NaOMe, 30 min.

The aromatic acetate is more easily cleaved due to the more stable anion formed in the reaction. Thus, a stoiciometric amount of base would only cleave the aromatic acetate, and different bases were tested in mixtures of dioxane and water. NaOH gave 0-27% product with poor reproducibility. LiOH gave approximately the same result and K_2CO_3 gave a slightly lower yield. The starting material, **69** is not very soluble in water and as soon as one acetate group is cleaved, the substrate is more soluble in water, generating small amounts of product and a mixture of fully deprotected material and starting material.[i]

We then turned to KCN in MeOH instead, a catalytic method with respect to the base. The method was first published my Mori et al. as a neutral transestrification method.[104] The method is however mild as Herzig has isolated partly deacetylated carbohydrates.[105] When this method was used the yield of **70** increased to a reasonable and reproducible 45%. The free phenol was then coupled with dansyl chloride as described by Lin et al. followed by deprotection using standard Zemplén conditions, to give **72**.[106]

4.3.2 Physical properties of second generation

The log *P* of labeled compound **72** was evaluated on HPLC and then compared to values obtained for **62** and **6**. This showed that **72** was a little more hydrophilic, but still much more lipophilic than **6** (Table 4.2). The absorbance and fluorescent spectra were also determined; from the absorbance spectrum the excitation wavelength was determined to 353 nm (Figure 4.5).

Table 4.2 Gradient HPLC retention times for the fluorescently labeled compounds and **6**.

Compound	Retention time (min)
6	17.73 ± 0.03
62	43.40 ± 0.02
72	38.48 ± 0.08

[i] Ellervik et al. have tried to evaluate if it is possible to remove acetates from **69** with stoiciometric amount of base. In most cases the aromatic acetate was cleaved first but no good trend or reaction times could be figured out.

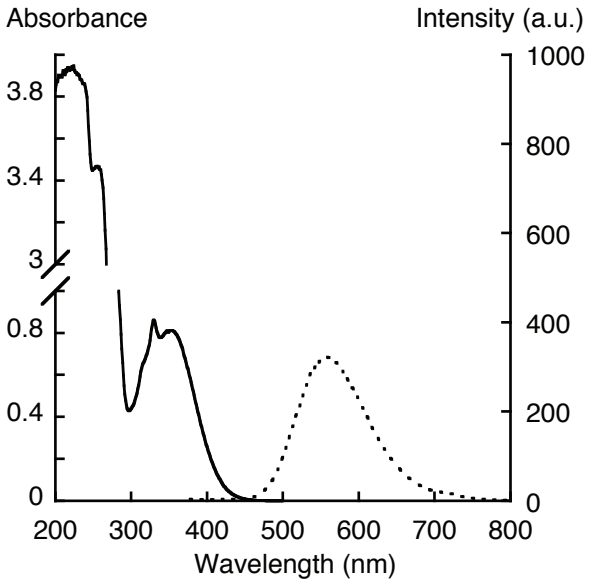

Figure 4.5 Absorbance spectrum of compound **72** (0.25 mM in MeCN, solid line) and fluorescence spectrum of compound **72** (0.25 mM in MeCN, λ_{Ex} = 353 nm, dotted line).

4.3.3 Biology of second generation

To evaluate if **72** was a good structural analog to **6**, it was tested for uptake and GAG priming ability on transformed T24 cells. T24 cells were thus treated with 0.100 mM **72** for 16 h, and then fixed and studied using fluorescence microscopy. **72** was taken up by the cells and was mainly located in the intracellular compartment, similarly to **62**.

The priming ability of **72** was also tested on transformed T24 cells, which were treated with 0.100 mM **72** over night. After priming, the GAG chains were separated from proteoglycans using size-exclusion, however no xyloside primed GAG chains could be isolated.

4.4 Summary of fluorescent labeling

Two different fluorescent analogs to **6** were synthesized to find out more of the biosynthesis of GAG chains. Both these analogs were taken up by the cells but did not initiate priming. These compounds are more lipophilic than **6**, but this is probably not the only reason for their failure to prime GAG. Another plausible reason is that the aglycon is too big, which means that they will not be located to the correct compartment of the cell to induce priming. It is known that labels such as fluorescein and rhodamin alter physico-chemical properties of small peptides.[107] In this case, the molar mass is 75% higher for **62** and 80%

higher for **72**, and this will alter the physical, chemical and biological properties of the system too much and the labeled analogs will not be relevant for studying the system. With this knowledge we left fluorescently labeled xylosides and turned to radioactive labeling.

5 RADIOACTIVE LABELING

5.1 Background

5.1.1 Radioactive labeling

When an unstable isotope of an element decays, it emits radiation in the form of particles or electromagnetic waves with the three most common being α-decay (emission of helium nuclei), β-decay (emission of electrons or positrons) and γ-decay (electromagnetic radiation).

Since the physical properties of the substances are, more or less unaltered, radioactive isotopes for labeling interesting compounds in biological systems are widely used. The use of radioactive substances in the treatment of diseases is also known, e.g. in the treatment of thyroid cancer with radioactive iodine.

In our project we were interested in the use of a radioactive label on our active compound **6**. The most convenient way was to exchange hydrogen for tritium via iodination. Tritium is widely used in labeling of biological material since hydrogen is present in most molecules and the synthesis of tritium labeled compounds is much easier compared to labeling with carbon-14.[108]

In the biological evaluation of the naphthoxylosides, the priming ability of the naphthoxylosides is evaluated using [^{35}S]-sulfate which is incorporated in the growing GAG chains during post-synthetic modifications (e.g. sulfation) Both ^{3}H and ^{35}S are β-emitters. ^{3}H has a maximum energy of 18.6 keV with an average of 6 keV whilst ^{35}S has a maximum energy 167 keV with an average of 56 keV. This means that it is possible to distinguish

between radiation from ^{3}H and ^{35}S, and compounds labeled with tritium in the aromatic residue can be traced through the cells simultaneously with the chain growth, which is followed by ^{35}S-incorporation.

5.1.2 Aromatic iodination

Aryl iodides are important synthetic intermediates in organic chemistry, useful in a variety of functional transformations, e.g. the Heck reaction and Stille and Negishi cross couplings.[109] The aryl iodides can also be hydrodehalogenated to incorporate deuterium or tritium in the molecule, and are, as such, important intermediates in medicinal chemistry.[110,108]

Direct aromatic iodination can be divided into five classes, depending on the reagents used; i) iodine and oxidant (most often nitric acid), ii) iodine monochloride, iii) insoluble metal iodides, iv) *N*-iodoamides and v) iodination in presence of base.[111] However, the low electrophilicity of molecular iodine renders direct aromatic iodination difficult in comparison to bromination and chlorination and, for example, the addition of an oxidant can degrade sensitive groups.

To improve a promoter system for glycosylation, the capabilities of different Lewis acid to generate iodonium ions from ICl and IBr was tested. We thus used the electrophilic aromatic substitution of acetanilide (**73**) as a model system to evaluate the formation of iodonium ions. As it turned out, the iodination reaction worked well and we decided to further evaluate the iodinating properties of ICl and IBr.

5.2 Aromatic iodination

5.2.1 Optimization of iodination

The activating properties of various Lewis acids were tested with ICl and IBr. Acetanilide was used as an aromatic model system (Scheme 5.1).

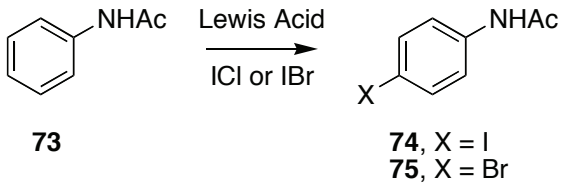

Scheme 5.1 Evaluation of Lewis acid catalyzed iodination.

The reaction was stirred for 15 minutes at room temperature in acetonitrile, extracted and the crude product was analyzed by NMR (results are summarized in Table 5.1). The most potent activator was $Hg(OTf)_2$ (entry 14, Table 5.1). This was not a surprise since mercury is strongly halophilic and a well known activator for iodinations.[109] More surprising was that $In(OTf)_3$ was a more potent activator than AgOTf. The halophilic properties of In(III) have been discussed recently.[112] In a preparative scale (0.5 mmol) **74** was synthesized in 99% yield with 1 equivalent of $In(OTf)_3$ and 1.5 equivalents ICl. There is no correlation between the yield in the iodination and the different Lewis acids based on HSAB-theory.[113]

Table 5.1 The halogenating properties of ICl and IBr with various Lewis acids.

Entry	Lewis acid	74 (%) (ICl)	74 (%) (IBr)	75 (%)
1	HOTf	0	0	3
2	$Sc(OTf)_3$	0	0	8
3	$Sn(OTf)_2$	0	0	0
4	$Al(OTf)_3$	14	0	14
5	$Yb(OTf)_3$	16	0	14
6	-[a]	21	0	21
7	$Mg(OTf)_2$	24	0	26
8	$Mn(OTf)_2$	25	0	17
9	LiOTf	25	0	18
10	$Cu(OTf)_2$	30	0	36
11	AgOTf	43	13	32
12	$Zn(OTf)_2$	46	0	19
13	$In(OTf)_3$	79	27	11
14	$Hg(OTf)_2$	100	100	0

a) No Lewis acid added.

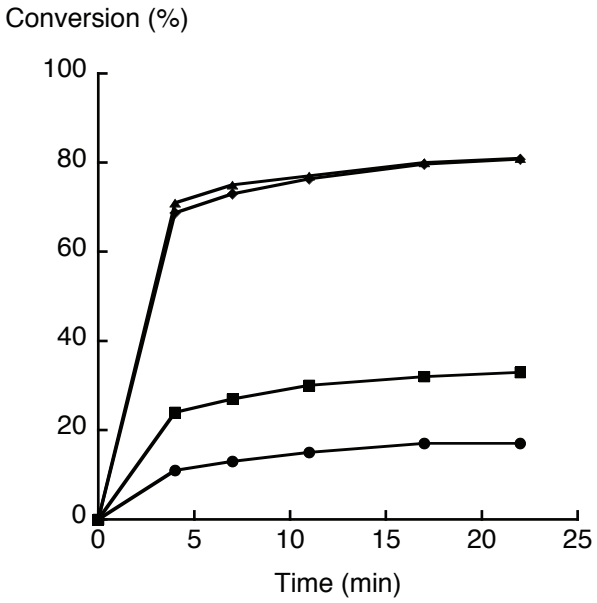

Figure 5.1 Iodination of **73** using various amounts of $In(OTf)_3$. ICl/acetanilide 1:1. 1 eq. $In(OTf)_3$ (▲); 0.5 eq. $In(OTf)_3$ (◆); 0.1 eq. $In(OTf)_3$ (■); 0 eq. $In(OTf)_3$ (●).

To investigate the role of $In(OTf)_3$ in the reaction, a sample with **73** in CD_3CN, and $In(OTf)_3$ (0, 0.1, 0.5 and 1.0 equivalents) was prepared. The reaction was started by the addition of 1.0 equivalent ICl and then followed by NMR and the amount of product formed was plotted versus time (Figure 5.1). As indicated from the plot, 0.5 equivalents of $In(OTf)_3$ are necessary for complete conversion.

5.2.2 Application of aromatic iodination

The standard conditions for the aromatic iodination were set to; aryl/$In(OTf)_3$/ICl 1:0.5:1.1 in acetonitrile and a reaction time of one hour. The reaction appeared to be rapid, albeit the reaction time was set to one hour for practical reasons. These conditions were applied to a wide range of aromatic compounds (Scheme 5.2). Deactivated and weakly activated aromatic rings (i.e. nitrobenzene, acetophenone, bromobenzene, benzene and toluene) were not iodinated under these conditions. However, toluene was iodinated if $In(OTf)_3$ was substituted for $Hg(OTf)_2$. The reaction gave a mixture of para- (**99**) and ortho-para-iodinated (**100**) toluene in 30 and 23% yield (Scheme 5.3).

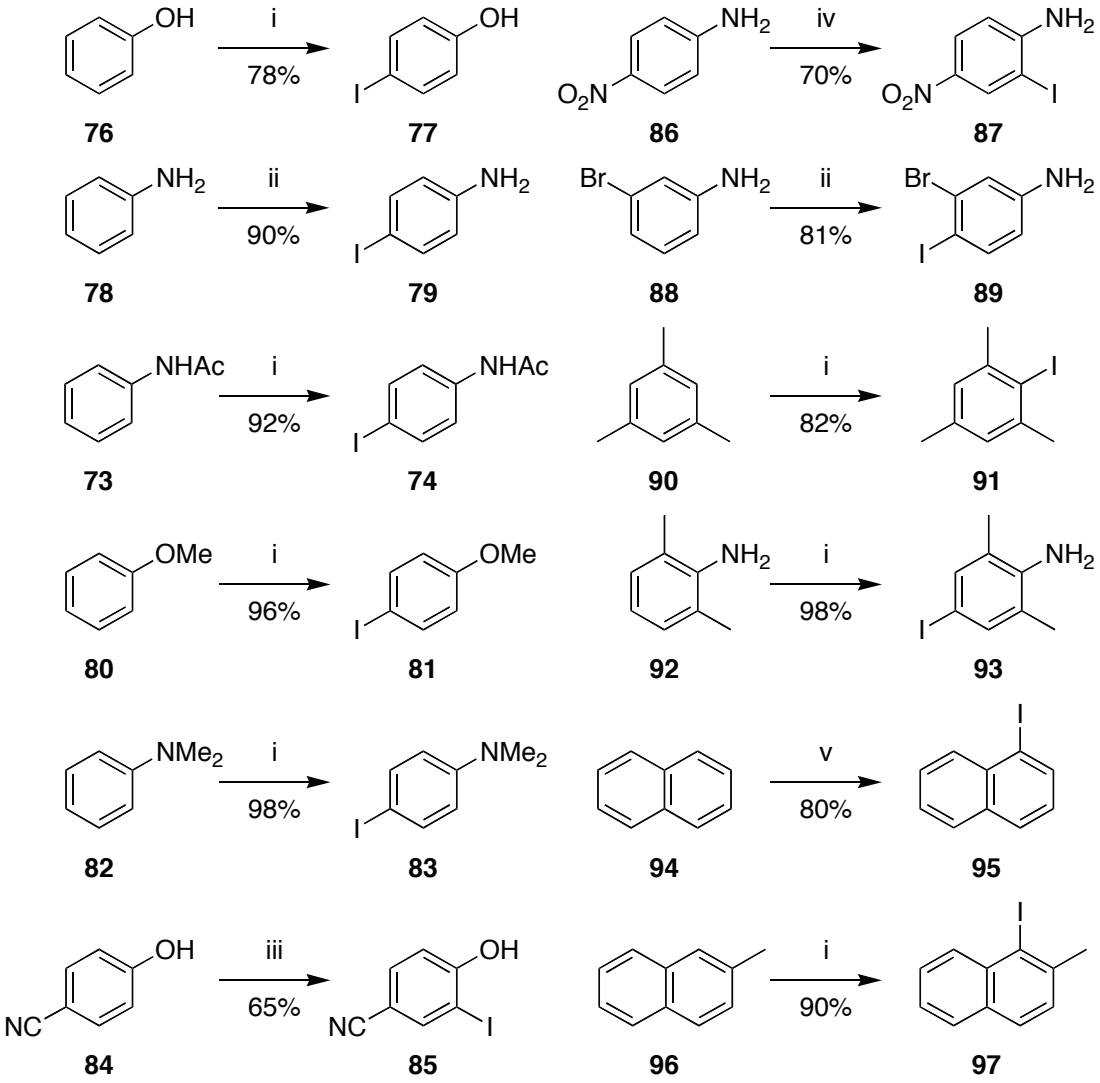

Scheme 5.2 The halogenation properties of ICl/$In(OTf)_3$. i) $In(OTf)_3$, ICl, MeCN, 1 h; ii) $In(OTf)_3$, ICl, MeCN, 0 °C, 1 h; iii) $In(OTf)_3$, ICl, MeCN, 0 °C, 12 h; iv) $In(OTf)_3$, ICl, MS 3Å, MeCN, 0 °C, 1 h; v) $In(OTf)_3$, ICl, MeCN, 12 h.

The reaction was first tested at room temperature and aniline, which is highly activated, gave some diiodination. The diiodination was minimized by lowering the temperature to 0 °C. For 4-hydroxynitrile (**84**), which is an easily reduced compound,[114] lower temperature and prolonged reaction time increased the yield from 16 to 65%. The yield of 4-nitroaniline (**86**) increased from 63% to 70% by lowering the reaction temperature and adding molecular sieves which act as a neutral acid scavenger (to remove formed HCl).[115] Also 3-bromoaniline (**64**) was isolated in better yield by lowering the temperature. Naphthalene (**70**), was the least activated compound in this series, and after 1 h only 40% could be isolated. If the reaction time was prolonged to 12 hours the yield of 1-iodonaphthalene (**71**) was increased to 80%.

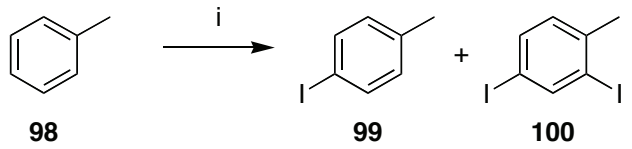

Scheme 5.3 Iodination of toluene. i) $Hg(OTf)_2$, ICl, MeCN, 1 h.

Carbohydrates are acid sensitive and to verify the mildness of the reaction conditions and to confirm that the system will work for the intended application, four carbohydrates with naphthol as aglycon were iodinated under these conditions in excellent yields (Scheme 5.4). The more acid sensitive 2-naphthyl 2,3-di-*O*-acetyl-4,6-*O*-benzylidene-β-D-glucopyranoside (**105**) was iodinated in the presence of molecular sieves. All attempts to iodinate unprotected carbohydrates failed and resulted in decomposition.

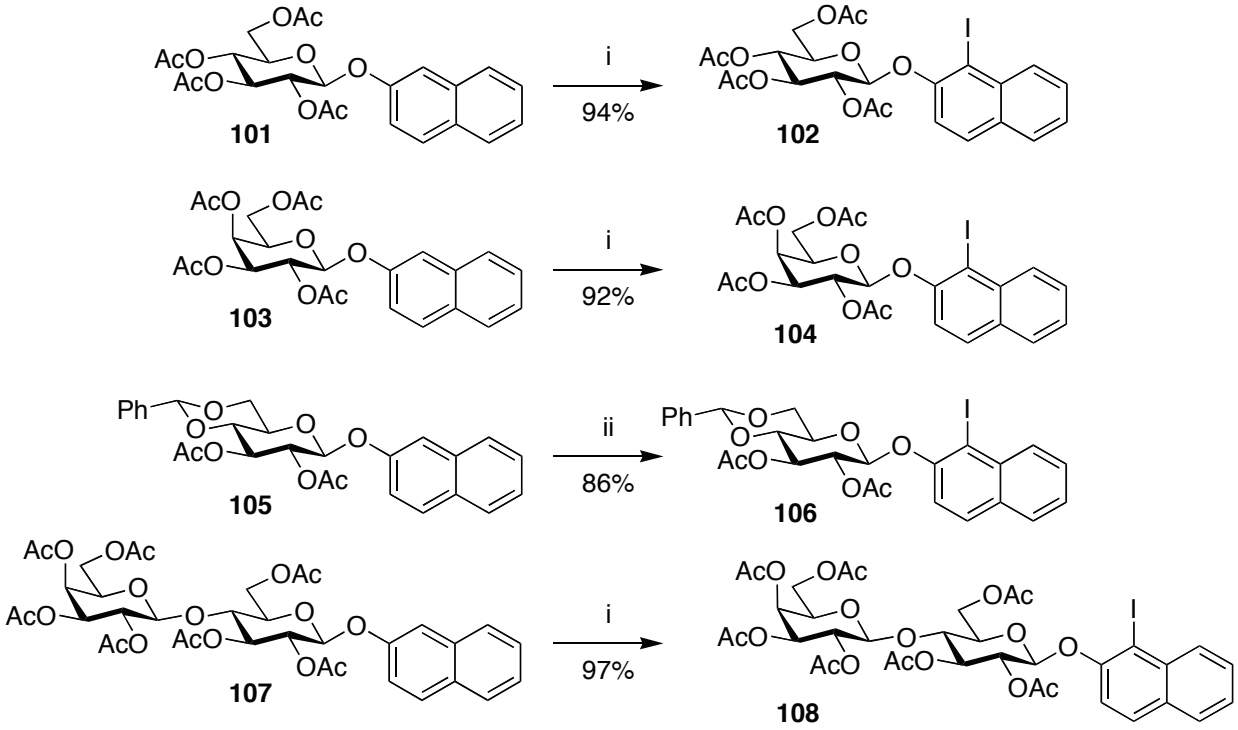

Scheme 5.4 The halogenation properties of ICl/$In(OTf)_3$. i) $In(OTf)_3$, ICl, MeCN, 1 h; ii) $In(OTf)_3$, ICl, MS 3Å, MeCN, 1 h.

5.2.3 Solvent dependence

The aromatic iodination was performed in acetonitrile. Since the method should be as versatile as possible, we also studied the reaction in different solvents. It is also anticipated by calculations that the activation energy of the iodination of anisole with ICl is decreased when the polarity of the solvent increases.[116] The reaction was set up with acetanilide (**73**) as

aromatic model system and 0.5 equivalents of $In(OTf)_3$ and 1.5 equivalents of ICl. The reaction was run for 1 hour and also overnight. The conversion into product was estimated by NMR analysis of the crude reaction mixture, after aqueous work-up.

Table 5.2 The starting material: Product distribution of iodination in different solvents.

Entry	Solvent	Dielectric constant	73:74 (1 h)	73:74 (18 h)
1	MeCN	37.5	0:100	0:100
2	DMF	36.7	0:100	0:100
3	$MeNO_2$	35.9	6:94	0:100
4	CH_2Cl_2	9.1	22:78	16:84
5	THF	7.6	42:58	0:100
6	EtOAc	6.0	0:100	0:100
7	$CHCl_3$	4.8	19:81	0:100
8	Et_2O	4.3	0:100	0:100
9	CS_2	2.6	55:45	3:97
10	Dioxane	2.2	42:58	0:100
11	Heptane	1.9	29:71	15:85

Methanol, toluene, benzene and the ionic liquid EMIm•OTf (1-ethyl-3-methyl-imidazolium trifluoromethanesulfonate) were also tested. Toluene and benzene gave low conversion, even after 18 hours, MeOH gave a mixture of three different products after 18 hours and EMIm•OTf was unable to mediate any reaction at all. It is clear that there is no correlation between the yield and the polarity/dielectric constant.

5.2.4 Summary of aromatic iodination

A protocol for mild and efficient iodination of activated aromatic systems was developed. It works well with acid sensitive systems such as the glycoconjugates that it was designed for. The iodination and bromination with IBr were also evaluated although to a much lesser extent.

5.3 Radioactive xylosides

5.3.1 Synthesis of tritiated compounds

For this study we decided to work with our reference compound **6** as well as **4** and **118**. **4** is considered a reference compound in studies regarding priming ability as it will prime the synthesis of GAG chains but do not show any antiproliferative activity. **118** does also prime GAG chains but show no antiproliferative activity, and is thus a dihydroxy analog to the reference compound **6**.

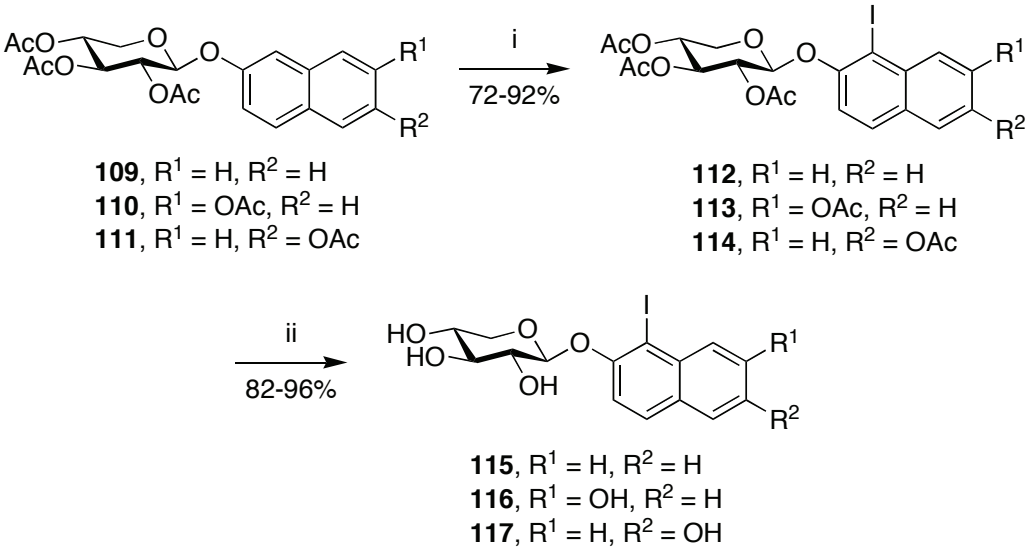

109, R^1 = H, R^2 = H
110, R^1 = OAc, R^2 = H
111, R^1 = H, R^2 = OAc

112, R^1 = H, R^2 = H
113, R^1 = OAc, R^2 = H
114, R^1 = H, R^2 = OAc

115, R^1 = H, R^2 = H
116, R^1 = OH, R^2 = H
117, R^1 = H, R^2 = OH

Scheme 5.5 Synthesis of iodinated naphthoxylosides. i) $In(OTf)_3$, ICl, MS 3Å, MeCN, 1 h; ii) NaOMe MeOH, 1 h.

109 and **111** are known compounds,[117,118] but **110** was synthesized from the corresponding mono acetylated dihydroxynaphthalene and peracetylated xylose in 85% yield. The three acetylated naphthoxylosides were then iodinated according to the method described above. The reactions worked well using molecular sieves, and the products were isolated in 72-92% yield. The iodinated naphthoxylosides were subsequently deacetylated using standard Zemplén conditions to give **115**-**117** in 82-96% yield. With the three compounds in hand, the hydrodehalogenation was tested. The most common way for hydrodehalogenation is by tributyltin hydride or by metal mediated reaction with hydrogen gas.[110,108] It was decided that the radioactive labeling should be done by contracting, and hence a method for hydrodehalogenation using tritium gas had to be developed.

To circumvent the potential problem of saturation of the aromatic moiety, the use of low pressure of hydrogen gas was explored. The use of hydrogen gas at one atmosphere, with Pd/C as catalyst and triethylamine in methanol was tested.[119] Tritium labeled compounds should preferably not be evaporated to dryness, since the product may degrade. After two hours reaction time, the product distribution was controlled by NMR. The lowest conversion was observed for **116** (90% product), followed by **117** (95%) and the hydrogenation of **115** went to completion.

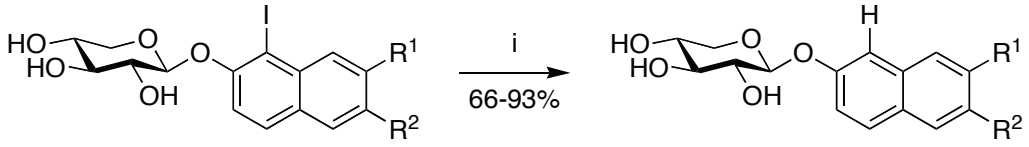

115, R^1 = H, R^2 = H
116, R^1 = OH, R^2 = H
117, R^1 = H, R^2 = OH

4, R^1 = H, R^2 = H
118, R^1 = OH, R^2 = H
6, R^1 = H, R^2 = OH

Scheme 5.6 Hydrodehalogenation. i) H_2, Pd/C, NEt_3, MeOH, 2 h.

The products were purified on HPLC and lyophilized to give the yields of 66-93% (Scheme 5.6). To further evaluate the hydrodehalogenation the reaction was performed with deuterium gas for **117** to give **119** in similar results as with hydrogen gas (**117**/**119** 25:75) (Scheme 5.7). With the working protocol the iodinated substances were sent for labeling and the products were received with data as seen in Table 5.3.[120]

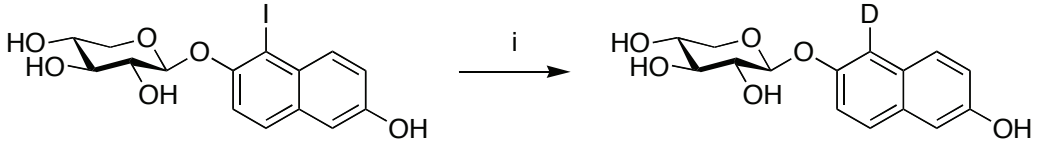

117 **119**

Scheme 5.7 Hydrodehalogenation with D_2. i) D_2, Pd/C, NEt_3, MeOH, 2 h.

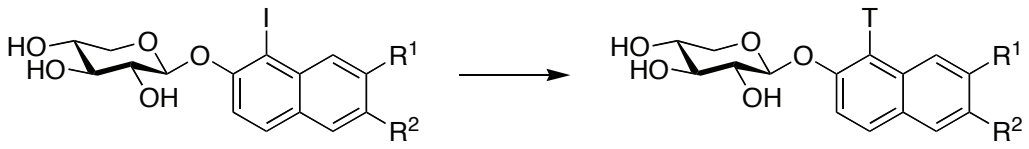

115, R^1 = H, R^2 = H
116, R^1 = OH, R^2 = H
117, R^1 = H, R^2 = OH

120, R^1 = H, R^2 = H
121, R^1 = OH, R^2 = H
122, R^1 = H, R^2 = OH

Scheme 5.8 Radioactive labeling of iodinated naphthoxylosides.

Tritium has a specific activity of 28.7 Ci/mmol, which means that if the conversion of iodine to tritium is 100% the specific activity will be 28.7 Ci/mmol for the product. However, it is more common to have an exchange of 60-90%. This does not mean that the product contains iodinated material, but that some iodine is exchanged for hydrogen instead. The hydrogen can come from the gas, or the catalyst. This then means that **120** has a specific activity of 68%, **121** 95% and **122** 331% (meaning that there is more than three tritium atoms in the molecule). Exchange of hydrogen by tritium is not uncommon, and Wilzbach observed an aromatic hydrogen-tritium exchange when toluene was stirred in room temperature under a sub-atmospheric pressure of tritium, even without catalyst.[121] It has also been shown that the addition of a palladium catalyst increased the conversion 50 times.[122] Any hydrogen-deuterium exchange was not observed in the reaction with deuterium, but the reactivity between deuterium and tritium varies.

Table 5.3 Data for radioactively labeled compounds.

Compound	Specific activity (Ci/mmol)	Radiochemical purity (%)	Concentration (mCi/mL)	Concentration (mmol/mL)
120	19.7	98.5	1.4	0.071
121	27.4	98.6	1.2	0.044
122	95.0	97.7	1.25	0.013

5.3.2 Biology of tritiated compounds

We decided to start the investigation by measuring kinetics in T24 and HFL-1 (human fetal lung fibroblast) cells, and follow the tritiated aglycon on **122** as well as [^{35}S]-sulfate in the growing GAG chains.

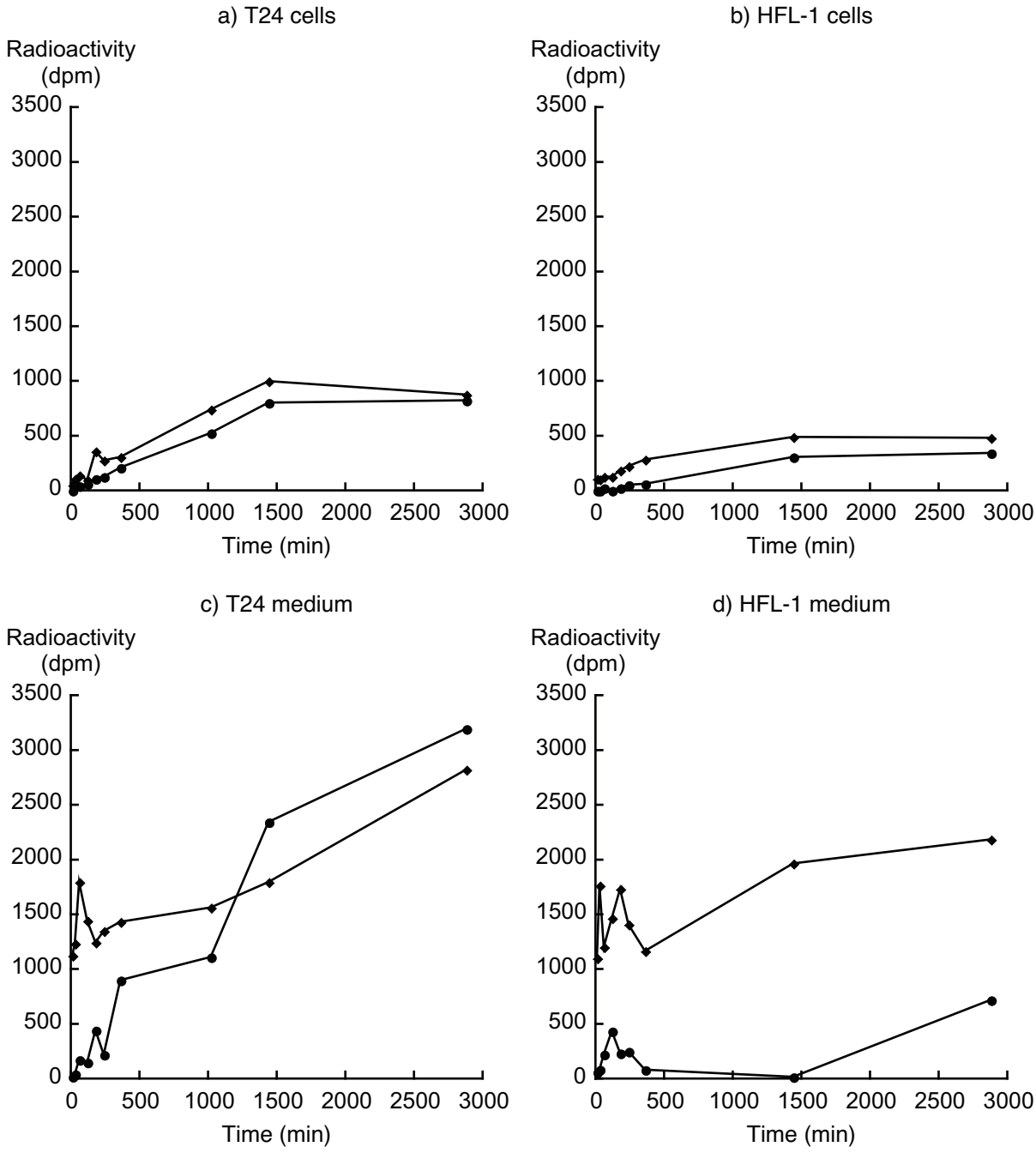

Figure 5.2 Amount of ^{3}H (♦) and ^{35}S (●)over a time period of 48 h. a) T24, whole cell; b) HFL-1, whole cell; c) T24, medium; d) HFL-1, medium.

Both cell lines accumulated **122**, indicating an uptake of the compound with a maximum after 24 hours (Figure 5.2a and b). These cells also had an increased amount of sulfated GAG chains, indicating that **122** primed biosynthesis of GAG chains. The T24 cells had a higher uptake and primed GAG chains to a higher extent than HFL-1.

The free xyloside primed GAG chains are usually secreted into the extracellular environment, and to examine to what extent, the amount xyloside and GAG were measured

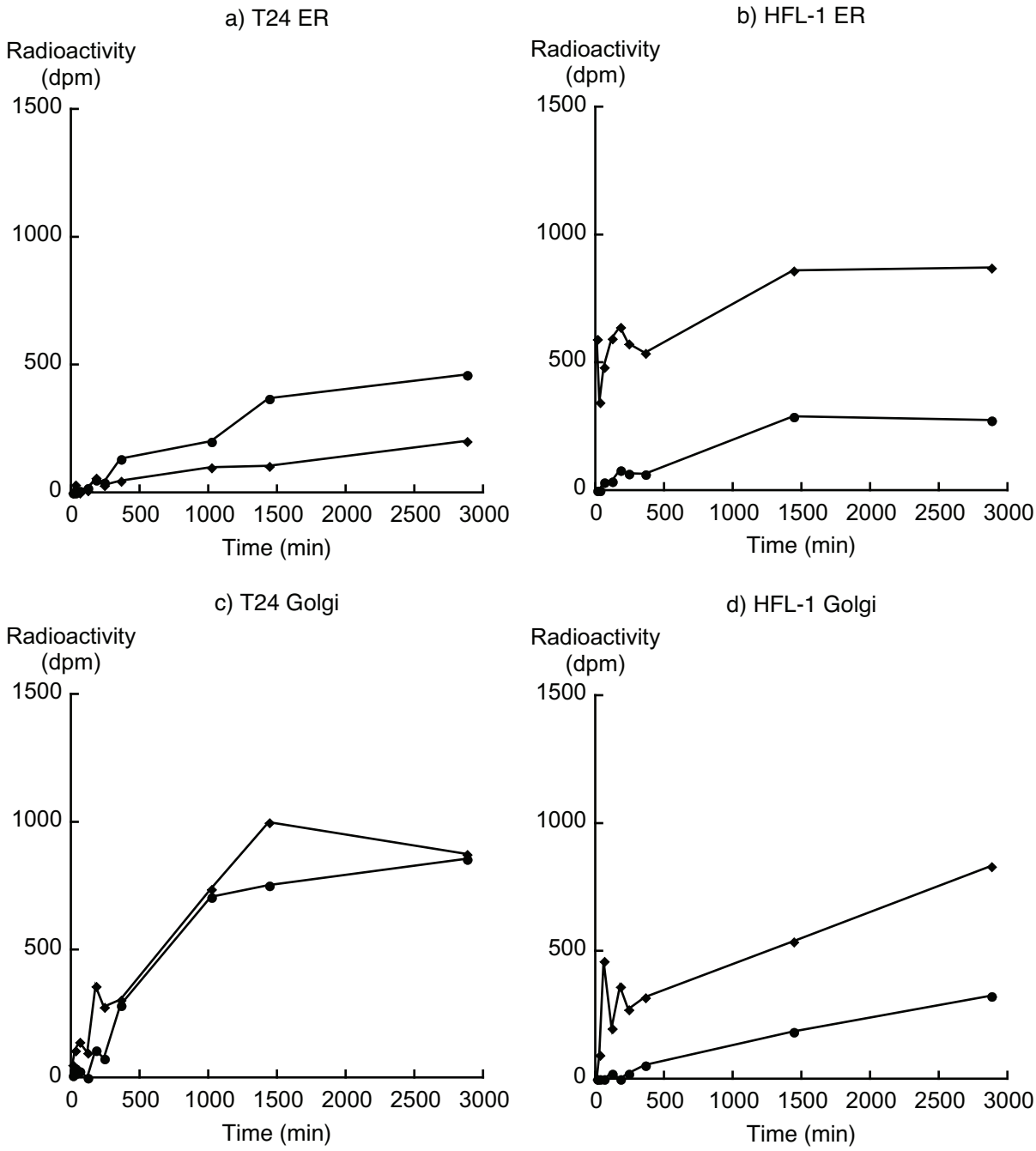

Figure 5.3 Amount of ^{3}H (♦) and ^{35}S (●)over a time period of 48 h. a) T24, ER; b) HFL-1, ER; c) T24, Golgi; d) HFL-1, Golgi.

in the culture medium. After the removal of PG, both T24 and HFL-1 cells secreted free xyloside primed GAG chains (Figure 5.2c and d). The accumulation of sulfated GAG chains indicated that the major part of the GAG chains were secreted to the medium, however internalization and binding to cell surface receptors cannot be excluded. T24 cells expressed higher amounts of both [^{3}H]-xyloside and [^{35}S]-sulfated GAG chains and they were sulfated to a higher extent than the GAG chains expressed by HFL-1 cells.

The biosynthesis of GAG chains is complex and involves numerous enzymes, and the secretory pathway also include the ER and Golgi, where assembly and modification of GAG chains take place. To find out more about the cellular pathways, the ER and Golgi was isolated with immunomagnetic methods and studied regarding radioactivity. There were generally small amounts of xyloside products in the ER, although slightly more in HFL-1 cells compared to T24 cells. We also observed an accumulation over time (Figure 5.3a and b). In the Golgi apparatus, the amount of [^{3}H]-xyloside was higher in T24 cells compared to HFL-1 cells, and the amount of [^{35}S]-sulfate was also higher with a maximum after 24 hours (Figure 5.3c and d). These results are consistent with the results from the whole cells.

5.3.3 Summary of tritiated compounds

To summarize, we have for the first time proven that the GAG chains are really primed by the naphthoxylosides, i.e. the isolated GAG chains contain both [^{3}H] and [^{35}S]. We can also see that the maximum amount of GAG chains is reached after 24 hours and that most of them are secreted into the cell medium. We also found an accumulation in the ER and Golgi apparatus, and a higher amount in the Golgi. Transformed T24 cells generally prime GAG chains to larger extent than normal HFL-1 cells.

6 ACETAL OPENINGS

6.1 Background

The first reported regioselective opening of an acetal was presented by Doukas and Fontaine, who regioselectively opened the spirostenol diosgenin with lithium aluminum hydride/hydrogen chloride gas in ether (Scheme 6.1).[123]

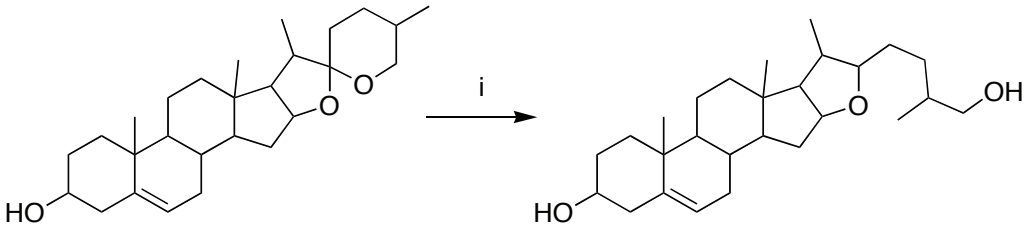

123 **124**

Scheme 6.1 Reductive opening of diosgenin. i) $LiAlH_4$, HCl, Et_2O.

Since neither lithium aluminum hydride nor hydrogen chloride affect **123**, Eliel and Rerick suggested that the active species was lithium aluminum hydride-aluminum chloride and they also showed the reductive capabilities of this reagent combination.[124,125]

In 1964, Legetter and Brown published a systematic study of reductive openings of 1,3-dioxolanes (Scheme 6.2).[126] They conclude that electron-donating groups speed up the reaction rate while electron-withdrawing groups decrease it, and that the substituent in position 4 and 5 directs the regioselectivity. They also suggested a mechanism, where aluminum chloride first coordinates to an acetal oxygen giving the oxocarbenium ion that subsequently is reduced by lithium aluminum hydride (Scheme 6.2).

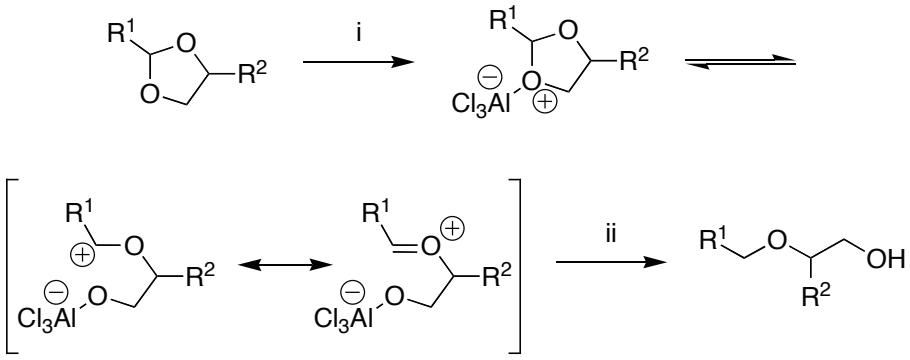

Scheme 6.2 Proposed mechanism by Legetter and Brown in their model system. i) $AlCl_3$; ii) $LiAlH_4$.

The benzylidene acetal is a versatile protecting group that is commonly used to protect 1,2- and 1,3-diols, with preference to 1,3-diols. The protecting group can be cleaved under neutral or acidic conditions. More interestingly, it can be regioselectively opened under reductive conditions, to yield a free hydroxyl group and a benzyl ether. Reductive openings of benzylidene acetals was introduced in carbohydrate chemistry by Bhattacharjee and Gorin in 1969.[127] They opened a number of benzylidene protected gluco-, galacto- and mannopyranosides with lithium aluminum hydride-aluminum chloride in 27-64% yield.

Lipták et al. further studied the regioselective opening of 4,6-benzylidene acetals of carbohydrates and found that neither the anomeric configuration nor the aglycon or the substituent on O-2 affect the regioselectivity. However, they found that the substituent in O-3 affect the regioselectivity, i.e. a more bulky substituent favors the formation of the 4-*O*-benzyl group.[128]

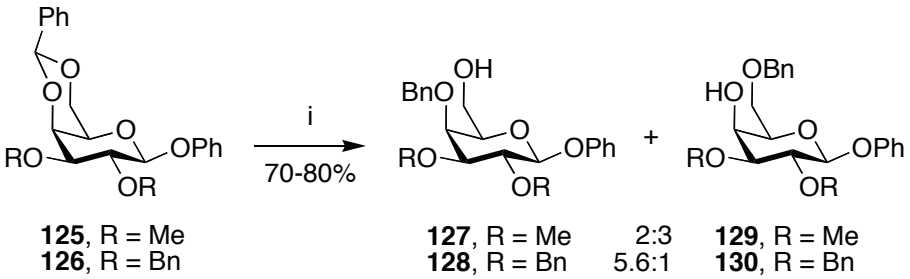

Scheme 6.3 The regioselective opening presented by Lipták et al. The less bulky O-3 substituent gives more 6-*O* benzyl ether. i) $LiAlH_4$, $AlCl_3$, CH_2Cl_2:Et_2O.

Lithium aluminum hydride is reactive and reduces esters, a common protecting group in carbohydrate chemistry. To find a more chemoselective reagent, Garegg and co-workers published a method with sodium cyanoborohydride in combination with dry hydrogen

chloride in ether, a method that do not affect esters.[93] Interestingly, this method gave reversed regioselectivity compared to the method with lithium aluminum hydride, i.e. predominantly the 6-*O*-benzyl ether. The regioselectivity was explained by the less steric demand of a proton compared to aluminum chloride.[129] To get back to the original regioselectivity, Garegg and co-workers turned their attention to boranes. The combination of borane-trimethylamine with aluminum chloride in tetrahydrofuran gave the 6-*O*-benzyl ether whilst the same reaction in toluene yielded the 4-*O*-benzyl ether.[94] The reactions in toluene gave a somewhat lower yield due to degradation, and the regioselectivity was explained by the stronger solvation of Lewis acid and cationic intermediates in tetrahydrofuran.

The opening of methyl 2,3-di-*O*-benzyl-4,6-*O*-benzylidene-α-D-glucopyranoside (**53**) has become somewhat of a standard reaction in comparing different methods, as summarized in Table 6.1.

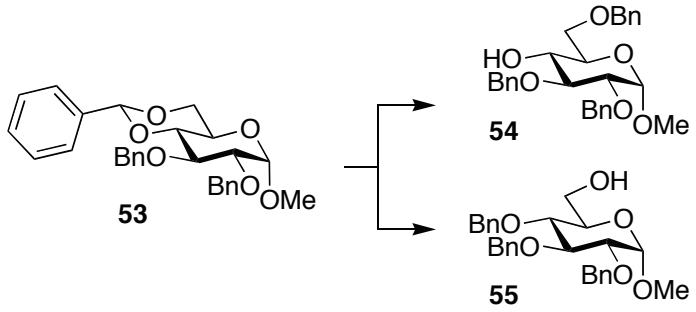

Scheme 6.4 Reductive opening of **53**.

It is well accepted that the Lewis acid has to coordinate to the oxygen that will become the free hydroxyl group. The proposed mechanism explain the regioselectivity by the differences in steric demand from the proton and aluminum chloride (Scheme 6.5).[140]

Table 6.1 Example of reagents for reductive opening of **53**.

Reagent combination	Conditions	54 (%)	55 (%)	Reference
BH_3•THF, Bu_2BOTf, THF:CH_2Cl_2	0 °C, 1 h	0	87	130
BH_3•THF, $Cu(OTf)_2$, THF:CH_2Cl_2	r.t., 45 min	0	94	131
BH_3•THF, $CoCl_2$, THF	r.t., 10 min	0	100	132
BH_3•THF, $M(OTf)_n$[a], CH_2Cl_2	r.t., 3-5 h	0	87-94	133
BH_3•SMe_2, $Cu(OTf)_2$, THF	r.t. 10 min	3	78	131
BH_3•SMe_2, BF_3•OEt_2, CH_2Cl_2	0 °C, 3.5 h	20	62	134
BH_3•NMe_3, $Cu(OTf)_2$, THF:CH_2Cl_2	r.t., 25 h	40	0	131
BH_3•NMe_3, $AlCl_3$, THF	r.t., several h	71	0	94
BH_3•NMe_3, $AlCl_3$, toluene	r.t., 5 min	0	50	94[b]
BH_3•$NHMe_2$, BF_3•OEt_2, CH_2Cl_2	0 °C-r.t., 1 h	3	73	135
BH_3•$NHMe_2$, BF_3•OEt_2, MeCN	0 °C-r.t., 1 h	30	55	135
9-BBN, $Cu(OTf)_2$, MeCN	r.t., 27 h	0	40	131
$NaCNBH_3$, HCl, THF	r.t., 5 min	82	0	129
Me_2EtSiH, $Cu(OTf)_2$, MeCN	0 °C, 30 min	84	0	131
Et_3SiH, BF_3•OEt_2, CH_2Cl_2	0 °C-r.t., 4 h	83	0	136
Et_3SiH, TFA, CH_2Cl_2	0 °C-r.t., 2-4 h	81	0	137
PMHS[c], $AlCl_3$, Et_2O:CH_2Cl_2	r.t., 12 h	0	80	138
$LiAlH_4$, $AlCl_3$, CH_2Cl_2:Et_2O	Reflux, 2 h	0	94	128
DIBAL, CH_2Cl_2	-30-40 °C, 5.5-21 h	4-8	57-88	139

a) M = V(O), Sc, Pr, Nd, Sm, Eu, Gd; b) low yield due to degradation; c) polymethylhydrosiloxane.

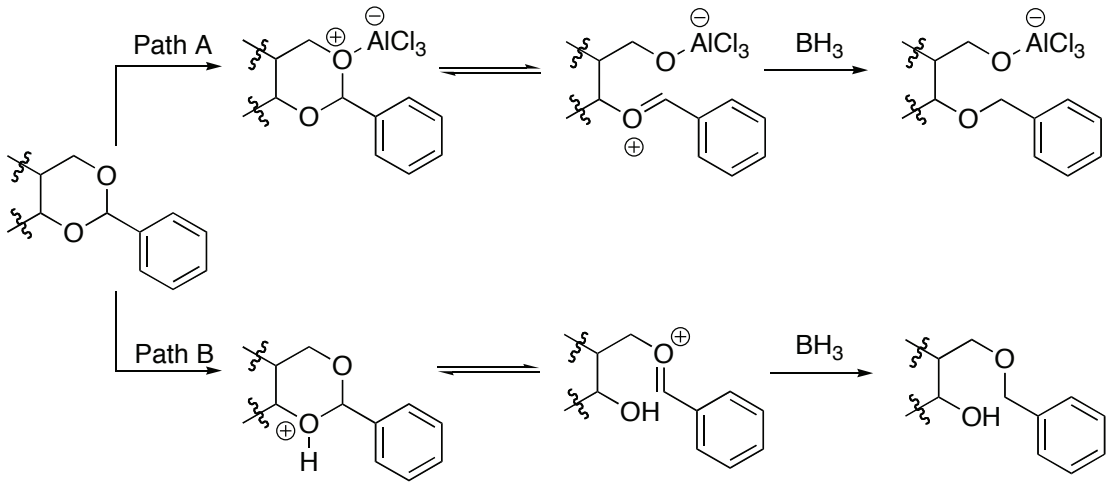

Scheme 6.5 Proposed mechanistic pathway for regioselective reductive opening of cyclic acetals.

This mechanism is however accompanied with some problems. The mechanism do not explain the regioselectivity in the BH_3•NMe_3 reduction, which follows path B, even though the aluminum chloride should associate with the less sterically demanding oxygen, giving the 4-*O*-benzyl ether.[94] This mechanism also fails to explain the regioselective outcome when copper triflate gives the 4-*O*-benzyl ether in combination with BH_3•THF complex, but the 6-*O*-benzyl ether in combination with BH_3•NMe_3.[131]

6.2 Preliminary study

Our interest for acetal openings started with the synthesis of the first fluorescent probe. We realized that the reductive opening of acetals is an interesting and versatile reaction with an unknown mechanism. As described in section 4.2 the opening of **52** gave solely **56** in THF but, when subjected to the conditions in toluene, which should give the reverse opening, only degradation was observed.

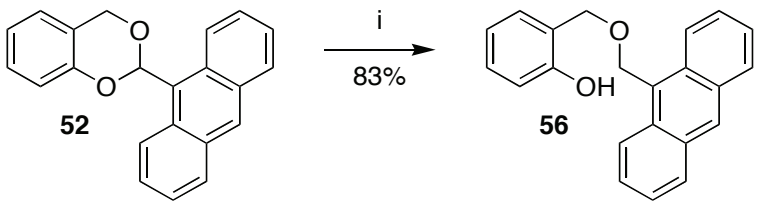

Scheme 6.6 Reductive opening of **52**. i) BH_3•NMe_3, $AlCl_3$, THF, 0 °C, 3 h.

To further investigate this, **52** was subjected to BH_3•NMe_3 in THF without $AlCl_3$, which gave no reaction. Similarly, no reaction was observed when the acetal was subjected to $AlCl_3$ in THF without the borane. Reverse addition order, i.e. first addition of $AlCl_3$ followed by BH_3•NMe_3 gave degradation. When the borane was exchanged to the supposedly more reactive BH_3•THF,[141] a low yield of **56** (10%) was isolated together with starting material and degradation products. When the acetal was subjected to $AlCl_3$ in toluene, only degradation was observed.

To shed some light on the regioselective openings, three new compounds were synthesized, one with an electron-donating group, (OMe, **133**), one with an electron-withdrawing group (NO_2, **136**) and one sterically demanding (**139**). **133** was synthesized from the 5-methoxy salicylic acid (**131**), which was reduced with BH_3•THF in 73% to give the corresponding salicylic alcohol (**132**). **132** was then coupled with anthraldehyde dimethyl acetal to give **133** in 32% (Scheme 6.7).[i]

The nitro-analog (**136**) was synthesized in the same way, starting from 5-nitro salicylic acid (**134**) (Scheme 6.8). However, the reduction did not go as well as for the methoxy analog, and gave only 31% yield. We did not optimize the yield, since the preferred product was produced in adequate amounts. For the coupling of the acetal, the solvent was replaced by acetonitrile and the reaction time was prolonged to 18 hours, still it only gave 22% yield.

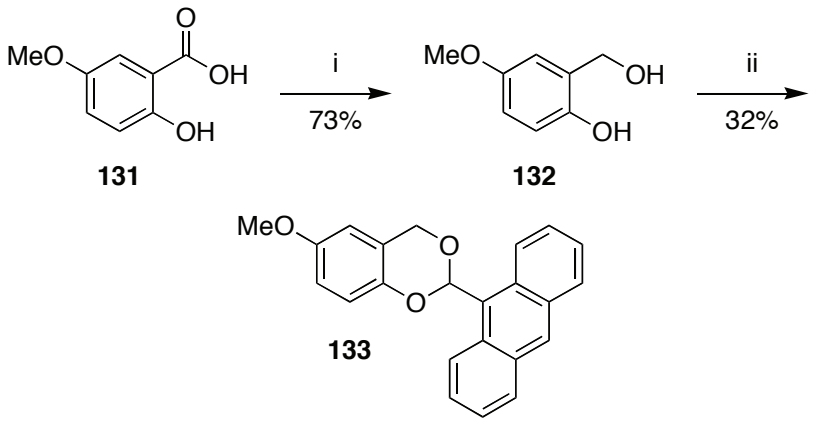

Scheme 6.7 Synthesis of benzylic-phenolic acetal **133**. i) BH_3•THF, THF, 0-60 °C, 3.5 h; ii) anthraldehyde dimethyl acetal, *p*TSA, THF, 3.5 h.

[i] The low yield in the acetal formation is also discussed in section 6.3.

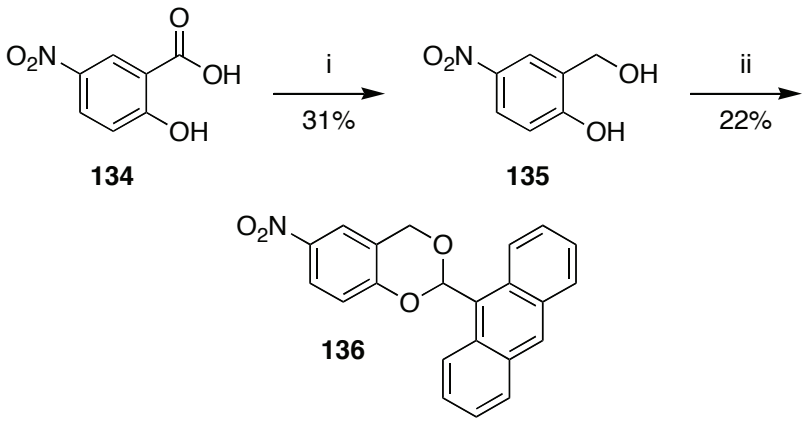

Scheme 6.8 Synthesis of benzylic-phenolic acetal **136**. i) BH_3•THF, THF, 0-60 °C, 3.5 h; ii) anthraldehyde dimethyl acetal, *p*TSA, MeCN, 18 h.

The sterically hindered **139** was synthesized from methyl salicylate (**137**), which was treated with MeMgCl to give the sterically demanding salicylic alcohol (**138**) in 88% yield, followed by acetal formation to give **139** in 52% (Scheme 6.9).

These three new acetals were subjected to the regioselective opening methods described above. The electron rich **133** was opened to the phenol (**140**) in 73% (Scheme 6.10), but neither the electron poor **136,** nor the sterically hindered **139** reacted and the starting materials were recovered.

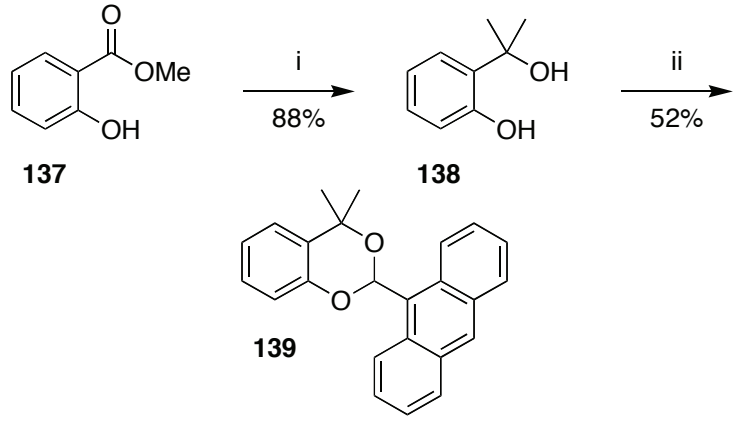

Scheme 6.9 Synthesis of benzylic-phenolic acetal **139**. i) MeMgCl, Et_2O, 4h; ii) anthraldehyde dimethyl acetal, *p*TSA, MeCN, 18 h.

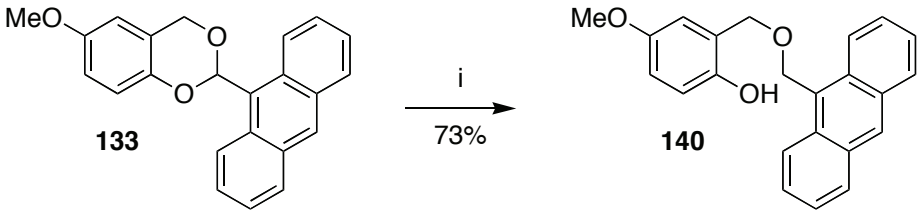

Scheme 6.10 Reductive opening of **133**. i) BH_3•NMe_3, $AlCl_3$, THF, 0 °C, 3 h.

The sterically hindered **139** was also subjected to reaction conditions in toluene, which only resulted in degradation.

These results indicate that the regioselective opening is directed by both electronic and steric effects. To understand more about the electronic effects, the electrostatic potential of the four acetals were calculated using density functional theory at the B3LYP/6-31G* level and default settings in Spartan '02 for Macintosh (Table 6.2).[85]

These results show that the benzylic oxygen is the most basic in all four compounds, indicating that this will react first with a Lewis acid. We now speculated in that, when BH_3 is added first, the borane will coordinate to the most basic oxygen, i.e. the benzylic oxygen. When $AlCl_3$ was added, it initiated the reductive opening, and gave the product. When the $AlCl_3$ was added first, the decomposition followed an unknown mechanism. The reaction is also sensitive to the electronic effect since the electron deficient nitro-acetal (**136**) did not open under these conditions.

Altogether these results indicate that the borane, that is added first, coordinate to the more basic, benzylic oxygen (Scheme 6.11).

Table 6.2 Electrostatic potential for acetal oxygen atoms.

Compound	Phenolic oxygen (kJ/mol)	Benzylic oxygen (kJ/mol)
52	-141.0	-149.8
133	-147.7	-154.0
136	-102.9	-116.7
139	-146.0	-151.0

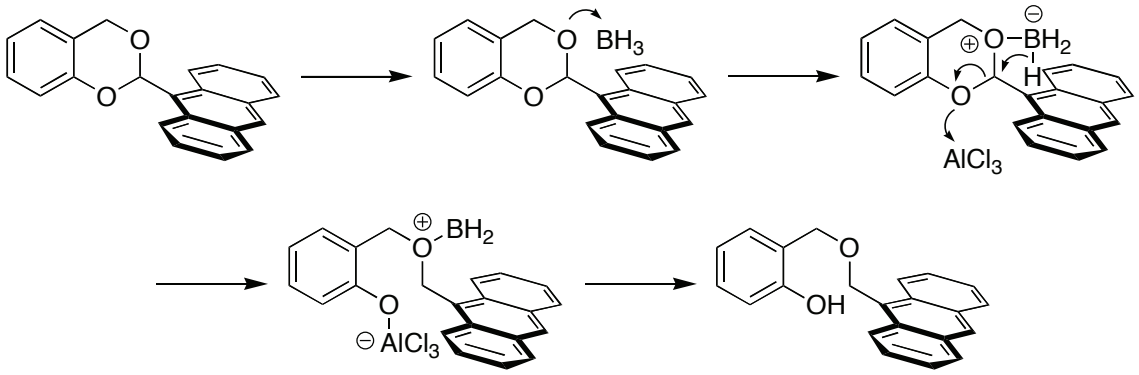

Scheme 6.11 Mechanistic proposal for the reductive opening of acetal.

The preorganization is highly sensitive to the electrostatic potential of the oxygens, since the electron deficient compound **136** did not react under these conditions. BH_3•THF complex gave more decomposition, indicating less discrimination between the two acetal oxygen atoms. Similarly **133** gave a lower yield than **52**. The sterically demanding **139** has similar electrostatic potential as **52**, but did not react, indicating a steric hindrance. Since the reactions in toluene only gave degradation, no conclusion could be drawn regarding that mechanism.

6.3 A model system for acetal openings

With our proposal for the mechanism of the reductive opening, we decided to investigate the mechanism further in order to induce reverse opening. The anthracene moiety is an electron-donating group, and it is known that electron-donating groups gives faster openings of the acetals.[92,142] Since the reverse opening did not work, it was of interest to change the anthracene moiety for another, not electron donating, group and hence give a slower system for the acetal opening. Since the study is related to the aromatic systems, we expanded the preliminary study to include substitutions in both rings. The advantage of studying the opening in an aromatic system, would be the facile fine-tuning of electronic properties.

The first generation of acetals was decided to be substituted in one ring at the time, with two electron-withdrawing groups (NO_2, and Br) two electron-donating groups (OMe and Me) and an unsubstituted (H), according to Chart 6.1.

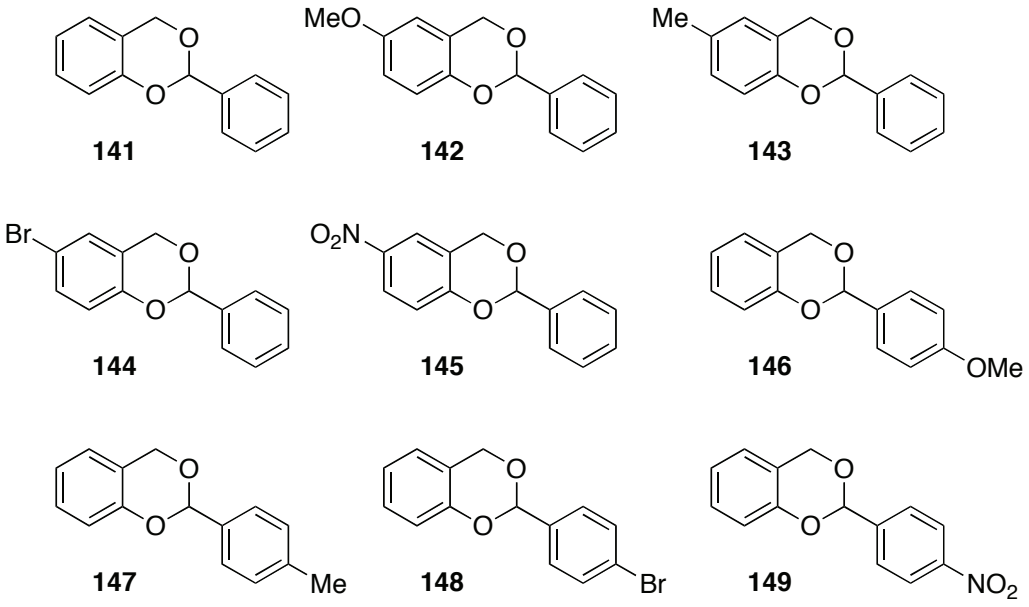

141 **142** **143** **144** **145** **146** **147** **148** **149**

Chart 6.1 Compounds for study of acetal openings.

To build a collection of substituted 2-phenyl-1,3-benzodioxines, we initiated a study to optimize the synthesis. Benzylidene acetals are commonly synthesized by trans acetalization, using the corresponding dimethyl acetals, rather than the more straightforward condensation of the aldehydes.

For **141**, the reaction was straightforward using commercially available starting material (salicylic alcohol (**150**) and benzaldehyde dimethyl acetal), which gave **141** in 73% yield. For the compounds with substitution in the salicylic alcohol part, the 2-hydroxy-5-bromobenzyl alcohol (**151**) and 2-hydroxy-5-nitrobenzyl alcohol (**135**)[i] are commercially available and these compounds were coupled with benzaldehyde dimethyl acetal to give 6-bromo-2-phenyl-4*H*-benzo[d][1,3]dioxine (**144**) and 6-nitro-2-phenyl-4*H*-benzo[d][1,3]-dioxine (**145**) in 57% and 56% yield.

[i] When **135** was synthesized in the preliminary study, the commercial availability was not controlled. The synthesis was copied from the naphthoic acid **57**, which is only available as acid and not as aldehyde.

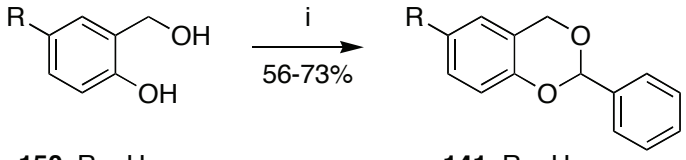

150, R = H
151, R = Br
135, R = NO_2

141, R = H
144, R = Br
145, R = NO_2

Scheme 6.12 Synthesis of acetals. i) benzaldehyde dimethyl acetal, *p*TSA, MeCN, 3-18 h.

The methoxy and methyl substituted salicylic alcohols are not available and, at first, we attempted to reduce the corresponding salicylic acids (as for **131** and **134**). This did not work adequately using BH_3•THF, and the method was complicated and involved several addition steps and different temperatures. Instead, the reduction was tested with $LiAlH_4$, which also gave several by-products. To circumvent these problems, the corresponding aldehydes were used instead, and reduction with $NaBH_4$ in methanol, gave 2-hydroxy-5-methoxybenzyl alcohol (**132**) and 2-hydroxy-5-methylbenzyl alcohol (**154**) in 65% and 69% yield.[143] The alcohols were then coupled to get the acetals **142** and **143** in 45% and 56% yield respectively (Scheme 6.13).

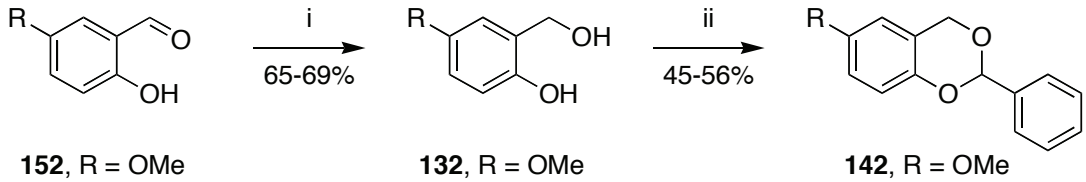

152, R = OMe
153, R = Me

132, R = OMe
154, R = Me

142, R = OMe
143, R = Me

Scheme 6.13 Synthesis of acetals. i) $NaBH_4$, NaOH, MeOH, 45 °C, 30 min; ii) benzaldehyde dimethyl acetal, *p*TSA, MeCN, 3.5-4 h.

We then turned to substitution in the aldehyde moiety. 4-bromobenzaldehyde dimethyl acetal (**160**) was easily available but the other three compounds [methoxy (**158**), methyl (**159**) and nitro (**161**)] had to be synthesized. There is a wide range of methods for the formation of dialkyl acetals from the corresponding aldehyde using either alcohols (MeOH or EtOH) and catalytic amount of acid (HBr,[144] Ce^{3+},[145] or $TiCl_4$[146]) or trialkyl orthoformates [$(MeO)_3CH$ or $(EtO)_3CH$] and a suitable catalyst (*p*TSA,[147] HCl,[148] decaborane ($B_{10}H_{14}$),[149] $HClO_4/SiO_2$,[150] $ZrCl_4$,[151] $Sc(NTf_2)_3$,[152] $InCl_3$,[153] $LiBF_4$,[154] Amberlyst-15,[155] NBS,[156,157] or DDQ[158]). Unfortunately the majority of these methods suffer from long reaction times (usually 12-48h), the use of expensive and/or not

commercially available reagents or the necessity of subsequent purification steps to remove the catalyst.

Based on our experience, the use of a resin bound acid (Amberlite IR-120 H^+) and microwave heating would enhance the reaction rates and also facilitate the work-up. The optimized reaction conditions turned out to be 15 minutes reaction time with trimethyl orthoformate at 110 °C in MeOH. Traces of unreacted aldehyde were easily removed by washing with aqueous $NaHSO_3$, which gave the pure dimethyl acetals **158**-**161** in 88-99% yield, without the need for further purification (Scheme 6.14). The dimethyl acetals were then coupled with salicylic alcohol to get the acetals.

All reactions gave reasonable yields (45-75%) except for the coupling to get 2-(4-methoxyphenyl)-4*H*-benzo[d][1,3]dioxine (**146**), which only gave 12% yield. Even though the reaction path is short, a 12% yield is not acceptable since it consumes a lot of material. The substances were synthesized to evaluate a mechanism and large quantities were needed. The coupling of the 4-methoxybenzaldehyde dimethyl acetal (**158**) with **150** was tested with a wide range of acids; *p*TSA, CSA, Amberlite IR-120 H^+, $ZnBr_2$ and TMSOTf. We also tested to couple 4-methoxybenzaldehyde (**155**) with **150** together with different acids; *p*TSA, CSA, Amberlite IR-120 H^+, $ZnCl_2$ and H_2SO_4. As it turns out, the best yield was obtained in the reaction between **155** and **150** in MeCN with Amberlite IR-120 H^+ as acid, giving **146** in 68% yield.

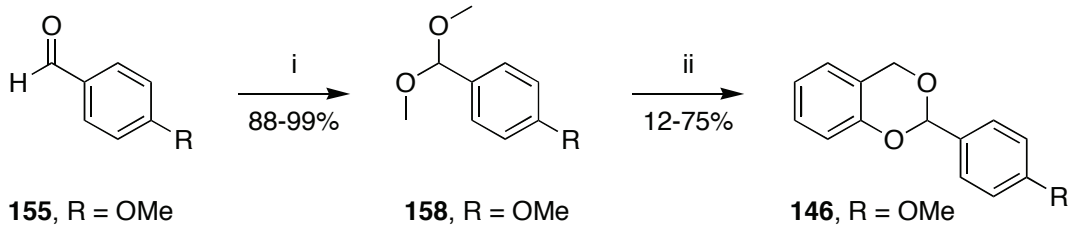

155, R = OMe
156, R = Me
157, R = NO_2

158, R = OMe
159, R = Me
160, R = Br
161, R = NO_2

146, R = OMe
147, R = Me
148, R = Br
149, R = NO_2

Scheme 6.14 Synthesis of acetals. i) $CH(OMe)_3$, Amberlite IR-120 H^+, MW 110 °C, 15 min; ii) 2-hydroxy benzyl alcohol, *p*TSA, MeCN, 3.8-7.8 h.

6.4 Evaluation of Lewis acid activation

6.4.1 Opening of acetals

The benzylic-phenolic acetals **141**-**149** were opened using BH_3•NMe_3 and $AlCl_3$ in THF at 0 °C, giving exclusively the free phenols (Scheme 6.15), as anticipated based on the preliminary study discussed in section 6.2. The reactions were followed by NMR and the identities of the products were verified by isolation and characterization after termination of the reactions.

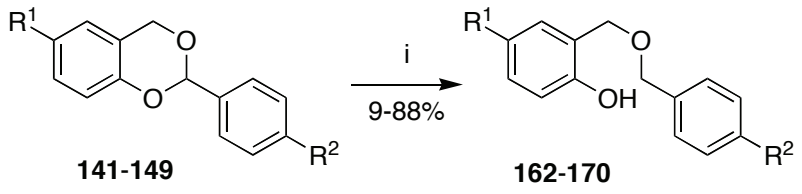

141, **162**, R^1 = H, R^2 = H
142, **163**, R^1 = OMe, R^2 = H
143, **164**, R^1 = Me, R^2 = H
144, **165**, R^1 = Br, R^2 = H
145, **166**, R^1 = NO_2, R^2 = H
146, **167**, R^1 = H, R^2 = OMe
147, **168**, R^1 = H, R^2 = Me
148, **169**, R^1 = H, R^2 = Br
149, **170**, R^1 = H, R^2 = NO_2

Scheme 6.15 Opening of acetals. i) BH_3•NMe_3, $AlCl_3$, THF, 0 °C, 6-23 h.

6.4.2 Computational chemistry on acetals

To gain more knowledge of the system, the electrostatic potentials of the acetals were calculated using density functional theory at the B3LYP/6-31G* level.[85] Throughout the series, the benzylic alcohol had a higher electrostatic potential, i.e. it is more basic. This is interesting in the sense that the more basic and also less sterically hindered oxygen, does not coordinate $AlCl_3$.[i] There can be two explanations, i) the energy of the two oxocarbenium ions direct the regioselectivity or ii) initial coordination of the borane, followed by coordination of the Lewis acid. To investigate these options, the energy of the two acetals coordinated with BH_3 as well as $AlCl_3$ and the energies of the two oxocarbenium ions were calculated using density functional theory at the B3LYP/6-31G** level (Figure 6.1).[159]

[i] The generally accepted mechanism always stipulate the Lewis acid on the oxygen that will become the free hydroxyl.

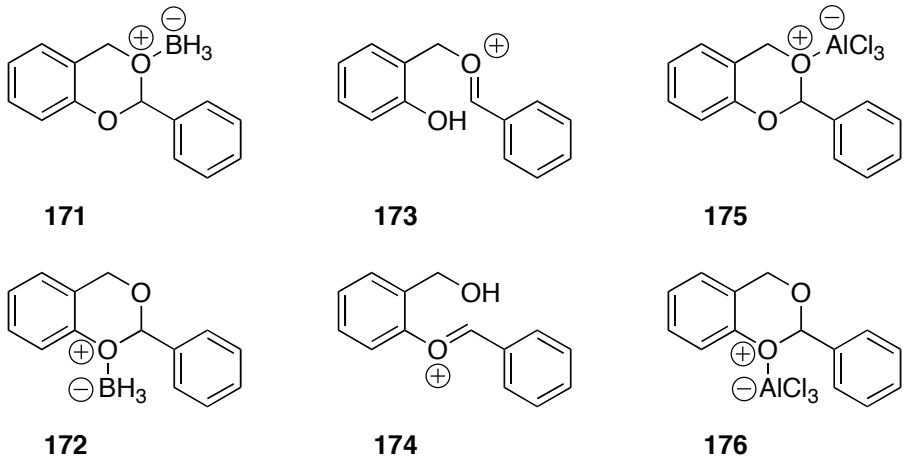

Figure 6.1 Calculated structures.

From these energies, the relative distributions were calculated using the Boltzmann distribution (Equation 6.1), which indicated exclusive formation of **171**, **173** and **175** (Table 6.3). This means that both the more stable oxocarbenium ion (**173**) and borane-associated acetal (**171**) gives the same product.

$$\frac{N_i}{N_j} = e^{-\frac{(E_i - E_j)}{RT}}$$

Equation 6.1 Boltzmann distribution.

Table 6.3 Boltzmann distribution of **171**-**176**.

Compound	E_i (hartrees)	E_j (hartrees)	E_i-E_j (J/mol)	N_j/N_i	N_i (%)	N_j (%)
171/172	-717.805985(**171**)	-717.795623(**172**)	-27209	161735	100	0
173/174	-691.535612(**173**)	-691.517865 (**174**)	-37516	15199764	100	0
175/176	-2314.440589(**175**)	-2314.432388(**176**)	-21521	13182	100	0

6.4.3 Hammett plots

To gain more insight into the mechanistic path, a study of Hammett plots was performed. The acetals (**141**-**149**) were subjected to BH_3•NMe_3 and $AlCl_3$ in THF at 0 °C. At different reaction times, samples were taken and quenched with aqueous $NaHCO_3$, extracted, concentrated and analyzed by NMR. The molar concentration of product, determined from NMR peak ratios, was plotted versus time, and all reactions were run in triplicate. Linear regression over the linear parts of the curves gave the initial reaction rates. The Hammett correlation for the alcohol ring was best fitted to σ_{para}-parameter (R^2 0.955) and for the aldehyde part, the best fit was to σ^+-parameters (R^2 0.959) (Figure 6.2). Both Hammett plots had negative ρ-values, with a more pronounced effect from the aldehyde part. The negative ρ-value indicates that electron-donating groups increase the reaction rate and since the ρ-value is lower for the aldehyde part, the substituents in this part of the molecule influence the system more. Since the reaction rate is more affected from the aldehyde part, the build-up of a positive charge on the acetal carbon is more important than the charge on the phenolic oxygen.

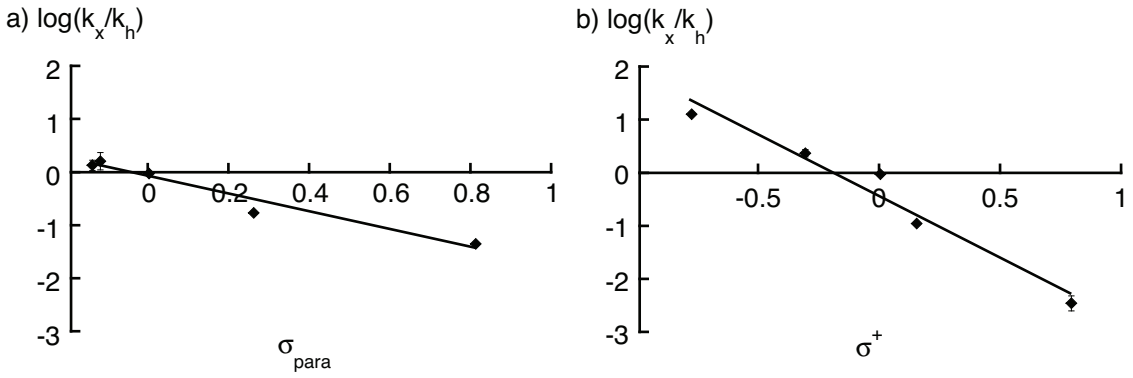

Figure 6.2 Hammett plots for a) substitution on the salicylic part and b) substitution in the aldehyde ring. Error bars show standard deviation.

6.4.4 Reaction order analysis

To further evaluate the mechanism, the reaction orders for the different components in the reaction were determined. The initial concentrations of **141**, BH_3•NMe_3 and $AlCl_3$ were varied systematically and the initial rates were calculated the same way as for the Hammett study. All reactions were run in at least duplicate. From these reactions it is seen that the

reaction is first order with respect to the acetal, higher order with respect to $AlCl_3$ and for BH_3•NMe_3 the relationship is complicated.

The first order kinetics for the acetal is easily explained. Moreover, a possible explanation for the result with $AlCl_3$ and BH_3•NMe_3 is a pre-activation of the borane by the Lewis acid, before the reductive opening. To further investigate this possibility, the formation energy for different complexes were estimated based on known dissociation energies[160-162] (Table 6.4) and calculated data for **171** and **175** (Table 6.3).

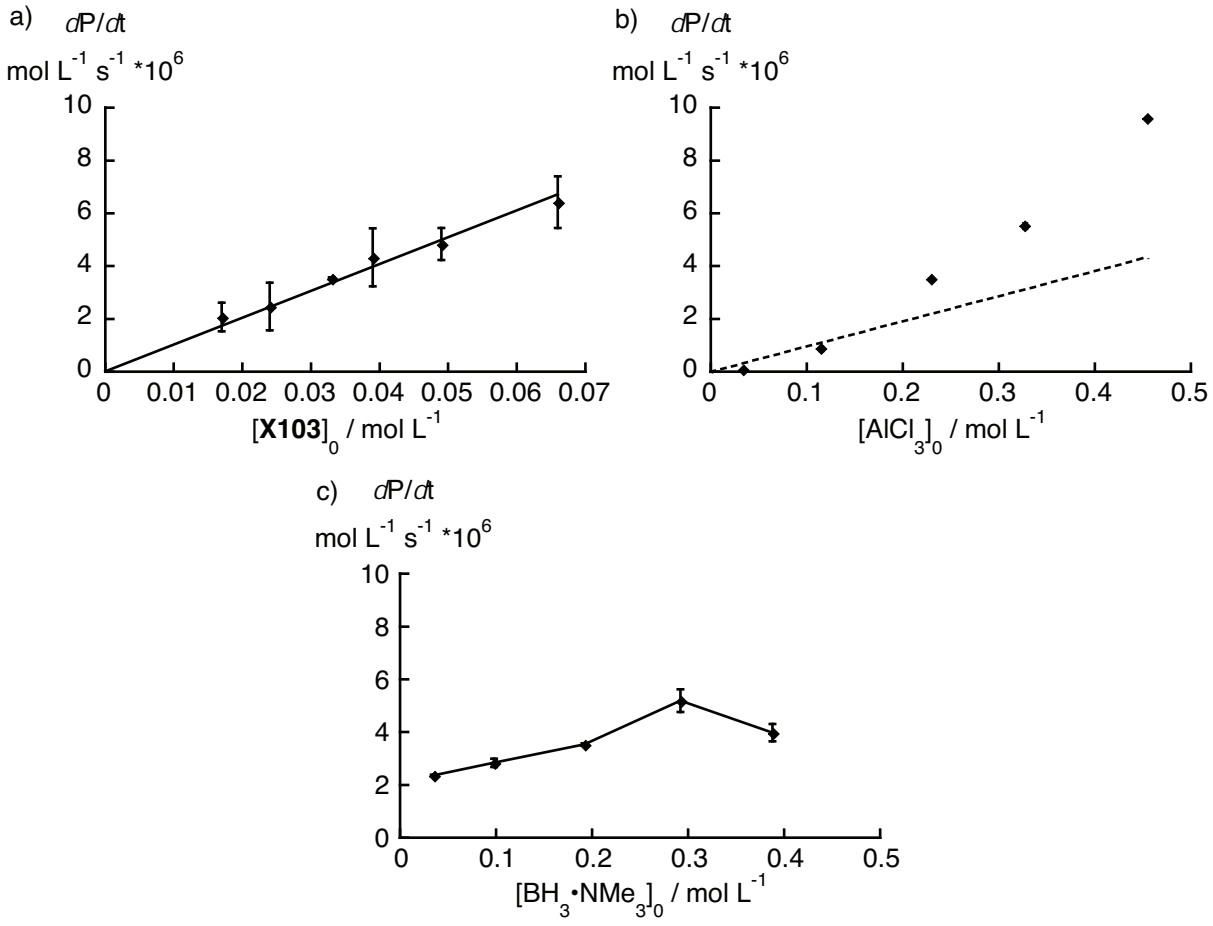

Figure 6.3 Initial rate analysis of the formation of **162**. Variation of a) **141**; b) $AlCl_3$; c) BH_3•NMe_3. Error bars show standard deviation. The dotted line in b) indicate first-order.

Table 6.4 Dissociation energies of Lewis acid-base complexes.[160-162]

Complex	Dissociation energy (kJ/mol)
BH_3•NMe_3	160
$AlCl_3$•NMe_3	199
$AlCl_3$•THF	90
$AlCl_3$•2THF	132

To summarize, the data indicate that reaction a), in Scheme 6.16, is thermodynamically unfavorable by 32 kJ/mol, reaction b) is thermodynamically unfavorable by 45 kJ/mol, but reaction c) is thermoneutral, with the formation of the highly stabilized $AlCl_3$•NMe_3 as driving force.

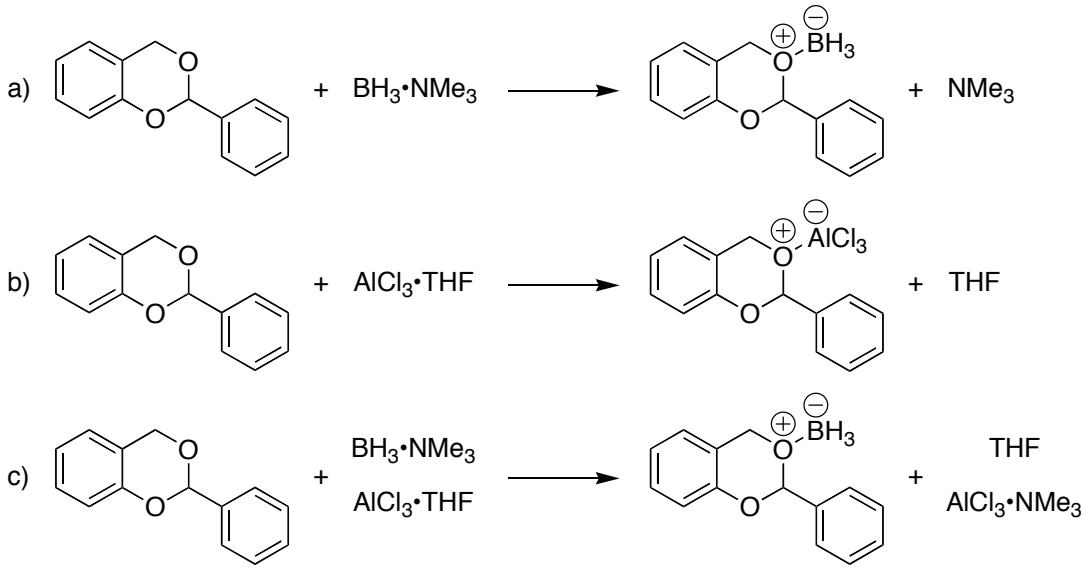

Scheme 6.16 Possible reactions between species in the mixture. a) and b) are thermodynamically unfavoured and c) is thermoneutral.

This pre-activation of the borane by $AlCl_3$, explains both the kinetic behavior of the borane and the Lewis acid. In the curve for variation of borane there are two irregularities, i) the reaction rate decrease when there is more than 9 equivalents of borane and ii) the reaction has a too high rate at the first point (1 equivalent borane). The relationship for the BH_3•NMe_3 and $AlCl_3$ is complicated and must be discussed in relationship to each other. When the amount of borane increases, the Lewis acid will generate the reactive species to the extent that is possible, at the most, the same as the amount $AlCl_3$ present. When the

amount of borane exceeds the amount of $AlCl_3$, no more active borane can be formed, and the reaction rate will decline. However, the released NMe_3 will also quench the $AlCl_3$, forming the stable $AlCl_3$•NMe_3 complex, and thus slow down the reaction. This will therefore give a reduced reaction rate based on borane. In the other end, when the amount of borane is low, compared to $AlCl_3$, the amount of free $AlCl_3$ is high. With the high amount of $AlCl_3$ present, the second step, i.e. the coordination of the $AlCl_3$ to the acetal oxygen, is fast and hence the reaction rate is higher than anticipated.

6.4.5 Boron NMR

To establish the fate of the borane, we turned to boron NMR. Since there is only one borane species at the start of the reaction, the reactant would be easy to follow. The reaction was performed in THF-*d*8 in an NMR tube and followed for 24 hours (first 45 minutes intensely) (Figure 6.4). At the start of the reaction (before addition of $AlCl_3$) only a quartet at –7.5 ppm is observed. This splitting (i.e. quartet) indicate that it is a B-H_3 species and the shift that it is BH_3•NMe_3.[163] In the course of the reaction, a new peak appeared at 8 ppm. This peak, a triplet, indicates that this is a BH_2 species, and that it probably is associated with oxygen. The species Me_3N•BH_2 would appear at 38 ppm. Since no peak was formed at 38 ppm, we conclude that the boron-nitrogen coordination is broken, probably by interaction with $AlCl_3$. A weak peak appears at 0 ppm within 45 minutes, this peak looks like a broad triplet, a BH_2, which is most likely coordinated to THF.

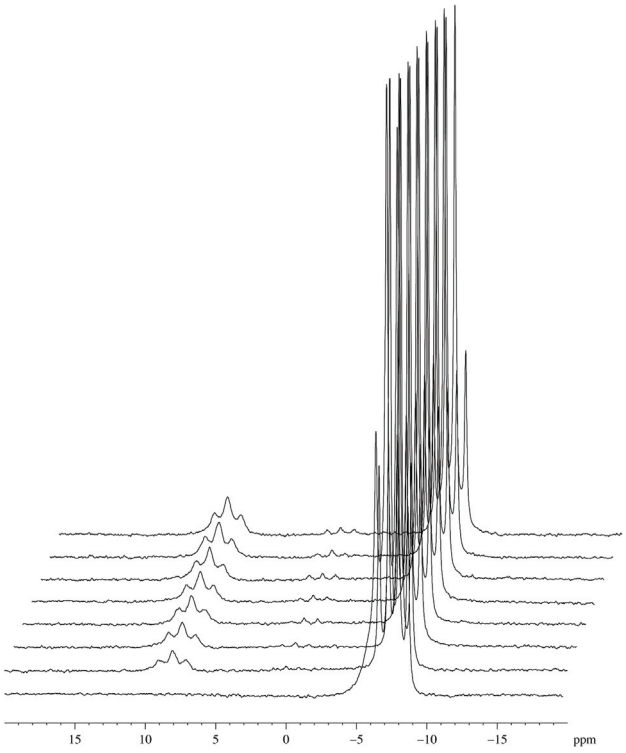

Figure 6.4 Stacked ^{11}B-NMR spectra of the reductive opening of **141** (0-45 min).

6.4.6 Reverse opening

In the original article for the reductive opening of acetals with BH_3•NMe_3/$AlCl_3$ the authors showed that the regioselectivity could be controlled by the solvent.[94] The focus for our next study was to further explore the mechanism to find conditions for reverse opening as well.

The acetal **141** was subjected to a wide range of different opening conditions. When BH_3•NMe_3 was substituted with BH_3•THF the reaction gave the same product, **162**, but the reaction rate was much lower. The addition of one equivalent of NEt_3 or 0.1 equivalent of BH_3•NMe_3 did not speed up the reaction. When BH_3•THF was used together with BF_3•OEt_2 as Lewis acid, product was formed over night, but degradation was also observed. $In(OTf)_3$, $Hg(OTf)_2$, $Cu(OTf)_2$ or AgOTf were also used as Lewis acids, but gave mainly degradation.

When BH_3•NMe_3 was used together with $AlCl_3$ the reaction was fast in dichloromethane, slower in toluene and acetonitrile and very slow in THF. If the Lewis acid was exchanged for $In(OTf)_3$ no opening could be observed and only degradation occurred. With $Hg(OTf)_2$, product was formed together with degradation, both in THF and CH_2Cl_2.

When we used AcOH as solvent, salicylic alcohol was isolated. With reverse addition, i.e. addition of $AlCl_3$ prior to BH_3•NMe_3, more or less everything was degraded, even before addition of borane.

In an attempt to trap the formed free hydroxyl group, methyl iodide was used. Methyl iodide together with BH_3•NMe_3 gave no reaction, not even at reflux over night. Using BH_3•THF, small amounts of normal opening was seen on crude NMR, but no methyl ether could be isolated.

In our proposed mechanism, the borane preorganizes to the more basic acetal oxygen followed by activation of the second oxygen with the Lewis acid. If the phenolic oxygen would be the more basic, the opening would then be reversed. Thus, the electrostatic potential for a range of different acetals were calculated. Since the substitution in the aldehyde part will affect the oxygens equally, only compounds varied in the alcohol part were calculated. It turns out that the only molecule found that had a reverse electrostatic potential is 6,8-dimethoxy-2-phenyl-4*H*-benzo[d][1,3]dioxine (**177**) (Figure 6.5). This substance was however not synthesized, since the steric effect on the phenolic acetal oxygen is too large to make this a suitable candidate.

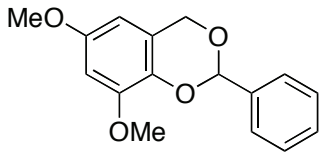

177

Figure 6.5 Compound **177**, with reversed electrostatic potential.

6.5 Evaluation of regioselectivity

6.5.1 Reductive opening of catechol acetals

To understand the acetal ring openings better, we designed a new model system based on catechol, where the difference in the steric hindrance of the two oxygen atoms would be minimized. The regioselectivity in this system should then only originate from electrostatic effects. At first, catechol was coupled with benzaldehyde dimethyl acetal in 22% yield and opened using BH_3•NMe_3/$AlCl_3$ in THF. As it turned out, the catechol acetals were much more difficult to open than the corresponding benzylic–phenolic acetals and the reactions

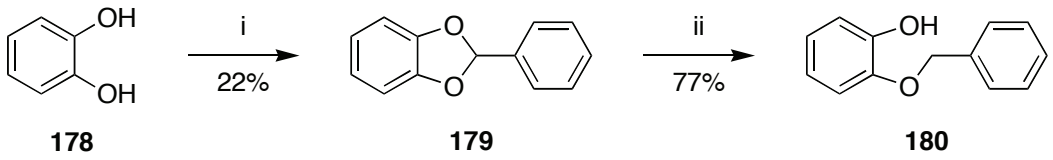

178 179 180

Scheme 6.17 Synthesis and opening of **179**. i) benzaldehyde dimethyl acetal, *p*TSA, MeCN, reflux, 18 h.; ii) BH_3•NMe_3, $AlCl_3$, THF, reflux, 1.3 h.

had to be run at refluxing THF for 1.5 hours to get 2-benzyloxy-phenol (**180**) in 77% yield (Scheme 6.17).

However this showed that the system worked for the regioselective openings and we continued by reacting 4-methoxycatechol and 4-nitrocatechol with benzaldehyde dimethyl acetal. 4-Nitrocatechol was hence coupled with benzaldehyde dimethyl acetal in acetonitrile with *p*TSA as acid, to give 5-nitro-2-phenyl-benzo[1,3]dioxole (**182**) in only 12% yield, however when the solvent was exchanged for toluene and the reaction was run at reflux the yield increased to 56% (Scheme 6.18).

4-Methoxycathechol **(184**) was synthesized from 4-methoxysalicylaldehyde (**183**) that was converted to the catechol with hydrogen peroxide and sodium hydroxide in 93% yield.[164] The catechol was then coupled to benzaldehyde dimethyl acetal with *p*TSA in acetonitrile. Unfortunately, no product was formed, not even at elevated temperature. The reaction was also tested with sulfuric acid in dichloromethane and *p*TSA in toluene, but no product could be isolated. We then changed the dimethyl acetal for benzal bromide and stirred it in acetonitrile with potassium carbonate as base, and we could then isolate a small amount of product.[165] It is reported earlier that the coupling of these acetals can be difficult, and exchanging the benzaldehyde dimethyl acetal for benzal bromide would increase the yield.[166] Since this reaction proceeds via an S_N2 mechanism, we decided to change the solvent to DMF, and use a stronger base, K_3PO_4, which increased the yield of **185** to 24% (Scheme 6.19).

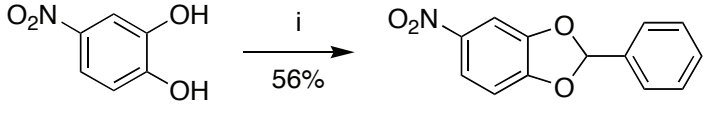

181 182

Scheme 6.18 Synthesis of **182**. i) benzaldehyde dimethyl acetal, *p*TSA, toluene, reflux, 5.6 h.

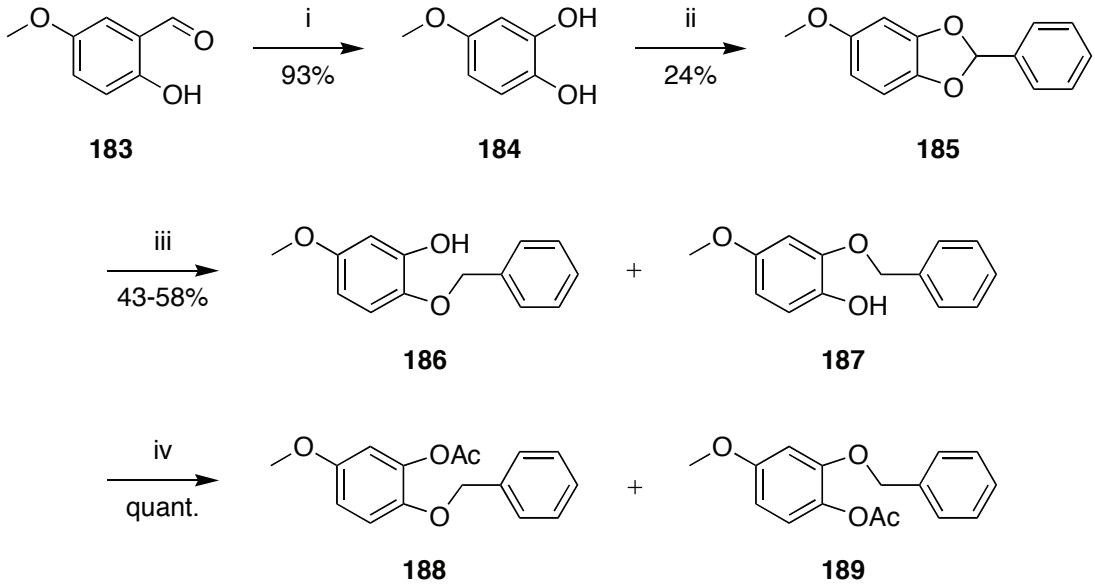

Scheme 6.19 Synthesis and opening of **185**. i) H_2O_2, NaOH, H_2O/THF, 5.2 h; ii) benzal bromide, K_3PO_4, DMF, 18h; iii) BH_3•NMe_3, $AlCl_3$, THF, reflux, 2 h, or BH_3•THF, $AlCl_3$, THF, reflux, 2 h; iv) Ac_2O, pyridine, 2.5 h.

The nitro (**182**) and methoxy (**185**) derivatized acetals were then reacted with BH_3•NMe_3/$AlCl_3$ in reflux THF. **185** opened to give a mixture of 66:34 of 2-benzyloxy-5-methoxy-phenol (**186**) and 2-benzyloxy-4-methoxy-phenol (**187**). The assignment of **186**/**187** was not possible due to overlapping signals in NMR and to distinguish between the two different products, the mixture was acetylated and the signals for 2-benzyloxy-5-methoxy-phenyl acetate (**188**)/2-benzyloxy-4-methoxy-phenyl acetate (**189**) were separated. All attempts to reductively open nitro analog **182** failed, and it appeared to be inert under these conditions, even at prolonged reaction times.

Since we needed another acetal to compare with, and we knew that unsubstituted **179** opens under these conditions we decided to use the 4-methylcatechol (**190**). The acetal was synthesized in 15% yield using K_3PO_4 in DMF. The acetal was opened according to the same method (BH_3•NMe_3/$AlCl_3$ in reflux THF) to give 2-benzyloxy-5-methyl-phenol (**192**)/2-benzyloxy-4-methyl-phenol (**193**) in a 53:47 ratio. The product distribution was easily determined based on the known NMR of **192**.[167]

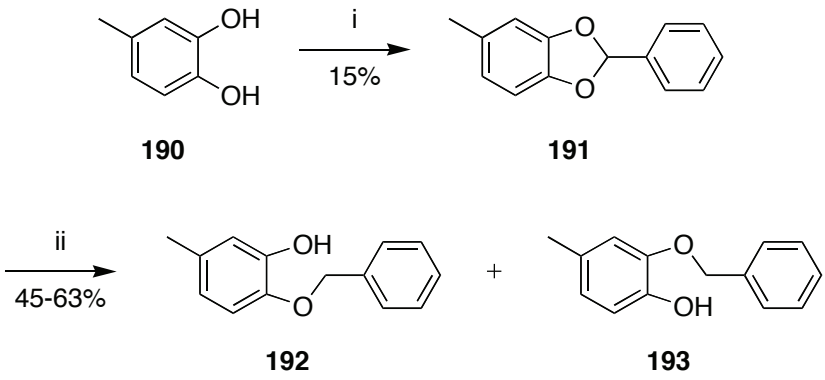

Scheme 6.20 Synthesis and opening of **191**. i) benzal bromide, K_3PO_4, DMF, 18h; ii) BH_3•NMe_3, $AlCl_3$, THF, reflux, 2 h, or BH_3•THF, $AlCl_3$, THF, reflux, 2 h.

We then tested the acetal ring opening with the same conditions using BH_3•THF complex instead, and isolated the same products, but in reverse distributions, i.e. 35:65 for **186**/**187** and 47:53 for **192**/**193**.

6.5.2 Computational chemistry on catechol acetals

There are three possible reactive intermediates that can direct the regiochemistry (Figure 6.6): i) BH_3 coordinated to the oxygen atom of the acetal (**194**-**197**), ii) $AlCl_3$ coordinated to the oxygen atom of the acetal (**198**-**201**) or iii) the oxocarbenium ions (**202**-**205**). The energies for **194**-**205** were calculated using density functional theory at the B3LYP/6-31G** level.[159]

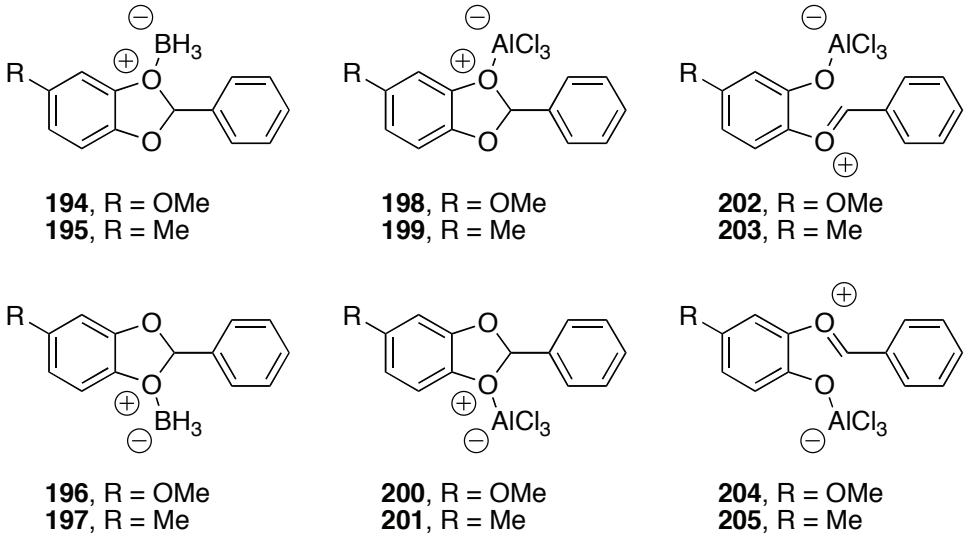

Figure 6.6 Calculated structures.

Table 6.5 Boltzmann distribution of **194**-**205**.

Compound	E_i (hartrees)	E_j (hartrees)	E_i-E_j (J/mol)	N_j/N_i	N_i (%)	N_j (%)
194/**196**	-793.007560(**196**)	-793.006895(**194**)	-1756.20	1.86	65	35
195/**197**	-717.803074(**197**)	-717.802922(**195**)	-399.13	1.15	54	46
198/**200**	-2389.643084(**200**)	-2389.642189(**198**)	-2350.16	2.31	70	30
199/**201**	-2314.439264(**201**)	-2314.439164(**199**)	-262.59	1.10	52	48
202/**204**	-2389.648326(**202**)	-2314.644316(**204**)	-10529.75	42.47	98	2
203/**205**	-2314.443969(**203**)	-2314.442638(**205**)	-3495.04	3.47	78	22

From the energies, the relative distributions were calculated using the Boltzmann distribution (Equation 6.1, Table 6.5). These results showed a remarkable agreement between initial coordination of the borane in the reaction with BH_3•NMe_3 as reducing agent and a similar correlation for the association of $AlCl_3$ in the reaction with BH_3•THF as reducing agent. It also seems less likely that the outcome is directed by the oxocarbenium ions.

These result indicate that BH_3•NMe_3 is activated by $AlCl_3$, giving a higher reaction rate and also, somewhat surprising, that the borane is the most electrophilic species and hence direct the regiochemistry. Probably no activation occurs in the reaction with BH_3•THF, and the regiochemical outcome in those reactions are directed by the Lewis acid, in agreement with earlier proposed mechanisms.

6.5.3 Reductive opening of carbohydrate acetals

With this new knowledge of the reductive openings we returned to carbohydrates and the reductive opening of methyl 4,6-benzylidene-2,3-*O*-acetyl-α-D-glucopyranoside (**53**). **53** was subjected to a range of different acetal opening reaction conditions. The reaction was performed with BH_3•NMe_3 as reducing agent and $AlCl_3$ as Lewis acid in different solvents; THF gave **54**, toluene gave **55**, acetonitrile gave a mixture of **54** and **55**, and dichloromethane only gave degradation. The Lewis acid was also varied; $In(OTf)_3$, AgOTf, $Cu(OTf)_2$ and BF_3•OEt_2 gave **54** in THF with BH_3•NMe_3 as reducing agent. **53** was also subjected to BH_3•THF with different Lewis acids; $In(OTf)_3$ only gave degradation whilst

AgOTf, $Cu(OTf)_2$ and BF_3•OEt_2 gave **55**. Reactions were also performed in neat acetic acid, and in THF with methyl iodide as acid. However, none of these reactions gave any product. We also noticed that the reaction rates were faster using BH_3•NMe_3 compared to similar reactions using BH_3•THF. This was unexpected, since it is believed that BH_3•THF is a more reactive borane.[141]

6.5.4 Reaction order analysis on carbohydrates

We then performed reaction rate studies on **53**, where we decided to vary the amount of $AlCl_3$, but holding the amount of borane and **53** constant. The reactions were performed with both BH_3•NMe_3 and BH_3•THF that gave **54** and **55** respectively (Scheme 6.21). The reactions were followed by quantitative TLC, and the initial rate kinetics were determined (Figure 6.7).[i,168,169]

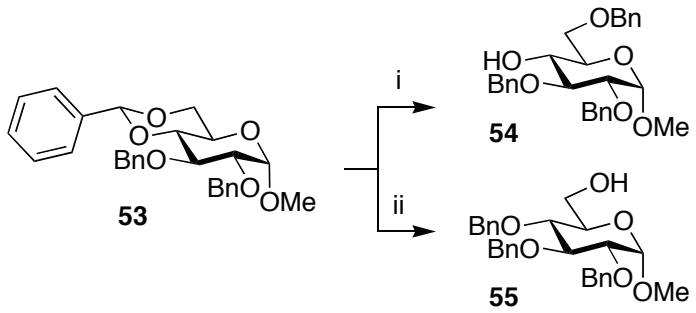

Scheme 6.21 Reductive opening of **53**. i) BH_3•NMe_3, $AlCl_3$, THF; ii) BH_3•THF, $AlCl_3$, THF.

[i] The method for quantitative TLC is discussed in detail in chapter 7.

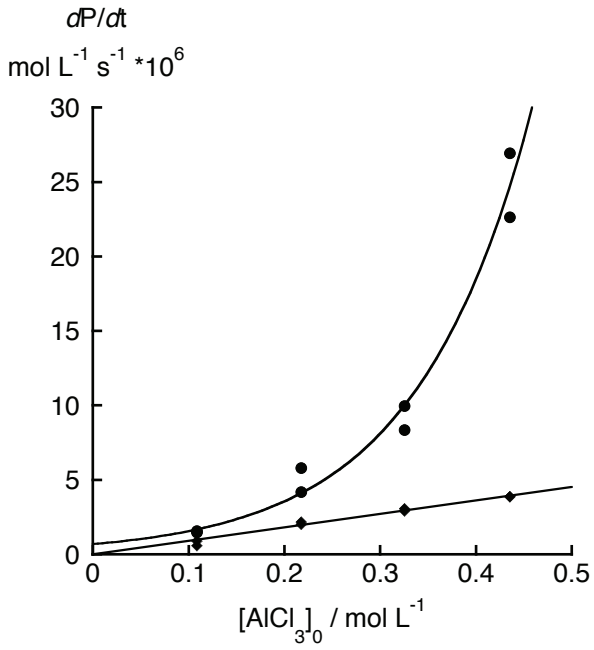

Figure 6.7 Initial rate analysis for the formation of **55** using BH_3•THF (♦) or **54** using BH_3•NMe_3 (●). All reactions were performed in duplicate.

From these experiments it was obvious that the reaction rate with BH_3•THF was slower compared to reaction with BH_3•NMe_3. It can also be seen that the reaction follows first order kinetics in the reaction with BH_3•THF and higher order for the reaction with BH_3•NMe_3, indicating an activation of the borane in this case.

6.6 Mechanistic proposal

With these results in hand we presented an improved mechanism for the acetal openings.[i] When $AlCl_3$ is added to the solution, it becomes solvated by THF forming an $AlCl_3$•THF complex. This weak complex breaks up, by reaction with BH_3•NMe_3, and generates a BH_3, coordinated to the most basic oxygen in the acetal, and $AlCl_3$•NMe_3. The BH_3 then reductively opens the acetal assisted by a second equivalent of $AlCl_3$•THF.

[i] This is an improvement based on the mechanism described in section 6.2.

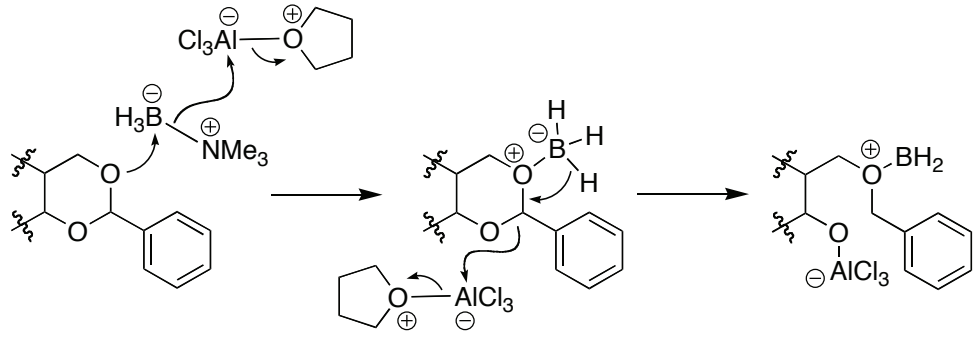

Scheme 6.22 Mechanistic proposal for the opening of benzylic-phenolic acetals.

This proposed mechanism can easily explain the higher order kinetics and the mechanism is also supported by the Hammett study.

6.7 Summary of acetal openings

We conclude that the mechanism for regioselective reductive opening of acetals can be controlled by the choice of borane. In the reaction with BH_3•THF, the Lewis acid $AlCl_3$ is the most electrophilic species and will thus coordinate to the more nucleophilic oxygen, (position 6 of carbohydrates and position 3 in the benzylic phenolic acetal) and direct the regioselectivity. In the reaction with BH_3•NMe_3, the most electrophilic species is the activated borane, which will coordinate to the more nucleophilic oxygen, thus giving reversed regioselectivity.

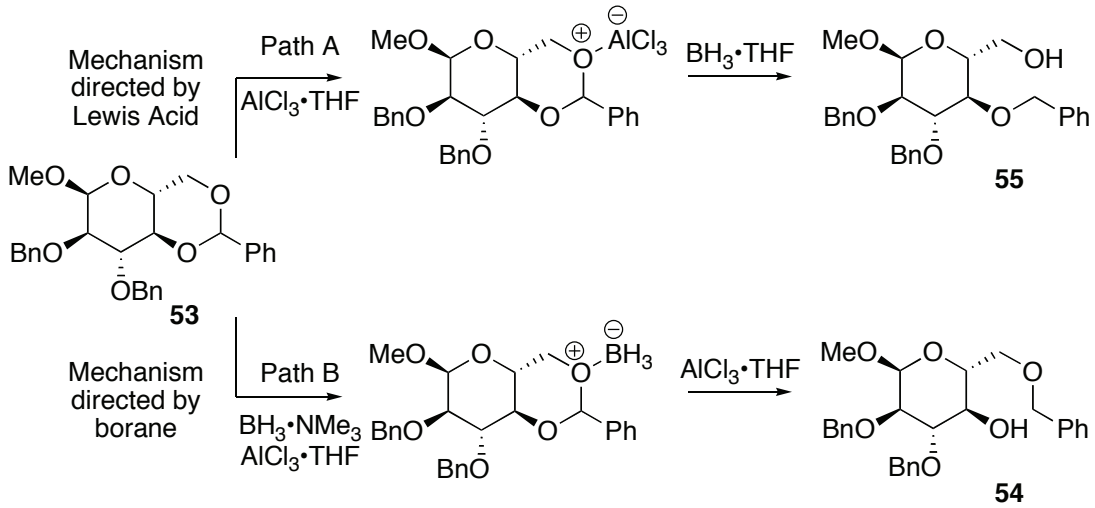

Scheme 6.23 The regiochemical outcome is directed by the relative nucleophilicity of the acetal oxygens towards the Lewis acid (Path A) or the activated borane (Path B).

7 QUANTITATIVE TLC

7.1 Background

Carbohydrates do not have any chromophores, which makes them difficult to quantify in a simple manner. TLC is on of the most widespread analytical methods in organic chemistry. It is a inexpensive method that only consumes small amounts of solvent and sample. There is a wide range of stationary phases, although the most used is SiO_2. The easiest way to analyze the sample is by scanning in the UV-region, but a wide range of staining methods are available, e.g. permanganate, sulfuric acid or anisaldehyde solutions. TLC can thus be used without requirements for UV-activity (HPLC), paramagnetic properties (NMR) or volatility (GC). Other important qualities are that TLC only uses the chromatographic surface once, which means that there is no risk of accumulation of the analyte on the stationary phase, and that the entire analyte is detected. TLC is also ideal for analyzing combinatorial reaction, since it is easy to analyze several samples simultaneously.

For long, TLC was not seen as a quantitative tool due to inadequate sample application, limited detectability, poor sensitivity and poor reproducibility. With the development of high-performance TLC, HPTLC, and the use of slit scanning densitometry the accuracy increased.[170] The drawback of the slit scanner was that the scanned lane had to be set to the largest spot, which increased the signal-to-noise ratio and that each lane had to be scanned individually.[171] The slit scanners are today exchanged for charge-coupled device (CCD). By using a CCD, the digitalization is much faster and much more efficient then a slit scanner and the results are more reliable.[170,172,173] The CCD has a low signal-to-noise ratio and it can detect samples from UV to near IR.[170]

The use of image analyzers are thought to be a powerful tool in use with TLC.[174] Today the research and development of software is scarce and only a handful of publications are available on the subject, which only analyze colored samples or generate the digital files in UV-light.[175-181] The use of staining reagents has not been evaluated.

To simplify the procedure we investigated the use of an ordinary office scanner. That makes the quantification fast, inexpensive and uncomplicated.

7.2 Software

We decided to work with the software JustTLC, which was developed in collaboration with the company Sweday.[168] The software treats the image as a three-dimensional topography. The digital image[i] is converted to grayscale at 400 dpi, followed by noise reduction and identification of the spots. The noise is reduced by a diffusion filter technique that preserves the spot shape but removes the random Gaussian noise in a robust manner. The spots are then detected, automatically or manually, and the volume of the spots are calculated by integration.

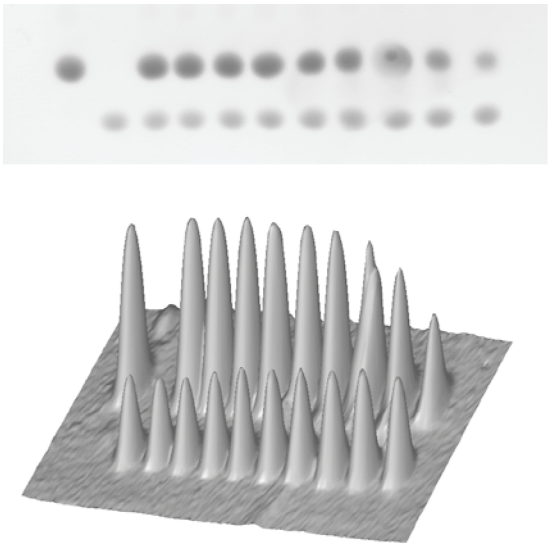

Figure 7.1 A TLC plate scanned with ordinary desktop scanner and the same plate as the three-dimensional topography that JustTLC works with.

[i] The software works with tiff, jpeg and bmp. However in this work only tiff images have been used.

7.3 Evaluation of the method

7.3.1 Useful detection range

The method is limited by the upper detection limit, i.e. full saturation of the peak intensity, and the lower detection limit with peak intensities close to the background variation. Too strong peaks are thus underestimated, while small peaks tend to be overrated.

The three different type of spots were investigated as can be seen in Figure 7.2. The weak spot is almost not detectable in the noise and the strong spot is flat at the top, indicating that the spot is saturated.

To evaluate the detection range, a series of solutions of 1,2,3,4,6-penta-*O*-acetyl-β-D-glucopyranose (**40**) in concentrations ranging from 0.0001 M to 0.5 M were prepared. Samples of 1 μL, hence giving amounts of 1 x 10^{-10} to 5 x 10^{-7} mol, were applied and eluted followed by staining with anisaldehyde, vanillin or sulfuric acid. Each experiment was performed in triplicate, scanned and evaluated using JustTLC (Figure 7.3).

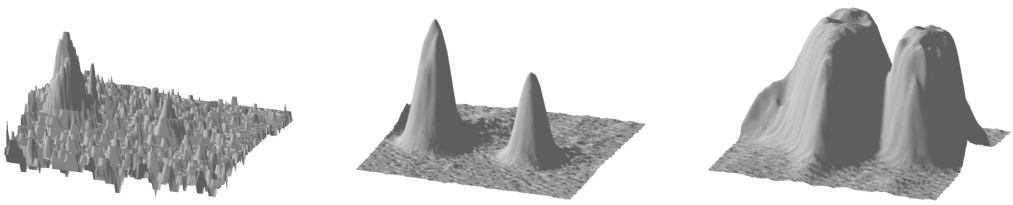

Figure 7.2 Illustration of weak spot, normal spot and saturated spot.

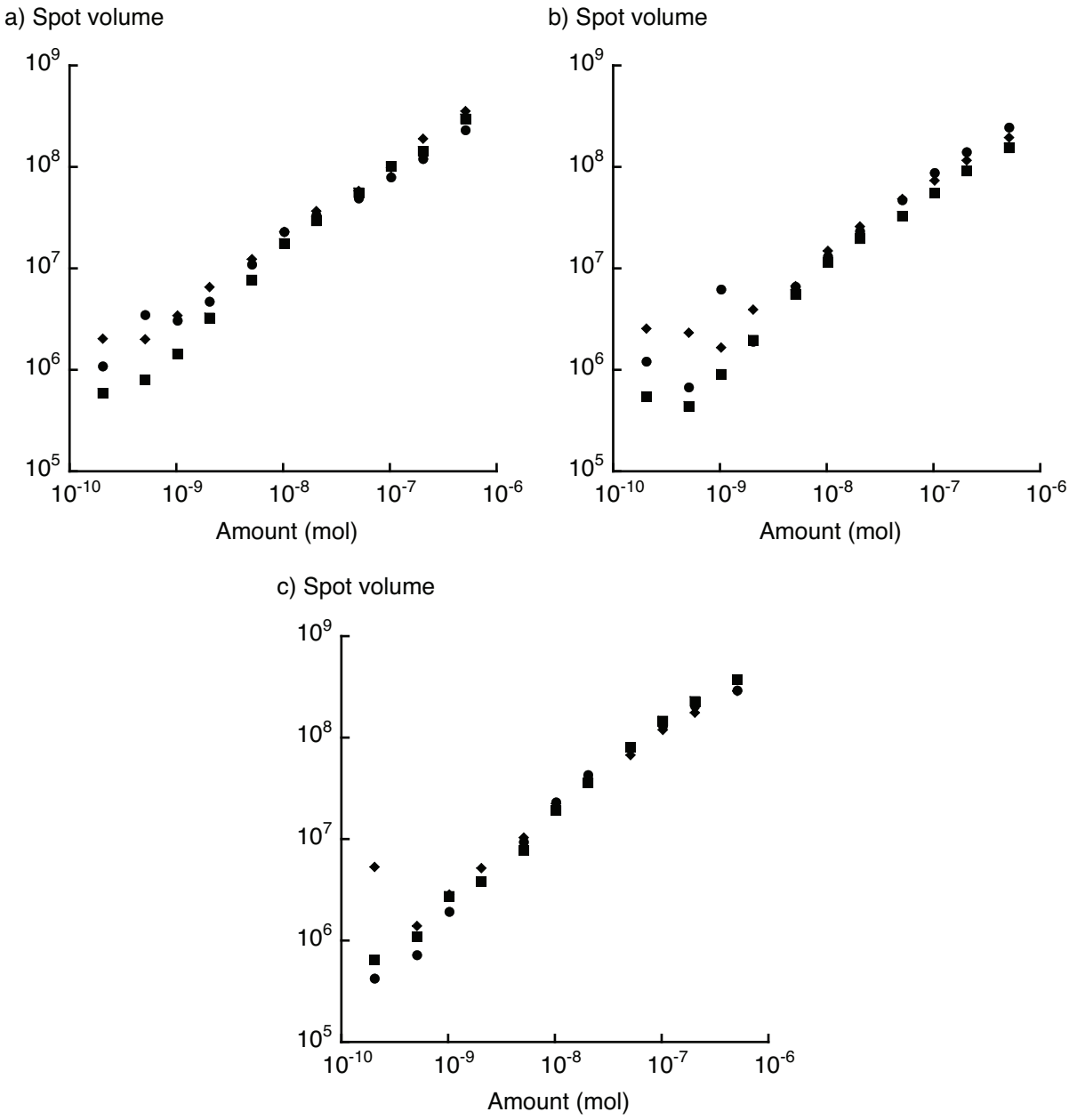

Figure 7.3 1,2,3,4,6-Penta-*O*-acetyl-β-D-glucopyranose stained with a) anisaldehyde, b) vanillin and c) sulfuric acid. Filled squares, circles and diamonds indicate three different series in each experiment.

Spots can be detected down to 2 x 10^{-10} mol but not quantified below 2 x 10^{-9} mol. Since the curve is slightly bent due to the underestimation of strong spots, and the fluctuation at low concentrations, the following work is based on 5 x 10^{-8} mol samples.

7.3.2 Estimation of errors

To estimate the errors in the process we investigated the scanning process, the sample application, and the staining process. The same plate, containing three spots of **40**,

developed with anisaldehyde, was scanned five times followed by analysis using JustTLC, and gave an error of 0.3%. The plate was also scanned at different resolutions ranging from 72 to 1200 dpi, with no difference in the relative intensities. The stability of the program's algorithm was also tested by analyzing the same digital file five times with the same result.

To evaluate the sample application, Rose Bengal[i] was spotted on a TLC plate using 'microcaps'. Ten spots of 1, 2 and 5 μL were applied to the plate, followed by scanning and analysis. This gave an error of 1.6, 1.8 and 5.0% for 1, 2 and 5 μL samples respectively. It is also possible to use more sophisticated methods of sample applications such as HPTLC applicators, but there is no need for that since the errors are small and the method convenient.

Finally, we evaluated the staining process. There are two main methods for applying staining reagents to TLC plates; spraying or dipping. Thus, ten plates with five spots of **40** were subjected to anisaldehyde by dip solution and ten plates were subjected to anisaldehyde by spraying. The plates were then heated with a hot air gun. The errors were generally lower using the dip solution, 7% versus 22%. The spray solution was applied with a hand pump and this gave rings on the plates, i.e. the first burst dried a little before the next burst of anisaldehyde was added. This could probably be minimized by using a consistent burst of staining solution.

The three different staining solutions were then developed using either a hot air gun or by heating in an oven. Ten plates, with five spots each of **40** were used for every experiment. For the hot air gun experiments the temperature was estimated to be 500-600 °C and the plates were heated until the spots did not grew any darker. For the oven experiments, the plates were heated for 15 minutes at 150 °C. The results are summarized in Table 7.1.

[i] Rose Bengal, 4,5,6,7-tetrachloro-2′,4′,5′,7′-tetraiodofluorescein disodium salt, is a colored compound.

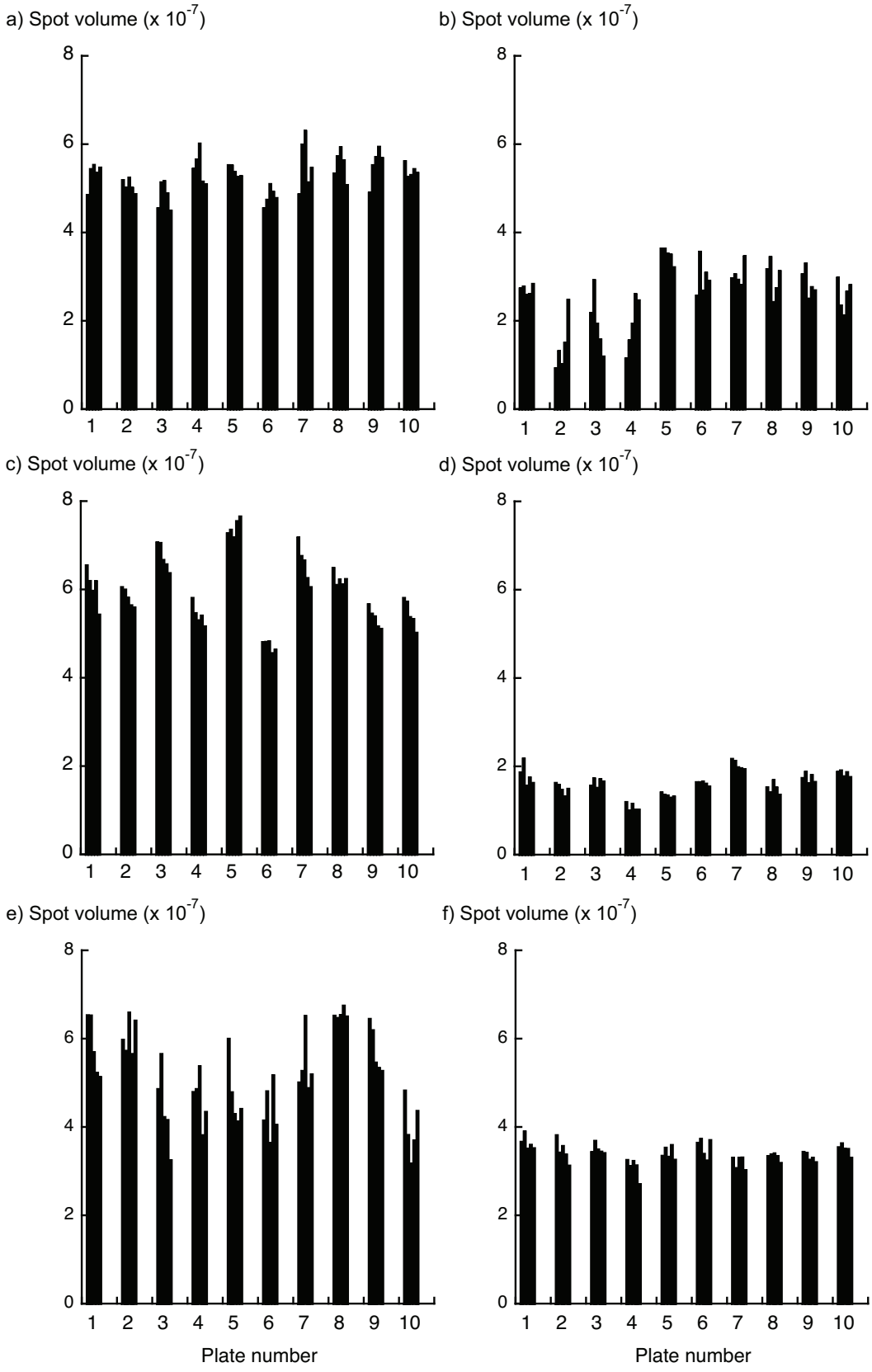

Figure 7.4 Errors using different staining reagents in combination with hot air gun or oven. a) anisaldehyde, hot air gun; b) anisaldehyde, oven; c) vanillin hot air gun; d) vanillin, oven; e) sulfuric acid, hot air gun; f) sulfuric acid, oven. Each column represents the five spots of one TLC plate.

Table 7.1 Errors using different developing techniques.

Entry[a]	Staining reagent	Heating method	Average spot volume (x 10^{-7})	Error (%)
a	Anisaldehyde	Hot air gun	5.3 ± 0.4	7
b	Anisaldehyde	Oven	2.6 ± 0.7	27
c	Vanillin	Hot air gun	6.0 ± 0.8	13
d	Vanillin	Oven	1.6 ± 0.3	17
e	Sulfuric acid	Hot air gun	5.2 ± 1.0	19
f	Sulfuric acid	Oven	3.4 ± 0.2	6

a) The entry refers to Figure 7.4.

It can be seen that the best method was sulfuric acid in oven followed by anisaldehyde with hot air gun. There is a substantial error in the staining process, especially between different plates.

7.3.3 Ratios

We conclude that the errors arise mainly from the staining process and that the errors are higher between different plates than within the same plate. One way to minimize the errors is measurement of ratios. To evaluate this method, a 1:1 anomeric mixture of isopropyl 2,3,4,6-tetra-*O*-acetyl-D-glucopyranoside was prepared and evaluated with anisaldehyde dip solution and hot air gun. The result, as shown in Figure 7.5, illustrate that the errors are much smaller than before and that different plates can be compared. Similar experiments were done with 10, 25, 75 and 90% α-glycoside, which gave the same result (Figure 7.6).

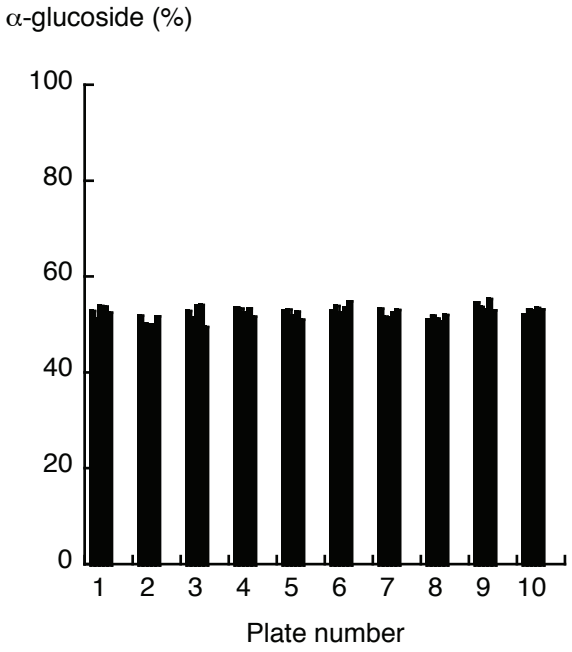

Figure 7.5 Percentage of α-glycoside in a mixture of α- and β-glycosides (1:1). In this figure it is shown that the errors are dramatically smaller both in each TLC plate but, and more importantly, between different plates. The average error is 2%.

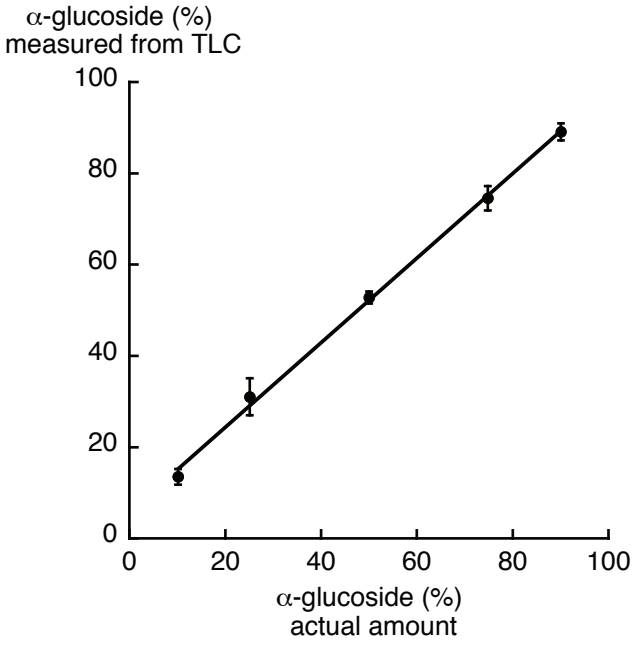

Figure 7.6 Plot of α-glycoside (%) measured from TLC versus the actual amounts. As can be seen from this figure, the result from TLC analysis correlates well with the actual ratios with excellent linearity (R > 0.99).

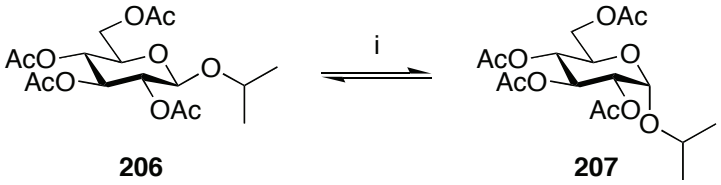

206 **207**

Scheme 7.1 Anomerization of **206** to **207**. i) BF_3•OEt_2, CH_2Cl_2, 2h.

Finally to evaluate the quantification of TLC in combination with staining reagents and JustTLC, the anomerization reaction of isopropyl 2,3,4,6-tetra-*O*-acetyl-β-D-glucopyranoside (**206**) in CH_2Cl_2 with BF_3•OEt_2 as promoter was followed (Scheme 7.1). The reaction was followed using TLC and NMR during 120 minutes, and each experiment was performed in triplicate. The outcome for both methods gave similar results (Figure 7.7).

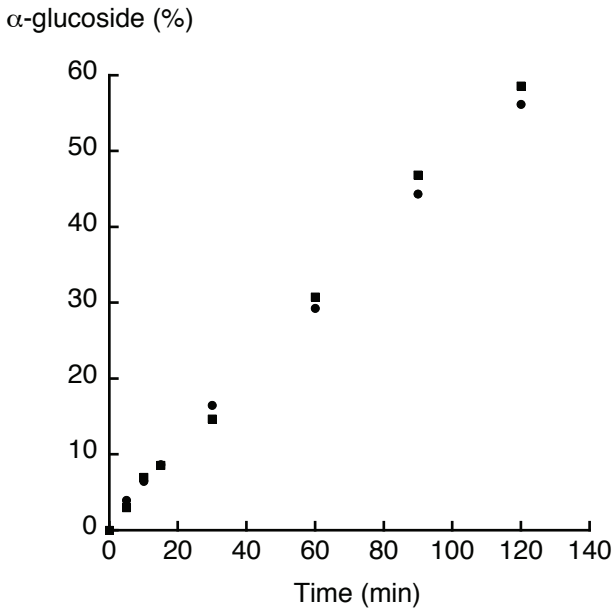

Figure 7.7 Anomerization of **206** followed by TLC (●) and NMR (■).

7.4 Summary of quantitative TLC

The software that was developed for the quantitative TLC works excellent with any form of digital image, generated from a flatbed scanner, a CCD or any other method. The errors were evaluated for the different parts of the process and the errors were very low in all parts except for the staining process. The errors for the whole process are summarized in Table 7.2.

Table 7.2 Total error in quantitative TLC

	Sample application	**Staining reagent application**	**Heating method**	**Scanning process**	**JustTLC**
Error	1.6-5.0%	7-22%	6-27%	0.3%	0.0%

The errors are large in the staining process, especially between plates. This error could arise from the difficulties with temperature, amount of developer and time for heating. The use of an internal standard minimizes the errors and the method is thus very useful.

8 SUMMARY

The understanding of biological systems and functions will help us to cure and prevent diseases. In this work we have synthesized, and evaluated, a number of labeled analogs to an antiproliferative naphthoxyloside. We have also interested us in the physical-organic investigation of the mechanism for regioselective reductive opening of benzylidene acetals. Finally, we have developed new synthetic methodology as well as analytical tools.

We conclude that the use of fluorescent probes in our assay is not a functioning method. The tested fluorescent probes are too large and alters the physical and biological properties of the small active compounds to a too large extent, which makes them poor structural analogs. To circumvent this problem we turned to radioactively labeled analogs. The choice fell on a tritiated compound and the preliminary biological data show interesting results. For example, we have proven that it is the naphthoxyloside that primes the GAG chains. We have also seen that the priming in the transformed cells is higher than in healthy cells and that it looks like an accumulation of GAG primed naphthoxylosides in the ER and Golgi apparatus.

The future perspectives in this project are to isolate the nuclei of the cells to find out if there is accumulation of GAG chains and tritiated compounds. We will also isolate endosomes to find out more about the secretory pathways. The isolated GAG chains will also be chemically degraded to find out their legths, and thus giving us knowledge where the glycosylation takes place. Of course, the two other tritiated xylosides will also be tested and some more cell lines will be used.

We have also shown that the mechanism of the regioselective reductive opening of acetals is dependant on borane, Lewis acid and solvent. We present a mechanistic proposal, where the borane is activated by the Lewis acid and gives a highly electrophilic borane, which directs the regioselectivity. On the other hand, if the borane is not activated, the Lewis acid is the most electrophilic species and hence directs the regioselectivity. However the experiment on the mixed benzylic-phenolic acetals show that the mechanism is also dependent on the substrate.

To understand more about this mechanism, other methods of regioselective opening will be examined, which will give insight in the solvent and Lewis acid dependency.

REFERENCES

1. Fischer, E. *Ber. Dtsch. Chem. Ges.* **1891,** *24*, 1836-1845.
2. Fischer, E. *Ber. Dtsch. Chem. Ges.* **1891,** *24*, 2683-2687.
3. Dwek, R. A. *Chem. Rev.* **1996,** *96*, 683-720.
4. Karlsson, K.-A. *Trends Pharmacol. Sci.* **1991,** *12*, 265-272.
5. Varki, A. *Glycobiology* **1993,** *3*, 97-130.
6. Collins, P. M.; Ferrier, R. J. *Monosaccharides: Their Chemistry and Their Roles in Natural Products*; John Wiley & Sons: Chichester, 1995.
7. Nicolaou, K. C.; Mitchell, H. J. *Angew. Chem., Int. Ed.* **2001,** *40*, 1576-1624.
8. Werz, D. B.; Seeberger, P. H. *Chem.-Eur. J.* **2005,** *11*, 3194-3206.
9. Stick, R. V. *Carbohydrates: The Sweet Molecules of Life*; Academic Press: London, 2001.
10. Lichtenthaler, F. W. *Angew. Chem., Int. Ed.* **1992,** *31*, 1541-1556.
11. Jacobsson, M.; Malmberg, J.; Ellervik, U. *Carbohydr. Res.* **2006,** *341*, 1266-1281.
12. Ellervik, U.; Jansson, K.; Magnusson, G. *J. Carbohydr. Chem.* **1998,** *17*, 777-784.
13. Lee, Y. S.; Rho, E. S.; Min, Y. K.; Kim, B. T.; Kim, K. H. *J. Carbohydr. Chem.* **2001,** *20*, 503-506.
14. Sokolov, V. M.; Zakharov, V. I.; Studentsov, E. P. *Russ. J. Gen. Chem.* **2002,** *72*, 806-811.
15. Kröger, L.; Thiem, J. *J. Carbohydr. Chem.* **2003,** *22*, 9-23.
16. Burger, K.; Kluge, M.; Koksch, B.; Fehn, S.; Böttcher, C.; Henning, L.; Müller, G. *Heterocycles* **2004,** *64*, 143-152.
17. Brewster, K.; Harrison, J. M.; Inch, T. D. *Tetrahedron Lett.* **1979,** *20*, 5051-5054.
18. Beejmohun, V.; Grand, E.; Mesnard, F.; Fliniaux, M.-A.; Kovensky, J. *Tetrahedron Lett.* **2004,** *45*, 8745-8747.
19. Watanabe, Y.; Shiozaki, M.; Kamegai, R. *Carbohydr. Res.* **2001,** *335*, 283-289.
20. Esko, J. D. In *Essentials of Glycobiology;* Varki, A.; Cummings, R.; Esko, J. D.; Freeze, H.; Hart, G.; Marth, J. Eds.; Cold Spring Harbor Laboratory Press: Cold Spring Harbor, New York, 1999; pp. 145-159.
21. Islam, T.; Linhardt, R. J. In *Carbohydrate-based Drug Discovery;* Wong, C.-H. Ed.; Wiley-VCH GmbH & Co. KGaA.: Weinheim, 2003; pp. 407-439.
22. Prydz, K.; Dalen, K. T. *J. Cell. Sci.* **2000,** *113*, 193-205.
23. Kjellén, L.; Lindahl, U. *Annu. Rev. Biochem.* **1991,** *60*, 443-475.

24. Prime, version 1.6, Schrödinger, LLC, New York, NY, **2007**.

25. Scott, P. G.; McEwan, P. A.; Dodd, C. M.; Bergmann, E. M.; Bishop, P. N.; Bella, J. *Proc. Natl. Acad. Sci. USA* **2004,** *101*, 15633-15638.

26. Chopra, R. K.; Pearson, C. H.; Pringle, G. A.; Fackre, D. S.; Scott, P. G. *Biochem. J.* **1985,** *232*, 277-279.

27. Meyer, K.; Palmer, J. W. *J. Biol. Chem.* **1934,** *107*, 629-634.

28. Fessler, J. H.; Fessler, L. I. *Proc. Natl. Acad. Sci. USA* **1966,** *56*, 141-147.

29. Fraser, J. R. E.; Laurent, T. C.; Laurent, U. B. G. *J. Intern. Med.* **1997,** *242*, 27-33.

30. Seno, N.; Toda, N. *Biochim. Biophys. Acta* **1970,** *215*, 544-546.

31. Stein, T.; Keller, R.; Stuhlsatz, H. W.; Greiling, H.; Ohst, E.; Müller, E.; Scharf, H.-D. *Hoppe-Seyler's Z. Physiol. Chem.* **1982,** *363*, 825-833.

32. Bhavanandan, V. P.; Meyer, K. *J. Biol. Chem.* **1968,** *243*, 1052-1059.

33. Brown, G. M.; Huckerby, T. N.; Morris, H. G.; Abram, B. L.; Nieduszynski, I. A. *Biochemistry* **1994,** *33*, 4836-4846.

34. Iozzo, R. V. *Lab. Invest.* **1985,** *53*, 373-396.

35. Linhardt, R. J.; Hileman, R. E. *Gen. Pharmac.* **1995,** *26*, 443-451.

36. Lidholt, K.; Kjellén, L.; Lindahl, U. *Biochem. J.* **1989,** *261*, 999-1007.

37. Bernfield, M.; Kokenyesi, R.; Kato, M.; Hinkes, M. T.; Spring, J.; Gallo, R. L.; Lose, E. J. *Ann. Rev. Cell Biol.* **1992,** *8*, 365-393.

38. Lindahl, U.; Feingold, D. S.; Roden, L. *Trends Biochem. Sci.* **1986,** *11*, 221-225.

39. Fransson, L.-Å. *Trends Biochem. Sci.* **1987,** *12*, 406-411.

40. Bernfield, M.; Götte, M.; Park, P. W.; Reizes, O.; Fitzgerald, M. L.; Lincecum, J.; Zako, M. *Ann. Rev. Biochem.* **1999,** *68*, 729-777.

41. Rider, C. C. *Glycoconjugate J.* **1997,** *14*, 639-642.

42. Tiwari, V.; O'Donnell, C. D.; Oh, M.-J.; Valyi-Nagy, T.; Shukla, D. *Biochem. Biophys. Res. Commun.* **2005,** *338*, 930-937.

43. Herold, B. C.; Visalli, R. J.; Susmarski, N.; Brandt, C. R.; Spear, P. G. *J. Gen. Virol.* **1994,** *75*, 1211-1222.

44. Horonchik, L.; Tzaban, S.; Ben-Zaken, O.; Yedidia, Y.; Rouvinski, A.; Papy-Garcia, D.; Barritault, D.; Vlodavsky, I.; Taraboulos, A. *J. Biol. Chem.* **2005,** *280*, 17062-17067.

45. Linhardt, R. J. *Chem. Ind.* **1991,** *2*, 45-50.

46. Cofrancesco, E.; Colombi, M.; Gianese, F.; Cortellaro, M. *Thromb. Res.* **1990,** *57*, 405-414.

47. Cöster, L. *Biochem. Soc. Trans.* **1991,** *19*, 866-868.

48. Zhang, L.; David, G.; Esko, J. D. *J. Biol. Chem.* **1995,** *270*, 27127-27135.

49. Chen, R. L.; Lander, A. D. *J. Biol. Chem.* **2001,** *276*, 7507-7517.

50. Helting, T.; Rodén, L. *Biochem. Biophys. Res. Commun.* **1968,** *31*, 786-791.

51. Helting, T.; Rodén, L. *J. Biol. Chem.* **1969,** *244*, 2790-2798.

52. Helting, T.; Rodén, L. *J. Biol. Chem.* **1969,** *244*, 2799-2805.

53. Okayama, M.; Kimata, K.; Suzuki, S. *J. Biochem. (Tokyo, Jpn.)* **1973,** *74*, 1069-1073.

54. Robinson, H. C.; Brett, M. J.; Tralaggan, P. J.; Lowther, D. A.; Okayama, M. *Biochem. J.* **1975,** *148*, 25-34.

55. Fukunaga, Y.; Sobue, M.; Suzuki, N.; Kushida, H.; Suzuki, S.; Suzuki, S. *Biochim. Biophys. Acta* **1975,** *381*, 443-447.

56. Lugemwa, F. N.; Esko, J. D. *J. Biol. Chem.* **1991,** *266*, 6674-6677.

57. Fritz, T. A.; Lugemwa, F. N.; Sarkar, A. K.; Esko, J. D. *J. Biol. Chem.* **1994,** *269*, 300-307.

58. Sarkar, A. K.; Fritz, T. A.; Taylor, W. H.; Esko, J. D. *Proc. Natl. Acad. Sci. USA* **1995,** *92*, 3323-3327.

59. Sarkar, A. K.; Esko, J. D. *Carbohydr. Res.* **1995,** *279*, 161-171.

60. Mani, K.; Havsmark, B.; Persson, S.; Kaneda, Y.; Yamamoto, H.; Sakurai, K.; Ashikari, S.; Habuchi, H.; Suzuki, S.; Kimata, K.; Malmström, A.; Westergren-Thorsson, G.; Fransson, L.-Å. *Cancer Res.* **1998,** *58*, 1099-1104.

61. Mani, K.; Belting, M.; Ellervik, U.; Falk, N.; Svensson, G.; Sandgren, S.; Cheng, F.; Fransson, L.-Å. *Glycobiology* **2004,** *14*, 387-397.

62. Jacobsson, M.; Ellervik, U. *Tetrahedron Lett.* **2002,** *43*, 6549-6552.

63. Jacobsson, M.; Ellervik, U.; Belting, M.; Mani, K. *J. Med. Chem.* **2006,** *49*, 1932-1938.

64. Malmberg, J.; Mani, K.; Säwén, E.; Wirén, A.; Ellervik, U. *Bioorg. Med. Chem.* **2006,** *14*, 6659-6665.

65. Jacobsson, M.; Mani, K.; Ellervik, U. *Bioorg. Med. Chem.* **2007,** *15*, 5283-5299.

66. Cheng, F.; Johnsson, R.; Nilsson, J.; Fransson, L.-Å.; Ellervik, U.; Mani, K. to be submitted for publication, **2008**.

67. Lichtenthaler, F. W.; Kläres, U.; Szurmai, Z.; Werner, B. *Carbohydr. Res.* **1998,** *305*, 293-303.

68. Johnsson, R.; Ellervik, U. *Synlett* **2005**, 2939-2940.

69. Mori, M.; Ito, Y.; Oqawa, T. *Carbohydr. Res.* **1990,** *195*, 199-224.

70. Excoffier, G.; Gagnaire, D.; Utille, J.-P. *Carbohydr. Res.* **1975,** *39*, 368-373.

71. Watanabe, K.; Itoh, K.; Araki, Y.; Ishido, Y. *Carbohydr. Res.* **1986,** *154*, 165-176.

72. Nudelman, A.; Herzig, J.; Gottlieb, H. E.; Keinan, E.; Sterling, J. *Carbohydr. Res.* **1987,** *162*, 145-152.

73. Herzig, J.; Nudelman, A.; Gottlieb, H. E. *Carbohydr. Res.* **1988,** *177*, 21-28.

74. Sambaiah, T.; Fanwick, P. E.; Cushman, M. *Synthesis* **2001**, 1450-1452.

75. Helferich, B.; Portz, W. *Chem. Ber.* **1953,** *86*, 604-612.

76. Itoh, T.; Takamura, H.; Watanabe, K.; Araki, Y.; Ishido, Y. *Carbohydr. Res.* **1986,** *156*, 241-246.

77. Fiandor, J.; García-Lopez, M. T.; del la Heras, F. G.; Méndez-Castrillón, P. P. *Synthesis* **1985**, 1121-1123.

78. Mikamo, M. *Carbohydr. Res.* **1989,** *191*, 150-153.

79. Rowell, R. M.; Feather, M. S. *Carbohydr. Res.* **1967,** *4*, 486-491.

80. Herzig, J.; Nudelman, A. *Carbohydr. Res.* **1986,** *153*, 162-167.

81. Zhang, J.; Kovác, P. *J. Carbohydr. Chem.* **1999,** *18*, 461-469.

82. Cook, B. N.; Bhaka, S.; Biegel, T.; Bowman, K. G.; Armstrong, J. I.; Hemmerich, S.; Bertozzi, C. R. *J. Am. Chem. Soc.* **2000,** *122*, 8612-8622.

83. Van, T. N.; Claessens, S.; Habonimana, P.; Tehrani, K. A.; Van Puyvelde, L.; De Kimpe, N. *Synlett* **2006**, 2469-2471.

84. Musso, H.; Matthies, H.-G. *Chem. Ber.* **1961,** *94*, 356-368.

85. Spartan '02 for Macintosh, Wavefunction, Inc. Irvine, CA.

86. Fransson, L.-Å.; Havsmark, B.; Sakurai, K.; Suzuki, S. *Glycoconjugate J.* **1992,** *9*, 45-55.

87. Fransson, L.-Å.; Karlsson, P.; Schmidtchen, A. *Biochim. Biophys. Acta* **1992,** *1137*, 287-297.

88. Foti, M. C.; Johnson, E. R.; Vinqvist, M. R.; Wright, J. S.; Barclay, L. R. C.; Ingold, K. U. *J. Org. Chem.* **2002,** *67*, 5190-5196.

89. O'Brien, P. J. *Chem. Biol. Interact.* **1991,** *80*, 1-41.

90. Scott, L. T.; Rozeboom, M. D.; Houk, K. N.; Fukunaga, T.; Lindner, H. J.; Hafner, K. *J. Am. Chem. Soc.* **1980,** *102*, 5169-5176.

91. Valeur, B. *Molecular Fluorescence: Principles and Applications.*; Wiley-VCH Verlag GmbH: Weinheim, 2001.

92. Ellervik, U. *Tetrahedron Lett.* **2003,** *44*, 2279-2281.

93. Garegg, P. J.; Hultberg, H. *Carbohydr. Res.* **1981,** *93*, C10-C11.

94. Ek, M.; Garegg, P. J.; Hultberg, H.; Oscarson, S. *J. Carbohydr. Chem.* **1983,** *2*, 305-311.

95. Andretti, G. D.; Böhmer, V.; Jordon, J. G.; Tabatabai, M.; Ugozzoli, F.; Vogt, W.; Wolff, A. *J. Org. Chem.* **1993,** *58*, 4023-4032.

96. Yoon, N. M.; Pak, C. S.; Brown, H. C.; Krihnamurthy, S.; Stocky, T. P. *J. Org. Chem.* **1973,** *38*, 2786-2792.

97. Sim, M. M.; Kondo, H.; Wong, C.-H. *J. Am. Chem. Soc.* **1993,** *115*, 2260-2267.

98. Ellervik, U.; Magnusson, G. *Tetrahedron Lett.* **1997,** *38*, 1627-1628.

99. Valkó, K.; Plass, M.; Bevan, C.; Reynolds, D.; Abraham, M. H. *J. Chromatogr., A* **1998,** *797*, 41-55.

100. Hanai, T.; Koizumi, K.; Kinoshita, T.; Arora, R.; Ahmed, F. *J. Chromatogr., A* **1997,** *762*, 55-61.

101. Westergren-Thorsson, G.; Önnervik, P.-O.; Fransson, L.-Å.; Malmström, A. *J. Cell. Physiol.* **1991,** *147*, 523-530.

102. Shively, J. E.; Conrad, H. E. *Biochemistry* **1976,** *15*, 3932-3942.

103. Kunesch, N.; Miet, C.; Poisson, J. *Tetrahedron Lett.* **1987,** *28*, 3569-3572.

104. Mori, K.; Tominaga, M.; Takigawa, T.; Masui, M. *Synthesis* **1973**, 790-791.

105. Herzig, J.; Nudelman, A.; Gottlieb, H. E.; Fisher, B. *J. Org. Chem.* **1986,** *51*, 727-730.

106. Lin, T.-S.; Xu, S.-P.; Zhu, L.-Y.; Cosby, L. A.; Sartorelli, A. C. *J. Med. Chem.* **1989,** *32*, 1467-1471.

107. Szeto, H. H.; Schiller, P. W.; Zhao, K.; Luo, G. *FASEB J.* **2005,** *19*, 118-120.

108. Saljoughian, M.; Williams, P. G. *Curr. Pharm. Des.* **2000,** *6*, 1029-1056.

109. Merkushev, E. B. *Synthesis* **1988**, 923-937.

110. Alonso, F.; Beletskaya, I. P.; Yus, M. *Chem. Rev.* **2002,** *102*, 4009-4091.

111. Hanson, J. R. *J. Chem. Res.* **2006**, 277-280.

112. Hayashi, R.; Cook, G. R. *Org. Lett.* **2007,** *9*, 1311-1314.

113. Ho, T.-L. *Chem. Rev.* **1975,** *75*, 1-20.

114. Canonica, S.; Hellrung, B.; Wirz, J. *J. Phys. Chem. A* **2000,** *104*, 1226-1232.

115. Weinstock, L. M.; Karady, S.; Roberts, F. E.; Hoinowski, A. M.; Brenner, G. S.; Lee, T. B. K.; Lumma, W. C.; Sletzinger, M. *Tetrahedron Lett.* **1975,** *16*, 3979-3982.

116. Wei, Y.; Wang, B.-W.; Hu, S.-W.; Chu, T.-W.; Tang, L.-T.; Liu, X.-Q.; Wang, Y.; Wang, X.-Y. *J. Phys. Org. Chem.* **2005,** *18*, 625-631.

117. Esko, J. D.; Lugemwa, F. N.; Fritz, T. A.; Primers of Heparan Sulfate Biosynthesis. PCT Patent WO 94/05678, March 17, 1994.

118. Johnsson, R.; Mani, K.; Ellervik, U. *Bioorg. Med. Chem. Lett.* **2007,** *17*, 2338-2341.

119. Faucher, N.; Ambroise, Y.; Cintrat, J.-C.; Doris, E.; Pillon, F.; Rousseau, B. *J. Org. Chem.* **2002,** *67*, 932-934.

120. Active Biotech AB, Scheelevägen 22, P.O. Box 724, SE-220 07 Lund, Sweden.

121. Wilzbach, K. E. *J. Am. Chem. Soc.* **1957,** *79*, 1013-1013.

122. Guillaume, M. *Bull. Soc. Roy. Sci. Liege* **1967,** *36*, 696-701.

123. Doukas, H. M.; Fontaine, T. D. *J. Am. Chem. Soc.* **1951,** *73*, 5917-5918.

124. Eliel, E.; Rerick, M. *J. Org. Chem.* **1958,** *23*, 1088-1088.

125. Eliel, E. L.; Badding, V. G.; Rerick, M. N. *J. Am. Chem. Soc.* **1962,** *84*, 2371-2377.

126. Leggetter, B. E.; Brown, R. K. *Can. J. Chem.* **1964,** *42*, 990-1004.

127. Bhattacharjee, S. S.; Gorin, P. A. J. *Can. J. Chem.* **1969,** *47*, 1195-1206.

128. Liptak, A.; Jodal, I.; Nanasi, P. *Carbohydr. Res.* **1975,** *44*, 1-11.

129. Garegg, P. J.; Hultberg, H.; Wallin, S. *Carbohydr. Res.* **1982,** *108*, 97-101.

130. Jiang, L.; Chan, T.-H. *Tetrahedron Lett.* **1998,** *39*, 355-358.

131. Shie, C.-R.; Tzeng, Z.-H.; Kulkarni, S. S.; Uang, B.-J.; Hsu, C.-Y.; Hung, S.-C. *Angew. Chem., Int. Ed.* **2005,** *44*, 1665-1668.

132. Tani, S.; Sawadi, S.; Kojima, M.; Akai, S.; Sato, K.-i. *Tetrahedron Lett.* **2007,** *48*, 3103-3104.

133. Wang, C.-C.; Luo, S.-Y.; Shie, C.-R.; Hung, S.-C. *Org. Lett.* **2002,** *4*, 847-849.

134. Ishikawa, T.; Shimizu, Y.; Kudoh, T.; Saito, S. *Org. Lett.* **2003,** *5*, 3879-3882.

135. Oikawa, M.; Liu, W.-C.; Nakai, Y.; Koshida, S.; Fukase, K.; Kusumoto, S. *Synlett* **1996**, 1179-1180.

136. Debenham, S. D.; Toone, E. J. *Tetrahedron: Asymmetry* **2000,** *11*, 385-387.

137. DeNinno, M. P.; Etienne, J. B.; Duplantier, K. C. *Tetrahedron Lett.* **1995,** *36*, 669-672.

138. Chandrasekhar, S.; Reddy, Y. R.; Reddy, C. R. *Chem. Lett.* **1998,** *27*, 1273-1274.

139. Mikami, T.; Asano, H.; Mitsunobu, O. *Chem. Lett.* **1987,** *16*, 2033-2036.

140. Garegg, P. J. In *Preperative Carbohydrate Chemistry;* Hanessian, S. Ed.; Marcel Dekker, Inc.: New York, 1997; pp. 53-67.

141. Smith, K.; Pelter, A. In *Comprehensive Organic Synthesis;* Trost, B. M.; Fleming, I. Eds.; Pergamon Press: Oxford, 1991; pp. 703-731.

142. Smith, M.; Rammler, D. H.; Goldberg, I. H.; Khorana, H. G. *J. Am. Chem. Soc.* **1962,** *84*, 430-440.

143. Hussain, H. H.; Babic, G.; Durst, T.; Wright, J. S.; Flueraru, M.; Chichirau, A.; Chepelev, L. L. *J. Org. Chem.* **2003,** *68*, 7023-7032.

144. Gopinath, R.; Haque, S. J.; Patel, B. K. *J. Org. Chem.* **2002,** *67*, 5842-5845.

145. Tateiwa, J.-i.; Horiuchi, H.; Uemura, S. *J. Org. Chem.* **1995,** *60*, 4039-4043.

146. Clerici, A.; Pastori, N.; Porta, O. *Tetrahedron* **1998,** *54*, 15679-15690.

147. Pério, B.; Dozias, M.-J.; Jacquault, P.; Hamelin, J. *Tetrahedron Lett.* **1997,** *38*, 7867-7870.

148. Fife, T. H.; Jao, L. K. *J. Org. Chem.* **1965,** *30*, 1492-1495.

149. Lee, S. H.; Lee, J. H.; Yoon, C. M. *Tetrahedron Lett.* **2002,** *43*, 2699-2703.

150. Kumar, R.; Kumar, D.; Chakraborti, A. K. *Synthesis* **2007**, 299-303.
151. Firouzabadi, H.; Iranpoor, N.; Karimi, B. *Synlett* **1999**, 321-323.
152. Ishihara, K.; Karumi, Y.; Kubota, M.; Yamamoto, H. *Synlett* **1996**, 839-841.
153. Ranu, B. C.; Jana, R.; Samanta, S. *Adv. Synth. Catal.* **2004,** *346*, 446-450.
154. Hamada, N.; Kazahaya, K.; Shimizu, H.; Sato, T. *Synlett* **2004**, 1074-1076.
155. Patwardhan, S. A.; Dev, S. *Synthesis* **1974**, 348-349.
156. Karimi, B.; Ebrahimian, G.-R.; Seradj, H. *Org. Lett.* **1999,** *1*, 1737-1739.
157. Karimi, B.; Seradj, H.; Ebrahimian, G.-R. *Synlett* **1999**, 1456-1458.
158. Karimi, B.; Ashtiani, A. M. *Chem. Lett.* **1999**, 1199-1200.
159. Jaguar, version 7.0, Schrödinger, LLC, New York, NY, **2007**.
160. Jonas, V.; Frenking, G.; Reetz, M. T. *J. Am. Chem. Soc.* **1994,** *116*, 8741-8753.
161. Richards, R. L.; Thompson, A. *J. Chem. Soc. A* **1967**, 1244-1248.
162. Rablen, P. R. *J. Am. Chem. Soc.* **1997,** *119*, 8350-8360.
163. Nöth, H.; Wrackmeyer, B. *Nuclear Magnetic Resonance Spectroscopy of Boron Compounds*; Springer-Verlag: Berlin, Heidelberg, New York, 1978.
164. Bernet, A.; Seifert, K. *Helv. Chim. Acta* **2006,** *89*, 784-796.
165. Alam, A.; Takaguchi, Y.; Ito, H.; Yoshida, T.; Tsuboi, S. *Tetrahedron* **2005,** *61*, 1909-1918.
166. Chan, K.-F.; Zhao, Y.; Chow, L. M. C.; Chan, T. H. *Tetrahedron* **2005,** *61*, 4149-4156.
167. Xing, X.; Padmanaban, D.; Yeh, L.-A.; Cuny, G. D. *Tetrahedron* **2002,** *58*, 7903-7910.
168. JustTLC, version 2.0, Sweday, Lund, Sweden.
169. Johnsson, R.; Träff, G.; Sundén, M.; Ellervik, U. *J. Chromatogr., A* **2007,** *1164*, 298-305.
170. Simon, R. E.; Walton, L. K.; Liang, Y.; Denton, M. B. *Analyst (Cambridge, U. K.)* **2001,** *126*, 446-450.
171. Vovk, I.; Prosek, M. *J. Chromatogr., A* **1997,** *779*, 329-336.
172. Liang, Y.; Baker, M. E.; Yeager, B. T.; Denton, M. B. *Anal. Chem.* **1996,** *68*, 3885-3891.
173. Petrovic, M.; Kastelan-Macan, M.; Lazaric, K.; Babic, S. *J. AOAC Int.* **1999,** *82*, 25-30.
174. Poole, C. F. *J. Chromatogr., A* **1999,** *856*, 399-427.
175. Pires Valente, A. L.; Augusto, F.; Lemes, A. C.; Lukjanenko, K. *Anal. Commun.* **1997,** *34*, 193-194.
176. Chau, F.-T.; Chan, T.-P.; Wang, J. *Bioinformatics* **1998,** *14*, 540-541.
177. Johnson, M. E. *J. Chem. Educ.* **2000,** *77*, 368-372.
178. Garbacia, S.; Touzani, R.; Lavastre, O. *J. Comb. Chem.* **2004,** *6*, 297-300.
179. Gerasimov, A. V. *J. Anal. Chem.* **2004,** *59*, 348-353.
180. Zhang, L.; Lin, X. *J. Chromatogr., A* **2006,** *1109*, 273-278.
181. Hess, A. V. I. *J. Chem. Educ.* **2007,** *84*, 842-847.

ACKNOWLEDGEMENTS

Efter tiden på avdelningen för bioorganisk kemi, sedermera organisk kemi så finns det ett antal personer som jag vill tacka.

Ulf Ellervik, min handledare, som gav mig en möjlighet att doktorera och som under den tiden delat med dig av din kunskap och ditt kemiintresse. Du har alltid idéer och är alltid engagerad i forskningen. Vi är ett bra team.

Katrin Mani, som har tagit hand om den biologiska delen av våra projekt.

Andréas Meijer, ett stort tack för ditt engagemang i min forskning, dels när du var i gruppen men också nu, långt senare.

Olov Sterner och Ulf Nilsson för ert intresse för kemi och forskning och för att ni gör avdelningen till ett trevligt ställe att jobba på.

Maria och Bodil för att ni ser till att allt fungerar. Karl-Erik Bergqvist för hjälp med NMR, Einar Nilsson för hjälp med masskörningar samt Anders Sundin för hjälp med beräkningar.

Alla tidigare och nuvarande medlemmar i grupp Ellervik, ett speciellt tack till Jesper och Mårten som har varit med nästan hela vägen. Särskilt stort tack till Dan för hjälp med acetaler och åter acetaler och Ulrika för alla biologidata på radioaktiva xylosider.

Gustav och Martin som gjorde TLC-projektet möjligt.

Christopher, 100 Mile House via Kelowna till Lübeck och Ryd med en del kolhydratsdiskussioner, Jakob för galna upptåg och trevliga diskussioner om mekanismer, samt Magnus som alltid är intresserad av att prata, kemi och annat.

Alla tidigare och nuvarande kollegor på avdelning för organisk kemi som gör att det är roligt att gå till jobbet.

Alla vänner utanför kemicentrum som trots allt finns kvar. Patrik, håll ställningarna i Stockholm.

Tack brorsan för all hjälp och stöd.

Mamma och pappa för att ni alltid står bakom mig och stöttar mig, oavsett vad jag gör.

Anastasia, min älskling och vän, för att du alltid står vid min sida.

SAMMANFATTNING

Cancer är ett samlingsnamn på en rad sjukdomar som beror på okontrollerad celltillväxt. År 2005 orsakades omkring 13 % av alla dödsfall i världen av cancer. Det finns många olika typer av cancer och överlevnaden varierar mellan 1 % för cancer i bukspottskörteln till 99 % för vissa typer av hudcancer.

Vi har arbetat med en kemisk substansklass som består av björksocker (xylos) kopplat till naftalen (samma ämne som i vissa malkulor) som hämmar cancertillväxten. Vad som gör att vissa av dessa ämnen, som vi kallar naftoxylosider, selektivt hämmar cancerceller är dock till stora delar ännu okänt. I detta arbete har vi försökt att ta reda på hur naftoxylosiderna rör sig i celler, för att förstå den tumörhämmande effekten.

Vi har arbetat med föreningar som är märkta på olika vis. I våra första försök använde vi fluorescenta grupper, som gör det möjligt att lysa på cellen och se var ämnet tagit vägen. Detta visade sig inte vara en bra metod, då den fluorescenta delen var för stor och påverkade naftoxylosidens biologiska och fysikaliska egenskaper för mycket.

Istället märkte vi in föreningarna med radioaktivt väte. De radioaktivt inmärkta analogerna påverkar inte de fysikaliska egenskaperna och är därför ett bättre sätt att följa ämnena i cellerna. Vi har studerat dessa molekyler i celler och våra preliminära resultat visar att friska och sjuka celler beter sig mycket olika. Bland annat går mekanismerna i de cancersjuka cellerna mycket snabbare.

Med resultaten från denna studie hoppas vi kunna förstå mer om den tumörhämmande effekten hos naftoxylosider och på det sättet kunna utveckla bättre cancermediciner.

Detta arbete inkluderar också ett antal undersökningar i syfte att i detalj förstå hur vissa kemiska reaktioner går till. För att göra detta har vi utvecklat dels nya metoder för att mäta mängden organisk förening och dels nya metoder för att bygga organiska molekyler.